University of Miami
Scholarly Repository

Open Access Dissertations

Electronic Theses and Dissertations

2016-08-05

Control Methods to Improve Non-Linear HVAC System Operations

Kaustubh P. Phalak

University of Miami, kpphalak@gmail.com

Follow this and additional works at: https://scholarlyrepository.miami.edu/oa_dissertations

www.manaraa.com

UNIVERSITY OF MIAMI

CONTROL METHODS TO IMPROVE NON-LINEAR HVAC SYSTEM
OPERATIONS

By
Kaustubh Pradeep Phalak

A DISSERTATION

Submitted to the Faculty
of the University of Miami
in partial fulfillment of the requirements for
the degree of Doctor of Philosophy

Coral Gables, Florida

August 2016

UNIVERSITY OF MIAMI

A dissertation submitted in partial fulfillment of
the requirements for the degree of
Doctor of Philosophy

CONTROL METHODS TO IMPROVE NON-LINEAR HVAC SYSTEM
OPERATIONS

Kaustubh Pradeep Phalak

Approved:

_____   _____
Gang Wang, Ph.D.   Wangda Zuo, Ph.D.
Assistant Professor   Assistant Professor
Civil, Architectural and   Civil, Architectural and
Environmental Engineering   Environmental Engineering

_____   _____
Matthew Jacob Trussoni, Ph.D.   Guillermo Prado, Ph.D.
Assistant Professor   Dean of the Graduate School
Civil, Architectural and
Environmental Engineering

_____
Shihab S. Asfour, Ph.D.
Professor and Associate Dean
Industrial Engineering

PHALAK, KAUSTUBH PRADEEP   (Ph.D., Civil Engineering)
<u>Control Methods to Improve Non-Linear HVAC System Operations</u>   (August 2016)

Abstract of a dissertation at the University of Miami.

Dissertation supervised by Professor Gang Wang.
No. of pages in text. (152)

The change of weather conditions and occupancy schedules makes heating ventilating and air-conditioning (HVAC) systems heavily dynamic. The mass and thermal inertia, nonlinear characteristics and interactions in HVAC systems make the control more complicated. As a result, some conventional control methods often cannot provide desired control performance under variable operating conditions.

The purpose of this study is to develop control methods to improve the control performance of HVAC systems. This study focuses on optimizing the airflow-pressure control method of air side economizers, identifying robust building pressurization controls, developing a control method to control outdoor air and building pressure in absence of flow and pressure sensors, stabilizing the cooling coil valve operation and, return fan speed control. The improvements can be achieved by identifying and selecting a method with relatively linear performance characteristics out of the available options, applying fans rather than dampers to control building pressure, and improving the controller's stability range using cascade control method.

A steady state nonlinear network model, for an air handling unit (AHU), air distribution system and conditioned space, is applied to analyze the system control performance of air-side economizers and building pressurization. The study shows that traditional controls with completely interlinked outdoor air, recirculated air, relief air dampers have the best control performance. The decoupled relief damper control may result in negative building static pressure at lower outdoor airflow ratio and excessively positive building static pressure at higher outdoor airflow ratio. On the other hand, return fan speed control has a better controllability on building pressurization. In absence of flow and pressure sensors fixed interlinked damper and linear return fan speed tracking control can maintain constant outside air ratio and positive building pressure.

The cascade control method is applied to improve the stability of cooling coil valve operation in single zone air handling unit systems, and return fan speed for building pressure control. The system dynamic response is studied using root locus analysis. It was found that the cascade control improved the stability range in two applications under consideration and made the HVAC feedback control loops more robust and adaptive.

ACKNOWLEDGEMENTS

TABLE OF CONTENTS

LIST OF FIGURES

ix

LIST OF TABLES

PUBLICATIONS

- Wang, G., L. Song., K. Phalak. 2015. Investigation on the Fan Energy and Control Performance of Different Damper Control Strategies in Air Handling Units. ASHRAE Transactions, Volume 121. Part 1. p 110-122

- Wang, G. K. Phalak. 2016. Reverse Relief Airflow Prevention and Building Pressurization with a Decoupled Relief Air Damper in Air Handling Units. ASHRAE Transactions. Volume 122. Part 1

- Phalak, K., G. Wang. 2016. Minimum Outdoor Air Control and Building Pressurization with Lack of Airflow and Pressure Sensors in Air Handling Units. Journal of Architectural Engineering. Volume 22. Issue 2. DOI: 10.1061/(ASCE)AE.1943-5568.0000190.

- Phalak, K., G. Wang. 2016. Performance Comparison of Cascade Control with Conventional Controls in Air Handling Units for Building Pressurization, 2016 ASHRAE Winter Conference, Jan 23-27, 2016, Orlando, FL

- Phalak, K.. G. Wang, J. Varona. 2016. Improving Valve Operation Using Cascade Control in Single Zone Air Handling Units. 2016 ASHRAE Annual Conference, June 25-29, St. Louis, MO.

CHAPTER 1. INTRODUCTION

The chapter provides a brief introduction to heating ventilating and air-conditioning (HVAC) systems and their control systems and then discusses the objectives and structure of the thesis.

1.1. HVAC Systems and Controls

1.1.1 HVAC Systems

The main purpose of HVAC systems is to provide a comfortable and healthy indoor environment for the occupants in buildings. This is achieved by eliminating building thermal loads, taking outdoor air and maintaining building static pressure in occupied zones.

To serve this purpose HVAC systems supply air at a controlled moisture and temperature. The temperature and moisture are maintained at specified level by either heating or cooling the supply air using a heating coil or a cooling coil. However, this process is highly energy intensive. According to the 2011 Buildings Energy Data Book by Pacific Northwest National Laboratory (D&R International, 2012), on an average, the HVAC system consumes about 50% of the total energy consumed in buildings.

In 2010, the United States (U.S.) contributed to 19% of global energy consumption. In the same year, only the U.S. building sector accounted for 7% of global primary energy consumption and about 41% of country's primary energy consumption. In terms of carbon dioxide emissions, the U.S. buildings represented a 40% the country's share in 2009. On an average space heating (37%), space cooling (10%) and ventilation (3%)

consume about half of the total energy consumption in buildings. Therefore, in buildings, major energy consumption is due to the HVAC systems.

1.1.2 HVAC Controls

The main objective of a control system is to regulate the behavior of other devices or to maintain a physical quantity at a specific value. The control system has become important in today's day to day life. It is involved in common devices like a toaster to complex machines like airplanes.

The control systems are broadly classified into two classes, an open loop control system and a closed loop control systems. In open loop control systems, the output is only the function of the current input to the system. The open loop control systems are inexpensive and less complex; however, the controlling efficiency of these systems is nearly zero. Figure 1.1 shows a basic schematic of open loop control systems.

Figure 1.1 Open loop control system

A closed loop control system compares the current output with the input (set-point) and takes a corrective action, therefore, this type of control loop is also called as feedback control loop. The feedback signal i.e. the actual output is compared with the desired output i.e. set-point to bring the output of the system back to the desired response. Figure 1.2 shows a basic schematic of feedback control loop systems.
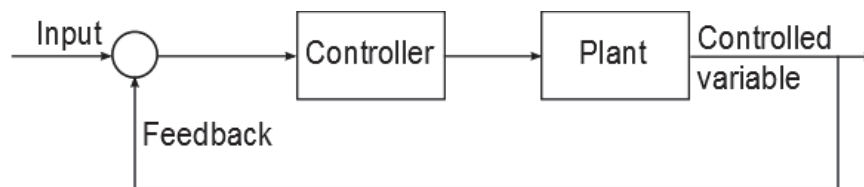
Figure 1.2 Closed or feedback control system

The proportional–integral–derivative (PID) controller is the most common form of controller used in control systems. More than 95% of the control loops used in process control is a proportional–integral (PI) controller (Astrom, 2002) with a zero D gain. PI controllers work well with linear systems.

From above discussion, it is clear that an HVAC system is an integral part of the building systems and contributes to high energy consumption. Also, control systems are required to achieve desired output from the HVAC system. The malfunctioning of the HVAC systems can lead to excessive energy consumption or negatively impact the indoor air quality (IAQ). For example, malfunctioning of the outdoor air damper in hot and humid ambient environments can either allow more than expected outdoor air that will put additional load on the cooling coil in summer or less than expected outdoor air that will degrade the IAQ.

1.2. Current State of HVAC Controls

The HVAC system is a dynamic system by nature due to change in weather conditions, occupancy and schedules. This dynamic nature makes the controller to adjust the control signal time to time to maintain the set-points of the system.

As mentioned earlier, the PI controllers are widely used in HVAC systems and they work well with linear systems. However, HVAC systems are known to be non-linear systems. The mass and thermal inertia of the equipment and fluids involved in the HVAC system

increases the order of the system. Non-linear system response is due to the response of the cooling coil, damper, duct and valve characteristics. In the non-linear system, the system gain varies with a change in operating condition. Therefore, the stability of the high-order HVAC systems also varies with change in operating conditions.

Even though in practice the HVAC control loops are divided into a multiple number of a single loop controlling a single controlled variable, the overall system is interdependent by nature. For example, in a single feedback control loop the supply fan speed is modulated to control the supply air duct static pressure, however, the supply fan speed ends up impacting the mixing chamber pressure, supply airflow rate, and building static pressure. Therefore, the change in the control input can lead to a change in multiple controlled variables and the interdependency of multiple dependent and controlled variables makes the HVAC system a multiple-input multiple-output (MIMO) system (Anderson, et al., 2005).

This dynamic, non-linear, MIMO, high-order HVAC system is most often treated as a group of uncoupled (or loosely coupled) individual HVAC subsystems, controlled using distributed single-input single-output (SISO) PI controllers. This unsophistication of the control system is often driven and impacted by the initial cost of the system, and unreliability and inaccuracy of sensors. Therefore, conventional control methods often cannot provide stable control performance under changing operating conditions. The objective of this study is to suggest low-cost and easy to implement control methods to stabilize control performance of the dampers, cooling coil valve and return fan of air-handling units (AHUs).

1.3. Problem Statement and Objectives

From above discussion, it is clear that the HVAC system encounters issues due to the simplistic nature of control systems often used in practice. Five common issues that are frequently observed in AHUs are listed below and this research addresses these issues and makes an attempt to find solutions.

1.3.1 Problem Statement

Following problem statements have been identified for this research related to the controls of AHUs. These problem statements help to clearly identify the objectives of the work.

- In AHUs, outside air damper, recirculating air damper and relief air damper are interlinked completely or partially in order to control the outdoor air flow (Wang et al., 2015). Based on the connections of these three dampers, five airflow-pressure control methods are suggested. These five available airflow-pressure control methods are often evaluated based on fan energy performance. The nonlinear response of the AHU dampers is not paid sufficient attention that may impact the control performance. A pre-tuned controller gain that work well at a minimum outdoor air condition may not work at economizer mode and vice versa if the controlled variables have nonlinear responses to their control inputs. The loss of control can degrade energy performance and IAQ.

- The reverse relief airflow might occur when relief plenum static pressure is not controlled (Wang and Phalak, 2016). One of the solutions is to decouple the relief air damper and maintain positive static pressure at the relief air plenum. Currently, two control methods have been suggested based on the control loop

design. The first control method uses the relief air damper to control the building static pressure and the return fan speed to control the relief air plenum static pressure and is called the passive building pressure control since damper controls are passive (Trane 2002). On the other hand the second control method uses the return fan speed to control the building static pressure and the relief air damper to control the relief air plenum static pressure by switching the control inputs and is called active building pressure control since fan controls are active. The building may loss the pressure control when the relief air damper reaches its fully open or fully closed position with the passive building pressure control.

- Ideally, minimum outdoor air (OA) and building static pressure are controlled through feedback controllers with the use of airflow and pressure sensors in AHUs. Unfortunately, since these sensors are not always installed in AHUs, it is common to use open loop controls to maintain the minimum OA by fixing the AHU control dampers at minimum positions and maintain the building static pressure by tracking the return fan speed with the supply fan speed (Phalak and Wang, 2016a). However, this open loop control method is not evaluated and the performance is not studied for wide range of operating conditions.

- For building pressurization, the conventional AHUs rely either on direct building pressure control or volume tracking control with a single loop PI controller to maintain a positive building static pressure. Even though this type of control structure is simplistic, it is observed that it may lead to hunting of return fan speed, especially with direct building pressure control as it is a high order, nonlinear system. In general cascade control provides a robust control in other

applications (Phalak and Wang, 2016b). The stability of cascade control on the building static pressure needs to be studied and compared.

- Single zone (SZ) AHUs are widely applied in conditioned spaces due to simple and low cost design. Traditionally, a single control loop is applied to modulate the control valve directly based on the space air temperature. The traditional control is simplistic in nature, however, suffers significant drawbacks. Due to the thermal capacity of both the water in the coils and the air in the conditioned space, the system is high order system and often becomes unstable due to nonlinear characteristics of SZ AHU system. This instability leads to hunting of the control valve and continuously varying supply air temperature, increasing the humidity level in the zone (Phalak et al., 2016). Cascade controls can be implemented to stabilize the operation. However, performance of cascade control needs to be studied and compared with the conventional control method.

1.3.2 Objectives

The primary purpose of the study is to identify control methods to stabilize the performance to HVAC systems. It is broadly divided into five objectives.

- To approach the first three problem statements a non-linear network model of variable air volume (VAV) single duct AHU model is developed. This non-linear network model is implemented in a FORTRAN program. Steady state simulations using this program are performed to achieve following objectives:

  - Select an airflow-pressure control method by evaluating both the fan energy and control performance of five airflow-pressure control methods.

- o Recommend a building pressure control from passive building pressure control and active building pressure control by evaluating the controllability of those two controls.

- o Develop alternative methods to control OA flow and building static pressure for an AHU with the lack of reliable and accurate airflow and pressure sensors through simulation.

- To study the dynamic response of cascade control and the conventional control methods initially, transfer functions for each segment and component in the system is derived and steady state gains are calculated. Using these transfer functions open loop plant transfer function is derived for each type of control method and root locus analysis is performed to achieve following objectives:

  - o Demonstrate the stability of the cascade control to maintain the building static pressure by comparing the performance of the two conventional control methods, i.e. direct pressure control and volume tracking, using the root locus analysis.

  - o Identify a solution to maintain the supply air temperature within an acceptable temperature range by applying cascade control.

1.4. Structure of the Thesis

After the introduction in Chapter 1, Chapter 2 provides a detailed literature review for the research work. Chapter 2 also explains the problem statement, the objectives of the research and the approach followed, in detail.

Chapters 3 and 4 address the first three objectives of this research. Chapter 3 explains the non-linear network model which provides a tool to evaluate the system steady state performance. Chapter 4 develops test case to simulate five pressure-airflow control methods, passive and active building pressure controls, and alternative control methods to control OA flow and building static pressure for an AHU with the lack of sensors, in the program based on the non-linear network model developed in the earlier chapter.

Chapters 5 and 6 address the last two objectives of the research. Chapter CHAPTER 5 discusses the basic control theory behind the conventional HVAC control, the cascade control and the root locus method. Chapter 6 applies the control theory addressed in Chapter 5 to evaluate the stability of building static pressure control and cooling coil valve control between conventional and cascade controls.

In the end, the conclusions of the entire study and future work are discussed in Chapter 7.

CHAPTER 2. LITERATURE REVIEW

AHUs are an integral part of centralized HVAC systems that supply conditioned air to space through connected air distribution ductwork. This chapter provides an extensive literature review of the past research work and existing industry standards in AHU controls. In the end, the issues in the existing system are identified that outline the objectives of the study and the approach is developed to solve the identified issues.

2.1. AHU Conventional Control

AHUs are widely applied to create a comfortable and healthy indoor environment in buildings by eliminating the cooling load generated by occupants, building power systems and heat gain through building envelopes in summer and the heating load mainly caused by heat loss through building envelopes in winter. To achieve its purpose, a conventional single duct AHU with economizer operation normally consists of a chilled water cooling coil, a supply fan (SF), a return fan (RF), and a set of three dampers: an outdoor air damper (OAD), a recirculating air damper (RCD), and a relief air damper (RLD). In conditioned space, terminal boxes with a hot water reheat coil maintain the desired space temperature by modulating a damper and a control valve.

Figure 2.1 shows schematic of a single duct variable air volume (VAV) AHU. Typically, both the SF and RF have a variable frequency drive (VFD) in VAV systems. In Figure 2.1 the actuator and damper, both are represented by the damper symbol.
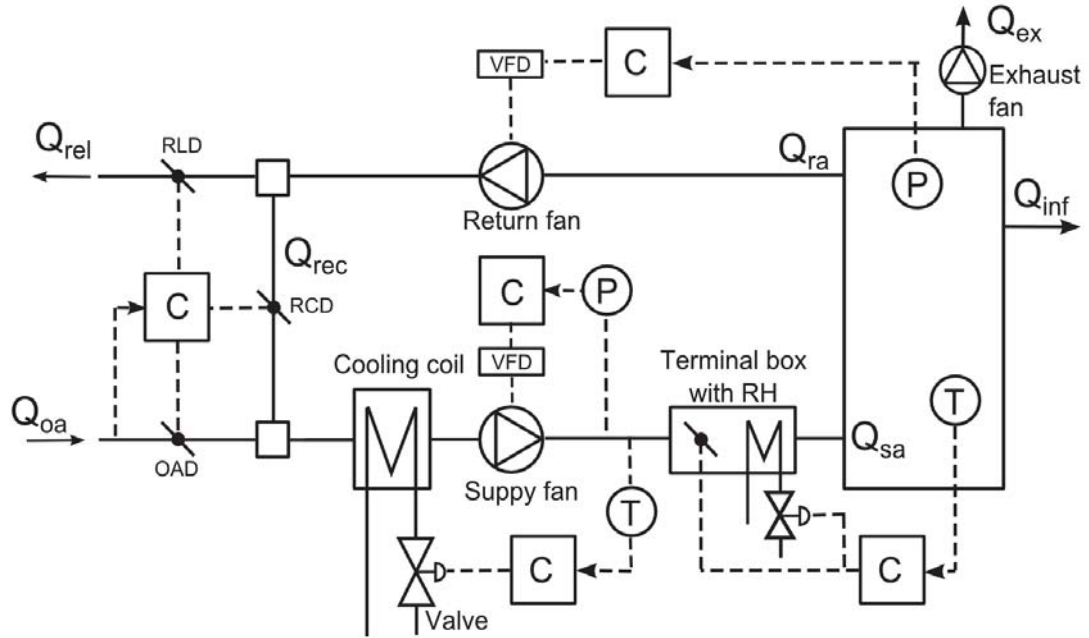
Figure 2.1 Conventional Single Duct VAV AHU with Control Loops

In addition to thermal control, supply air duct static pressure, building static pressure, and outdoor airflow rates need to be controlled. This is accomplished by use of feedback control loops that control the individual components of the AHU.

2.1.1 AHU Thermal Control

The supply air temperature is controlled using the cooling coil valve. Supply air temperature is thermally controlled at a set point, typically 13˚C (55˚F) (Wang and Song, 2012), to ensure that supply air is cool and dry enough to remove sensible and latent cooling load in spaces.

2.1.2 AHU Outdoor Airflow Control

The outside airflow is controlled by the set of three dampers. The damper command signal is often modulated by the proportional–integral (PI) controller. The outdoor airflow rate is maintained at a desirable level depending on outdoor air conditions. The outdoor airflow rate is either set at a minimum level for indoor air quality (IAQ) control

required by ASHRAE Standard 62.1 (ASHRAE, 2010a) or adjusted up to 100% for the economizer operation required by ASHRAE standard 90.1 (ASHRAE, 2010b). This feedback control loop compares the signal from the outdoor airflow meter with the desired setpoint during minimum outdoor air operation and compares the supply air temperature with the desired setpoint during economizer operation by modulating the damper command.

There are multiple ways in which the three dampers can be connected; however, conventional or often called the interlinked airflow-pressure control method is one of the widely used methods. In conventional airflow-pressure control method, all three dampers are interlinked and one single command is used to maintain the right amount of outdoor airflow in AHU.

As shown in Figure 2.2, the three dampers are completely interlinked and modulated for outdoor air control (Levenhagen, 1998; Underwood,1999; McQuiston et al., 2005). With one damper command, the OAD and RLD respond with a direct action while the RCD responds with a reverse action.
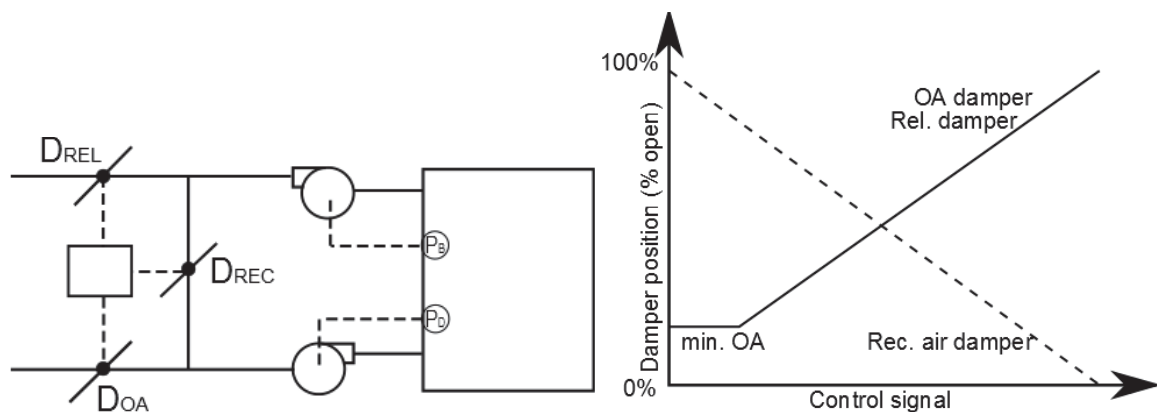
Figure 2.2 Conventional OA Control (a) schematic (b) operation

Apart from the conventional methods, several other methods have been suggested that can improve the energy performance of the AHU operation. Four other damper connection methods are discussed in section 2.2.

2.1.3 AHU Supply Air Duct and Building Static Pressure Controls

As shown in Figure 2.2 the SF speed is modulated using VFD in order to maintain the duct static pressure. The supply air duct static pressure is controlled at a set point, typically 374 Pa (1.5 inch of water) (Montgomery and McDowall, 2008), which ensures that all terminal boxes can receive required supply air to maintain comfortable space conditions.

As shown in Figure 2.2 a positive building static pressure is often maintained by modulating the RF speed using the VFD. A slightly positive building static pressure, 1 to 20 Pa (0.005 to 0.08 inch of water) is generally desired to avoid outdoor air infiltration to conditioned spaces (ASHRAE, 2015).

In few systems, positive relief plenum pressure is maintained to avoid the revised relief airflow. As shown in Figure 2.3, the RLD is decoupled with the interlinked OAD and RCD and is modulated to maintain a positive relief plenum pressure. The relief air plenum pressure controls with decoupled RLD are also discussed in section 2.2.
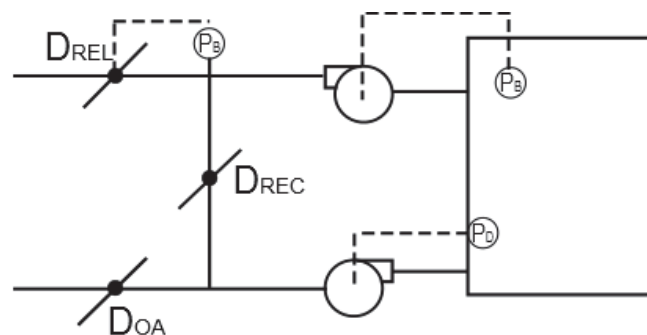
Figure 2.3 Duct Static Pressure and Building Pressure Control

2.1.4 Terminal Box Control

The space air temperature in each thermal zone is controlled by a VAV terminal box unit with a hot water reheat coil where the supply airflow can adjusted by a modulation damper and the discharge air temperature can be adjusted by a hot water control valve (Liu, Zhang, & Dasu, 2012).

When the required supply airflow is more than the minimum airflow set point, the damper is modulated to maintain the space temperature at its setpoint. As the required airflow reaches to the minimum airflow setpoint, the damper is modulated to maintain the airflow at the minimum airflow setpoint and the reheat coil valve is modulated to maintain the space temperature at its setpoint. As scope of this study is limited to the controls associated with AHUs this control loop is not under consideration for the research.

2.2. Pressure-Airflow Control Methods

From a controls point of view, in AHU pressure-airflow controls, five control inputs, including the speed of the SF and RF and the positions of the OAD, RCD, and RLD, are available to control three controlled variables: the supply air duct static pressure, the building static pressure, and the outdoor airflow rate. Besides the three dampers are interlinked completely in the conventional airflow-pressure control , which is discussed in section 2.1, in order to reduce the number of independent control inputs needed to match the number of the controlled variables, practically the three dampers can also be interlinked partially. Based on how the three dampers are interlinked, five different airflow-pressure control methods exist for pressure-airflow control in VAV AHUs.

The conventional method in which all three dampers are completely interlinked is a most widely used method. However, when all three dampers are interlinked, reverse airflow through the RLD might occur when the OAD and RLD are in a most closed position (Seem et al., 2000). As a result, IAQ could be jeopardized if the relief air louver is located near a pollution source. Moreover, since all three dampers always remain partially closed due to the interaction, the traditional control method causes an excessive system pressure drop that results in more fan power usage (Nassif and Moujaes, 2008; Nassif, 2010).

To avoid the reverse airflow, Seem et al. (2000) proposed that the OAD be decoupled from the interlinked RCD and RLD and always remain fully open. Alternatively, ASHRAE guideline 16 (2010c) recommends that the RLD be decoupled from the interlinked OAD and RCD and is modulated to maintain a positive relief air plenum pressure. Moreover both the OAD fully open control and the decoupled RLD control can have either sequenced or overlapping action. These damper connections and the sequenced and overlapping methods are discussed in this section.

2.2.1 Open OAD Methods
Except for the OAD, the other controls remained the same as the traditional control method. Simulation, laboratory, and field results demonstrated that a fully open OAD prevented air entering through the RLD. The RLD has a direct action and the RCD has a reverse action with the damper command. Since the RLD and RCD positions are overlapping, this method is called the overlapping control method with the OAD fully open. The fully open OAD also improves the energy performance of the SF; however, the

overlapping RCD and RLD still cause the RF to have poor energy performance (Nassif, 2010).

To improve the RF energy performance, Nabil and Moujaes (2008) proposed an airflow-pressure control method with only one damper partially closed and other two dampers fully open. The approach actually converts the RCD and RLD from an overlapping action to a sequenced action while the OAD remains fully open.

Figure 2.4 shows schematic of open OAD control method with sequenced and overlap operation. Given a damper command range from 0 to 0.5, the RLD acts from 0 to 100% open while the RCD is kept fully open. With a damper command range of 0.5 to 1, the RCD acts from 100% to 0% open while the RLD is kept fully open. This method is called the sequenced control method with OAD open. Nabil (2010) demonstrated that the potential fan energy savings would be 5% to 30% over the traditional control method.

(a)

(b)

(c)
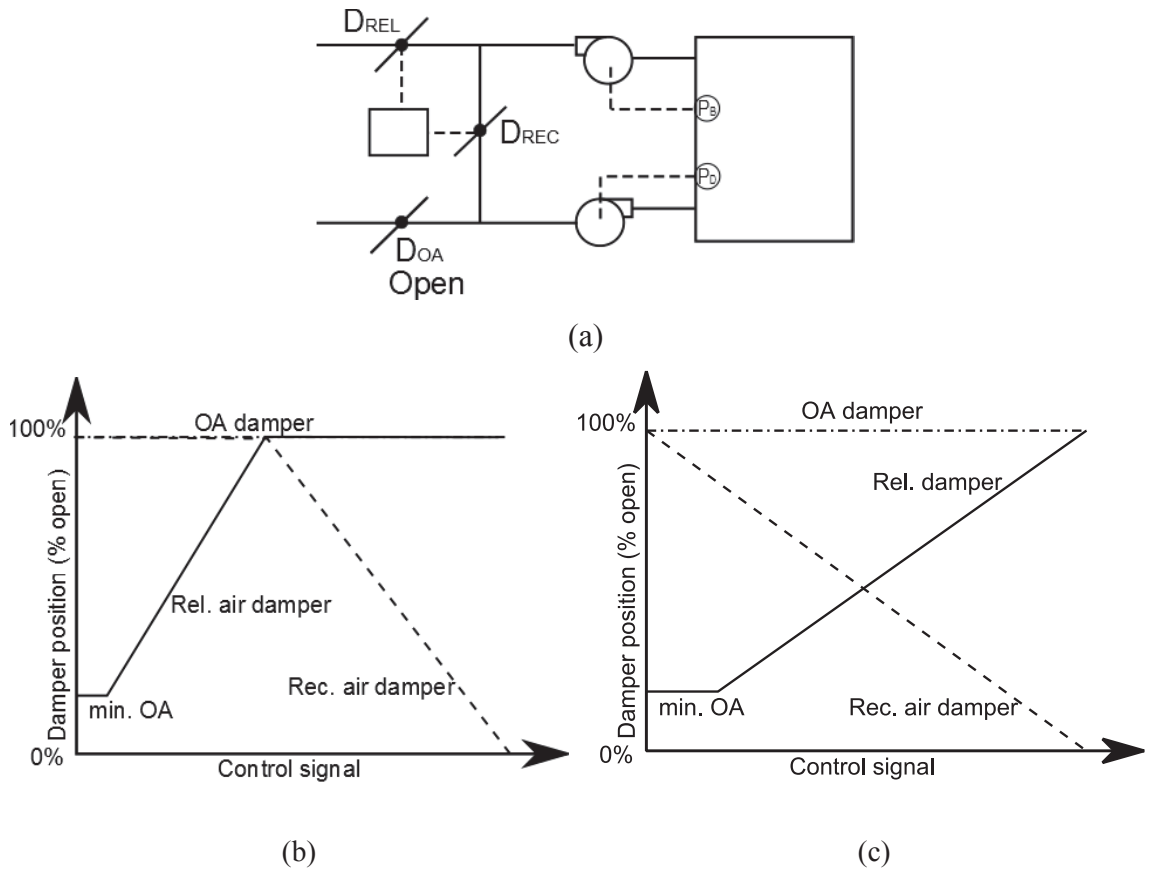
Figure 2.4 Open OAD airflow-pressure method (a) schematic (b) sequenced operation (c) overlap operation

2.2.2 Decoupled RLD Method

ASHRAE guideline 16 (2010c) recommends two different airflow-pressure control methods to avoid the reverse airflow from the RLD in the traditional method. The RLD is decoupled from the interlinked OAD and RCD to form a new control input, while the relief air plenum static pressure is controlled to form a new controlled variable with a set point from 25 to 75 Pa (or 0.1 to 0.3 inch of water).

Figure 2.5 shows schematics of decoupled RLD method with sequenced and overlapping operation. For a damper command range from 0 to 0.5, the OAD acts from 0 to 100% open while the RCD is kept fully open. With a damper command range of 0.5 to 1, the RCD acts from 100% to 0% open while the OAD is kept fully open. This control method

is called the sequenced control method with OAD open. In overlapping controls for a damper command range from 0 to 1, the OAD acts from a minimum position to 100% open while the RCD is closed from fully open position.

ASHRAE guideline 16 (2010c) recommends that the RF speed be modulated to maintain the desired relief air plenum static pressure while the decoupled RLD be modulated for building static pressure control. Figure 2.5 shows a schematic of decoupled relief damper method with sequenced and overlapping operation. The interlinked OAD and RCD control the outdoor air with either an overlapping action or a sequenced action. As a result, the overlapping control has two dampers at partially closed positions while the sequenced control always maintains at least one damper at a fully open position. Therefore, the ASHRAE-sequenced control method normally is recommended over the ASHRAE overlapping control method due to better fan energy performance (CEC, 2003).

(a)

(b)   (c)
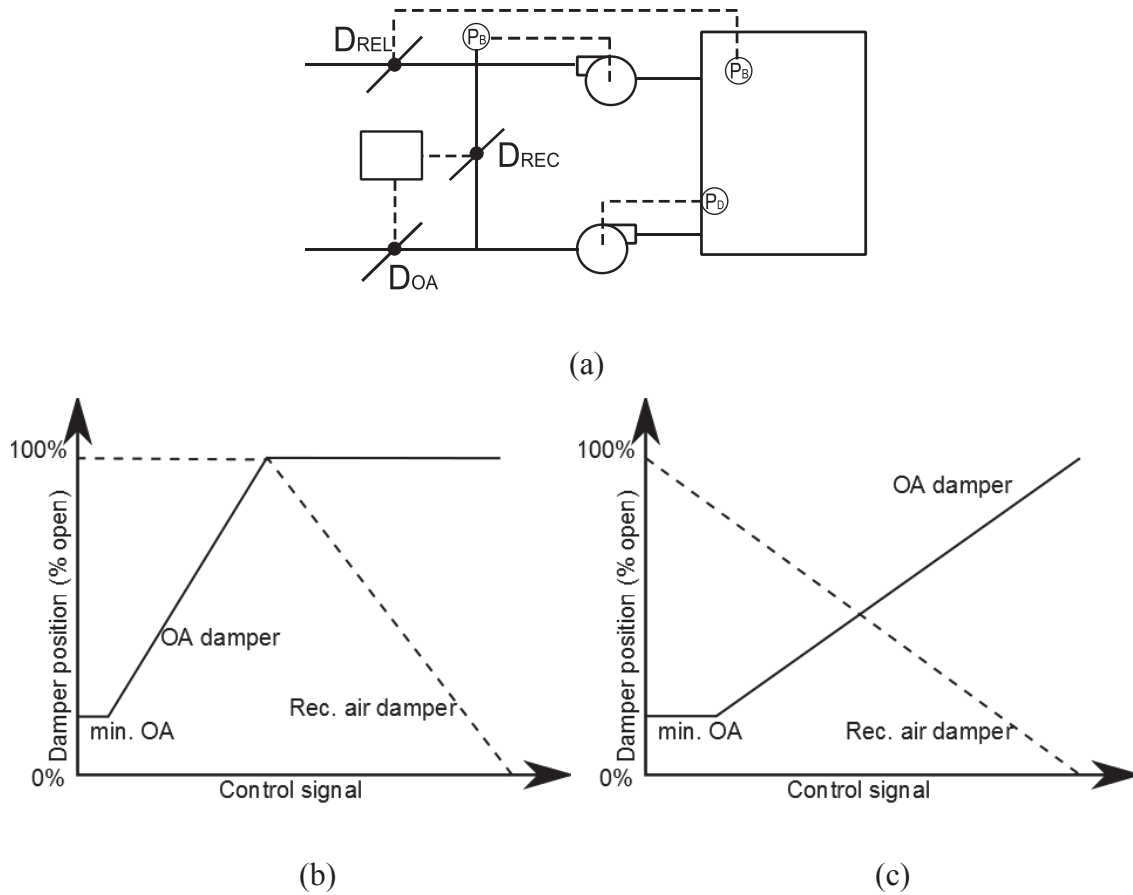
Figure 2.5 Decoupled relief damper method (a) schematic (b) sequenced operation (c) overlap operation

2.2.3 Passive and Active Control

As shown in Figure 2.5(a) building static pressure ASHRAE guideline 16 (2010c) recommends building static pressure should be controlled with the decoupled RLD. On the other hand Pennsylvania State University (PSU, 2010) Standard Sequences of Operation Guideline proposed alternative method in which the RF speed is modulated to maintain the building static pressure control and the decoupled RLD is modulated to maintain a positive relief air plenum pressure. Figure 2.6 shows the alternative decoupled RLD control method.
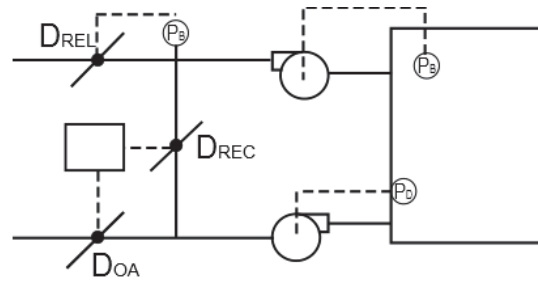
Figure 2.6 Decoupled RLD method by Pennsylvania State University's Standard Sequences of Operation Guideline

The control inputs and controlled outputs of the ASHRAE decoupled RDL controls (shown in Figure 2.5) and the PSU decoupled RDL controls (shown in Figure 2.6) are actually same under steady states if the control inputs is within their control range. However, the controllability of the damper and fan is quite different. The controlled variable can always be maintained by modulating the fan speed if the fan is sized appropriately.

On the other hand, the controlled variable associated with the airflow-pressure control is not only determined by the damper position but also limited by the fan speed. For example, the outdoor airflow cannot be higher than the supply airflow, which is determined by the supply fan speed, even though the OAD is fully open. Consequently, the method in which the building static pressure control using relief damper position as suggested in ASHRAE guideline 16 will be referred as Building Pressure Passive (BPP) Control. And the method in which the building static pressure control using RF speed as suggested by the Pennsylvania State University's Standard Sequences of Operation Guideline will be referred as Building Pressure Active (BPA). The controllability of the damper and fan will be discussed in further section.

2.2.4 Summary of Airflow-Pressure Control Methods

Table 2.1 categorizes and summarizes all the airflow-pressure control methods discussed above. This summary helps in identifying the methods those need to be simulated for the first two objectives of this research. The method 4 and 5 can further be subcategorized in two control types i.e. BPP and BPA. To study the gains of airflow-pressure control methods, the BPA and BPP control type is irrelevant as in these cases it is assumed that the building pressure and relief plenum pressure is well controlled. However, to study the controllability of RLD and RF speed over the building pressure the control type BPP and BPA is important. Therefore to study the controllability method 4 is simulated for BPP and BPA control.

Table 2.1 Summary of airflow-pressure control methods

Sr. No.	Method	Operation	Control Type	Controlled Variable		
				Building Static Pressure	Outdoor Airflow Rate	Relief Plenum static Pressure
1	Traditional	-	-	RF speed	OAD, RCD, and RLD	-
2	OAD open	Overlapping	-	RF speed	RCD and RLD	-
3	OAD open	Sequenced	-	RF speed	RCD or RLD	-
4	Decoupled RLD	Overlapping	BPP	RLD	OAD and RCD	RF speed
			BPA	RF speed	OAD and RCD	RLD
5	Decoupled RLD	Sequenced	BPP	RLD	OAD and RCD	RF speed
			BPA	RF speed	OAD and RCD	RLD

2.3. Nonlinear Characteristics of Airflow-Pressure Control Methods

From the discussion above, it is clear that multiple airflow-pressure control methods suggested in various materials. Currently, all these airflow-pressure control methods in an AHU are only evaluated based on fan energy performance, with an assumption that the AHU is always perfectly controlled. The improved energy performance is moot if the system is unstable or/and has a slow transient response. Not sufficient material and

research are available that discusses the transient response of these methods. One of the methods to evaluate the transient response is by studying the system gain over the operational range of the AHU. In the following discussion, the reason for the system for being non-linear and current methods used to handle the non-linearity is discussed.

The classical proportional–integral (PI) controllers are dominant in AHUs with pre-tuned constant controller gains, a linear system response of a controlled variable, such as outdoor airflow, to its corresponding control input, such as a damper command, is always desired for a perfectly controlled performance (ASHRAE, 2010c). Unfortunately, the pressure-airflow control in AHUs is highly nonlinear.

Air dampers have a nonlinear inherit characteristic curve. Since damper authority affects the installed characteristic curve of an ideal duct-damper path, which has a controlled differential static pressure between its two connected nodes, in order to obtain approximate linear installed characteristic curve, a parallel blade damper is preferred for the paths with high damper authority and an opposed blade damper is preferred for the paths with low damper authority (ASHRAE, 2010c; Lizardos and Elovitz, 2000; Taylor, 2014b). However, only the relief air path in AHUs with BPP control methods can be treated as an ideal duct-damper path because the differential pressure across the path is controlled by a fixed set point.

The damper curves and the nodal differential static pressure have a nonlinear relationship with airflow for each path. The system gain is the derivative of a controlled variable to its corresponding control input and varies under different operating conditions in a nonlinear network. Therefore a pre-tuned controller gains that work well at a full-load condition may not work at a partial load condition and vice versa. In general, an increased system

gain tends to make the system unstable while a reduced system gain tends to have a slow transient response and a higher steady state error (Burns, 2001; Nise, 2011). Due to the interdependency of the multivariable HVAC system the SF and RF speed change or damper position change has a unintentional effect on other variables of the HVAC system for example SF speed, a control input for duct static pressure control is a disturbance input for outdoor airflow.

Therefore, in order to select an appropriate airflow-pressure control method for AHUs, both the fan energy and control performance of five airflow-pressure control methods is one of the goals of this study.

2.4. Controllability of Dampers and Fans

As discussed earlier BPP and BPA are two decoupled RLD controls. As shown in Figure 2.5 and 2.6 the RLD is decoupled from the interlinked OAD and RCD to form a new control input, while the relief air plenum static pressure forms a new controlled variable. The static pressure setpoint at the relief air plenum is determined to overcome the losses through the RLD and associated ductwork, normally ranging from 25 to 75 Pa (or 0.1 to 0.3 inch of water).

In both the decoupled RLD controls, the SF speed is modulated to maintain the desired supply air duct static pressure while the interlinked OAD and RCD are modulated to maintain the desired outdoor airflow rate with either an overlapping action or a sequenced action. On the other hand, the control loop design for the space and relief air plenum static pressure is different. The BPP control proposes the RF speed to maintain the desired relief air plenum static pressure and the decoupled RLD to maintain the desired building static pressure. The BPA control proposed the RF speed to maintain the

desired building static pressure and the decoupled RLD to maintain the desired relief air plenum static pressure.

Unfortunately, the controlled variable of the airflow-pressure control may not be maintained at its set-point when the damper reaches either the fully open position or the fully close position. Since the BPP control uses the RLD to control the building static pressure and the BPA control uses the RLD to control the relief air plenum static pressure, the building static pressure may lose control with the BPP control and the reverse relief airflow may occur with the BPA control once the RLD reaches its limits, either the fully closed position or the fully open position. This study evaluates the system performance of both controls when the RLD reaches its limits. Since the relief air flow increases as the outdoor air increase and vice versa, the RLD may reach the fully closed position at low outdoor airflow ratio and the RLD may reach the fully open position at high outdoor airflow ratio. A nonlinear network solution is discussed first in order to mathematically describe the nonlinear network that consists of the SF, RF, and three air dampers in an AHU, along with the air distribution ductwork and conditioned space. Then, the system performance with both the BPP and BPA controls is simulated using the nonlinear network solution at both low and high outdoor airflow ratio. Finally, conclusions are drawn based on the simulation results.

2.5. Alternative Controls without Pressure and Flow Sensors

The control loops discussed in above sections rely on a reliable, accurate and stable operation of sensors. However, this is not the case in most of the applications in HVAC industry. For example, the building static pressure is maintained slightly above the atmospheric pressure and relatively small, wind and thermal effects significantly affect

the accuracy of the building static pressure measurement (Hitchings, 2001). For the accurate operation of the flow sensors the the flow need to be completely developed and they need to be recalibrated time to time. Another factor that affects the use of conventional flow sensors in the feedback control loops of the HVAC systems is the higher cost. Considering these issues alternative control methods for building static pressure and OA control are used.

The conventional AHUs rely either on direct building pressure control (Stanke & Bradley, 2002) or volume tracking control (Siemens, 2003) with a single loop PI controller to maintain positive building pressure.

In the building static pressure feedback control loop, the building static pressure is measured by a differential pressure sensor and is controlled by modulating the RF speed. Since the controlled building static pressure is relatively small, wind and thermal effects significantly affect the accuracy of the building static pressure measurement. This makes the direct building static pressure control difficult.

The building static pressure could also be controlled by the difference between the supply and return airflow rates. Using this technique the building static pressure could be indirectly controlled by maintaining the airflow rate difference at its setpoint (Trane 2002). Two airflow sensors are installed to measure the supply and return airflow rates and the RF speed is modulated to maintain the airflow rate difference at its setpoint, which needs to be calibrated based on the desired building static pressure. This building pressure control is known as flow or volume tracking control.

Direct building pressure control is simplistic; however, it is observed that it may lead to hunting of return fan speed. For the direct building pressure control, accurate and stable

building static pressure measurement is challenging due to the wind and intermittent pressure changes caused by the opening of doors. On the other hand, the building static pressure is highly sensitive to the differential airflow, therefore; the error in airflow measurement makes the volume tracking method unfavorable.

From above discussion it is clear that reliable pressure and airflow sensors are essential to control the minimum outdoor airflow rate and building static pressure. However, in current heating, ventilating and air-conditioning (HVAC) industry practice, the AHU controls are often not ideal, as their operation is limited by the accuracy of physical sensors installed. The costs of hardware and installation along with the unreliability and inaccuracy of sensors are usually cited as the reason for not installing physical sensors (Song et al. 2013).

This inaccuracy and unreliability of measurement by sensors are due to multiple reasons. As discussed previously, the wind and thermal effects affect the accuracy of the building static pressure measurement. For airflow measurements, airflow rate is often determined by measuring pressure differences across an orifice, nozzle or venturi tube (ASHRAE 2009). Since dampers, bends and fittings close to the airflow measurement devices can cause errors, long, straight ducts should be installed upstream and downstream of the flow measurement devices to assure fully developed flows (McFarlane, 2012). These conditions are hard to satisfy in actual systems.

For AHUs with the lack of pressure and airflow sensors, as a compromise, the common practice is to set the three control dampers at fixed positions to maintain minimum outdoor airflow (Apte 2006) when the outdoor airflow sensor is not installed.

2.5.1 Return Fan Speed Tracking

Often the building static pressure sensor, as well as the supply and return airflow sensors, are not installed. In such case, the RF speed tracks the SF speed as a compromised control to maintain the building static pressure (Krarti 2011, Honeywell 1998, Trane 2002). Since a part of the supply airflow exits the building at a constant flow rate as exhaust and exfiltration and the supply air duct has a constant static pressure setpoint regardless of the supply airflow, the RF speed is slightly less than the supply fan speed. In practice, the return fan speed tracks the supply fan speed using either an offset tracking which maintains a constant difference between supply and return fan speed (Krarti 2011) or by proportional tacking in which the RF speed is a constant fraction of the SF speed (ABB 2008).

Krarti (2011) found that the RF speed tracking using the offset tracking method is unacceptable due to mismatched fan flow characteristics over the typical range of operation, even though it is an inexpensive and easy to implement the method on existing systems. Besides the RF speed offset tracking, the proportional tracking and the tracking with a linear relationship are equally simplistic and inexpensive methods. Another objective of this study is to evaluate the building static pressure control with different RF tracking methods.

To achieve the two purposes, the outdoor airflow and building static pressure of an AHU is simulated using a nonlinear network solution, which is studied by Wang et al. (2015). The simulation will include two applications both with a perfect control of the supply air duct static pressure. In the first simulation application where the outdoor airflow sensor is not installed, the minimum outdoor airflow is controlled by the fixed damper position

method while the building static pressure is perfectly controlled. In the second application, the minimum door airflow is controlled by the fixed damper position method and the building static pressure is controlled by the compromise return fan control, i.e. RF speed tracking methods.

2.5.2 Outdoor Air Control without Outdoor Air Flow Sensor

The outdoor airflow rate is maintained at a desirable level depending on outdoor air conditions. The outdoor airflow rate is either set at a minimum level for indoor air quality (IAQ) control required by ASHRAE Standard 62.1(ASHRAE, 2010a) or adjusted up to 100% for the economizer operation required by ASHRAE standard 90.1 (ASHRAE, 2010b). The minimum outdoor airflow rate, which is monitored by an outdoor airflow sensor, is normally controlled by modulating the three control dampers, the OAD, RCD, and RLD, in an AHU.

Janu et al. (1995) found that the outdoor air intake controlled by the fixed damper position method is much closer to a constant outdoor airflow ratio rather than a constant airflow rate. As a result, the fixed damper position method cannot directly control the minimum outdoor airflow rate. However, a consistent correlation between the outdoor airflow ratio and damper position will provide a chance to calculate the outdoor airflow rate based on the damper position along with measured supply airflow rate. Wang et al. (2013) have developed and validated a virtual fan airflow meter, which can accurately determine the fan airflow rate based on the fan power and head measurements without the need of physical airflow sensors. If the consistent correlation exists, the outdoor airflow rate can be virtually measured based on the damper position, fan power and head, and finally can be indirectly controlled. Therefore, one of the objectives of this research is to

verify the consistent correlation between the outdoor air ratio and damper positions for different damper connections.

2.6. Control Loops with Large Capacity Plants

Above discussion mentions various control loops in HVAC systems. The responses of the control loops are largely dependent on the systems gains and the time constants offered by components and mediums (e.g. chilled water or air) in the loop. The number of components i.e. the sensors and the actuator is limited, however, depending on the way the loop is been setup and the capacity of the system the quantity of the medium can vary (Siemens, 2013). A large quantity of the medium in the system of feedback control loop can offer significant time constant and this can lead to the instability of the control loop. Some of the common places where this problem is observed are building static pressure control and zone temperature control in single zone (SZ) AHU system.

2.6.1 Building Static Pressure Control

As discussed earlier the return fan in the AHU is either directly controlled by the building static pressure or indirectly with the difference in supply and return airflow. In the direct building pressure feedback control loop, the building static pressure is measured by a differential pressure sensor and is controlled by modulating the return fan speed. The large quantity of air in the building offers a significant time constant. The controlled building static pressure is slightly above the atmospheric pressure therefore, the wind and thermal effects significantly affect the accuracy of the building static pressure measurement. Fluctuations in the reading of pressure get passed on to the return fan control signal and that could lead to erratic changes in return fan speed. This makes the direct building static pressure control difficult.

On the other hand, the building static pressure could also be controlled by the difference between the supply and return airflow rates. Using this technique the building static pressure could be indirectly controlled by maintaining the airflow rate difference at its setpoint (Trane 2002) or return fan linearly tracking supply fan (Phalak, 2015). Airflow sensors installed at the supply and return duct measure the supply and return airflow rates and the return fan speed is modulated to maintain the airflow rate difference at its setpoint. This needs calibration for the desired building static pressure. This building pressure control technique is known as flow or volume tracking control. Even though it is considered one of the stable control methods this often does not account for the variation in exhaust airflow and the infiltration. Exhaust airflows are often not measured and infiltration could not be exactly determined and is affected by multiple factors like daily use if the building, occupant behavior, and age of the building. Also, the airflow difference is dependent on airflow meters which need calibration, fully developed flow, and are not often accurate.

Therefore, the calibrated volume tracking control may not be able to maintain positive building static pressure for change in operating condition. Therefore, a cascade control method is been suggested which stabilizes the system, does not need frequent calibration and can eliminate the inaccuracy of the flow meters. Cascade control is often considered as an adaptive and robust type of control method and widely used in other applications where PI controllers are used. In this type of control method, two controllers are used. In this case, the first controller uses the instantaneous building static pressure measured to determine the corrected reference differential flow. This reference differential flow is then compared with actual differential flow and return fan is

modulated accordingly.

To compare the control performance of direct pressure control, volume tracking control and cascade control, initially, a model is developed for single duct VAV system. Equations for steady state gains are derived using the mass conservation equation. Using these steady state gain constants and time constants, plant transfer functions are derived.

2.6.2 Space Temperature Control in SZ AHU

SZ AHUs system is the type of centralized HVAC systems in which the heating or cooling operation in AHUs is controlled by a single thermostat located in the space. This type of system is widely used in residential and small commercial buildings due to the simple design and low cost. SZ AHU is an effective system for such applications because the loads in different areas of small buildings do not vary significantly.

In a conventional feedback control loop of SZ AHU system, the control valve of either the heating or cooling coil is modulated by zone air temperature and supply air temperature is neglected. In this type of system, the thermostat in the zone through single loop PI controller controls the chilled or hot water flow depending it is in the heating or cooling mode. The dependent variable, in this case, the space temperature, and the independent variable, the valve position are linked through HVAC equipment and two mediums, chilled water in the coil and air. The HVAC equipment and the mediums offer time delay due to inertia and heat capacity.

As mentioned earlier the conventional control method for SZ AHU is simplistic and low cost, however, suffers drawbacks. This type of control does not take into consideration the supply air temperature. It is often observed that the supply and diffuser air temperature fluctuates over a wide range, as high as 9°C (16°F) even if, the space air

temperature is maintained in a close ±1°C (3°F) range. Following examples explain the problems observed in practical cases.

Figure 2.7 shows the supply air temperature recorded for 10 days at a test facility in the University of Miami where the conventional single loop PI controller is used to maintain the space air temperature. It can be observed that the supply air temperature fluctuates from 14°C (57F) to as high as 23°C (73F). During this period, the space air temperature was maintained between desired 22°C (72°F) to 24°C (75°F) range. Even if the space temperature is maintained in the desired range the relative humidity of the space was much higher for a certain period of the day than the setpoint 50%. The increased supply air temperature due to the fluctuations increases the relative humidity of the space. This continuous variation also puts an additional burden on the pump and leads to energy consumption.
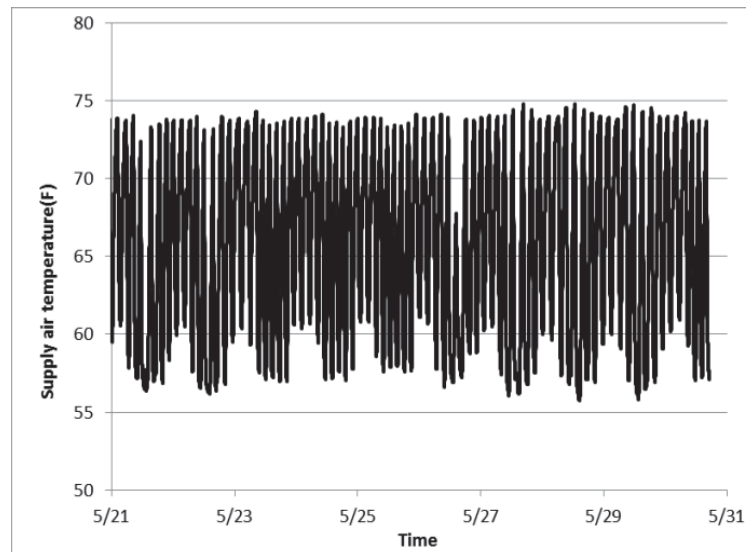
Figure 2.7 Variation in supply air temperature in SZ AHU system

Another problem is explained in Figure 2.8 which shows the cooling and heating control signals, which are sent to the chilled water valve and the electrical reheat coil of AHU measured in a building. Due to continuous and high variations in the supply air

temperature, the system was switching between heating and cooling modes cyclically. This continuous change in modes leads to significantly high energy consumption.
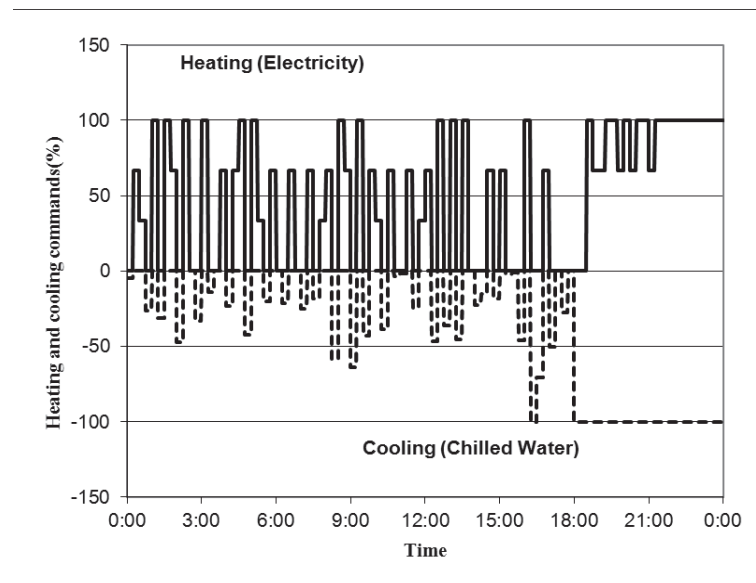
Figure 2.8 Switching between heating and cooling mode

2.7. Objectives and Approaches

From above discussion, it is clear that the dynamic, non-linear, multivariable, high-order HVAC system encounters issues due to the simplistic nature of control systems often used in practice. Some of the common issues are listed below and they summarize the problem statement for this research.

- The nonlinear response of the AHU dampers is generally not evaluated and that may impact the control performance negatively. A pre-tuned controller gain that work well at a design condition may not work at economizer mode or any other operating condition. The loss of control can degrade energy performance and IAQ.

- To avoid reverse relief airflow RLD is decoupled. There are two decoupled RLD control methods available based on passive and active type of control, BPP and

BPA. The controllability is affected at limiting cases of the damper position. In BPP as the RLD reaches its fully open or fully closed position it will lose the control over building static pressure. Therefore both BPP and BPA control methods need to be evaluated for controllability when the RLD reaches its operating limits.

- Often pressure and airflow sensors are not always installed in AHUs. it is common practice to maintain the minimum outdoor airflow by fixing the AHU control dampers at minimum positions and maintain the building static pressure by tracking the return fan speed with the supply fan speed. This common practice need to be evaluated.

- The direct building pressure control and volume tracking control are simplistic methods used for building pressurization. However, direct building pressure control often leads to unstable operation of return fan and volume tracking control does not account for building pressure changes when infiltration or exhaust airflow change. A stable and accurate control method is required to maintain the building pressure. In practice, cascade control is used for a robust control in other applications. The stability of cascade control with conventional control methods needs to be studied and compared.

- In SZ AHUs, often a single control loop is applied to modulate the control valve directly based on the space air temperature. Despite the simplicity of this control method hunting of the cooling coil control valve is commonly observed. This leads to higher humidity in conditioned spaces and continuously varying supply air temperature. A cascade control can provide a stable control. Its application and

the performance need to be evaluated and compared with the conventional control method.

2.7.1 Objectives

As mentioned in the earlier chapter the primary objective of the study is to select, identify and develop control methods to stabilize the performance to HVAC system. From above problem statements the objectives of the research are listed as below.

- The first three problem statements are solved with a non-linear network model of VAV single duct AHU model. FORTRAN program is developed based on the non-linear network model for steady state simulations to achieve following objectives:

  - Select an airflow-pressure control method with fairly constant system gain, for a stable response, out of all the airflow-pressure control methods discussed earlier and compare the control performance along with the fan energy performance.

  - Recommend a control method to control building static pressure by comparing the controllability of RLD and return fan at minimum OA condition and economizer mode. These methods (BPP and BPA) need to be analyzed and appropriate controlling variable for building static pressure is to be identified.

  - Develop and evaluate the performance of alternative methods to control OA flow and building static pressure for an AHU with the lack of reliable and accurate airflow and pressure measurement, with simulation.

- The dynamic response of cascade control and the conventional control methods is analyzed using root locus analysis d to achieve following objectives:

  o Demonstrate the stability of the cascade control on return fan to maintain the building static pressure and compare the control performance of the two conventional return fan control methods, i.e. direct pressure control and volume tracking, using the root locus analysis.

  o Check the applicability of cascade control to stabilize the cooling coil valve operation and eliminate the wide variation in supply air temperature and high humidity in conditioned space.

2.7.2 Approach

The objectives mentioned above are addressed with four approaches, development of a nonlinear network model (chapter 3), steady state simulations for the first three problem statement (chapter 4), cascade control and root locus analysis (chapter 5), and its application for dynamic simulation to approach the last two problem statement (chapter 6). For steady state simulation a non-linear network model was developed and implemented in a FORTRAN program. For dynamic simulation MATLAB and Simulink are used.

- A non-linear network model of variable air volume (VAV) AHU model is developed. The sections of the network are divided as paths and depending on the operation in each path they are categorized and equations are applied in the model.

- Above model is then applied to simulate the three applications. For the first problem statement the responses for each airflow-pressure control method and system gains are calculated using the simulation. The systems gains are then compared with varying OA ratio. The airflow-pressure control method with relatively constant system gain is selected for better control performance. Using the same non-linear network model with decoupled damper the controllability for building static pressure is studied. The two BPP and BPA control methods are simulated using the FORTRAN code. Each method is simulated for minimum OA condition and economizer mode and based on that appropriate controlling variable for building static pressure is identified. This non-linear network model is then used to evaluate the practical case of unavailability of pressure sensors and airflow meter to control the OA flow and building static pressure. For the fixed OA damper position the OA flow rate as well as the OA ratio is studied. The results will provide an insight about the effectiveness of this method. Return fan speed tracking is studied for offset, proportional and linear correlation with supply fan speed. The correlation that provides a positive building static pressure is selected.

- To evaluate the control performance of cascade control with the conventional control methods dynamic simulation is used. Initially, a model is developed for building pressure control and space air temperature in SZ AHU. Using steady state gains and time delays, plant transfer functions are derived. With the plant transfer functions and the conventional and cascade control method, open loop transfer functions are derived.

- Root locus analysis is performed to check the stability of the systems. The control method with roots in stable range of the plot is selected.

CHAPTER 3. NON-LINEAR NETWORK MODEL

In this chapter, development of nonlinear network model for single duct variable air volume (VAV) AHUs is discussed. To address the first objective of selecting a stable airflow-pressure control method, identifying better building pressure control method from the two decoupled RLD control methods, and developing the control for the AHUs when sensors are unavailable, a non-linear network model for single duct VAV AHUs is developed.

First, the components, paths, nodes, terminology and the assumptions for the single duct VAV AHUs are discussed. Then, the model is developed using the components of the schematic in Figure 3.1. The next section discusses the correlation between the damper positions and damper commands. For the five airflow-pressure control methods discussed in chapter 2, the correlations for OAD, RCD and RLD are given. The different goals of the first objective of the study have different set of independent variables. Finally, to simulate the test cases total five procedures are been developed and the code is modified for these procedures. The approaches are described in this chapter.

3.1. Single Duct VAV AHU Model

In this section, the components, paths, nodes and the terminology used in the single duct VAV AHU are discussed. Then, in the later part, the sign convention for the pressure drop and the pressure-airflow characteristic function for the paths in the network are discussed. Next, separate equation for each type of path i.e. a simple path, a damper path, and a fan path are given. Finally, mass conservation is applied at the three nodes i.e. relief air plenum, the mixed air plenum, and the room.

3.1.1 Description and Schematic

Figure 3.1 presents a schematic of a single duct VAV AHU with economizer operation as well as its air distribution ducts and conditioned space, which is equipped with a constant speed exhaust fan (EF). Each OAD, RCD, and RLD has its own actuator so that it can be interlinked or decoupled easily. The AHU system network has seven paths: supply air (sa), return air (ra), relief air (rel), recirculating air (rec), outdoor air (oa), exhaust air (ex), and building envelope infiltration (inf). Both infiltration and exfiltration is unintentional airflow through building envelope driven by the pressure difference between indoor and outdoor air. The negative building static pressure generates infiltration while the positive building static pressure generates exfiltration. Since the building static pressure is a controlled variable, in this thesis the infiltration is used to generally describe unintended air exchange through envelopes, negative infiltration representing air entering the space and positive infiltration representing air leaving space. For building pressurization, the entering OA flow should be avoided. The AHU system network also has three nodes: a relief air plenum (RE), a mixed air plenum (MA), and a space or room (RM). It is assumed that the outdoor air static pressure is zero and that the outdoor air is not treated as a node.
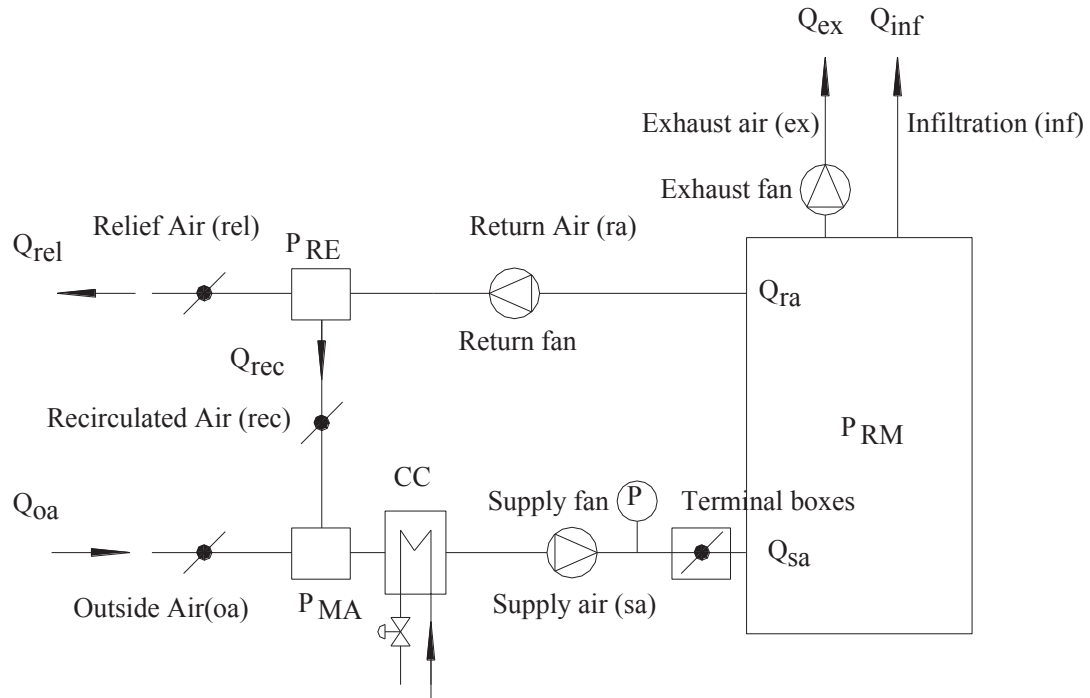
Figure 3.1 Network schematic of a Single Duct VAV AHU

3.1.2 Path Characteristic Functions and Mass Conservation

The pressure-airflow characteristic function for each path relates the airflow rate through each path to differential static pressures at two connected nodes. The three node static pressures are named as P_{RE}, P_{MA}, and P_{RM}, respectively. Since a path has a static pressure drop along the airflow direction, the path functions depend on the path airflow direction. For this thesis, the path airflow direction convention is shown in Figure 3.1. A reverse airflow causes a reverse pressure drop. An airflow sign is used in the path functions to represent this relationship.

Three different types of paths are treated in the AHU network: a simple path, a damper path, and a fan path. Building envelope infiltration can be treated as a simple path because it does not possess any dampers and fans. Infiltration airflow (Q_{inf}) relates to the

differential static pressure between the space node and outdoor air, which is equal to the space static pressure since the outdoor air static pressure is zero.

$$P_{RM} = S_{inf} \cdot Q_{inf}^n \cdot sign(Q_{inf}) \tag{3.1}$$

The resistance factor (S_{inf}) and exponent (n) depend on the nature of infiltration. The exponent (n) ranges between 1 and 2.5 (McQuiston et al., 2005).Within a given building, the resistance factor (S_{inf}) keeps constant.

A damper path has an air duct as well as a modulation damper. The damper paths include the relief air (rel), recirculating air (rec), and outdoor air (oa) paths. The resistance factor includes the fixed resistance factor of the air duct (S_{rel}, S_{oa} and S_{rec}), and an adjustable resistance factor of the damper (S_{reld}, S_{oad} and S_{recd}), which varies with the damper position ($\theta_{RLD}, \theta_{OAD}$ and θ_{RCD}).

$$P_{RE} = [S_{rel} + S_{reld}(\theta_{RLD})] \cdot Q_{rel}^2 \cdot sign(Q_{rel}) \tag{3.2}$$

$$-P_{MA} = [S_{oa} + S_{oad}(\theta_{OAD})] \cdot Q_{oa}^2 \cdot sign(Q_{oa}) \tag{3.3}$$

$$P_{RE} - P_{MA} = [S_{rec} + S_{recd}(\theta_{RCD})] \cdot Q_{rec}^2 \cdot sign(Q_{rec}) \tag{3.4}$$

The damper resistance factor depends on the damper type (opposed blade or parallel blade damper), and can be expressed as a function of the damper blade position, θ, for a given damper.

$$S(\theta) = f(\theta)S_d \tag{3.5}$$

The damper blade position (θ) is presented as a ratio of the fully open position. The damper is fully open when θ =1 and the damper is fully closed when θ =0. The resistance factor when the damper is fully open (S_d) is a design parameter for damper selection. The

damper correction factor (f) is a function of the damper blade position (θ) and can be found in different references (ASHRAE, 2010c; Felkers, 2010; Brandemuel et al., 1993).

A fan path has an air duct as well as a fan, which overcomes the pressure drop in the path. The differential static pressure or fan static head (H) is a function of relative fan speed (ω) and fan airflow rate (Q) for a given fan. The fan paths include the return air duct (ra), supply air duct (sa), and exhaust air duct (ex). The duct in the supply fan path actually includes an air distribution section (ad) and a terminal box section (TB) separated at the supply air duct static pressure sensor.

$$P_{MA} - P_{RM} = (S_{ad} + S_{TB}) \cdot Q_{sa}^2 \cdot \text{sign}(Q_{sa}) - H_{SF}(Q_{sa}, \omega_{SF}) \qquad (3.6)$$

$$P_{RM} - P_{RE} = S_{ra} \cdot Q_{ra}^2 \cdot \text{sign}(Q_{ra}) - H_{RF}(Q_{ra}, \omega_{RF}) \qquad (3.7)$$

$$P_{RM} = S_{ex} \cdot Q_{ex}^2 \cdot \text{sign}(Q_{ex}) - H_{EF}(Q_{ex}) \qquad (3.8)$$

The fan head and power curve under the design speed for the SF, RF, and EF can be regressed as

$$H_d(Q) = a_H Q^2 + b_H Q + c_H \qquad (3.9a)$$

$$W_d(Q) = a_W Q^2 + b_W Q + c_W \qquad (3.9b)$$

The fan head and power curve of the SF and RF under partial speeds can be deduced using the fan laws. Under a relative fan speed (ω), a ratio of actual fan speed to the design fan speed, the fan head and power curves can be expressed as

$$H(Q, \omega) = a_H Q^2 + b_H \omega Q + c_H \omega^2 \qquad (3.10a)$$

$$W(Q, \omega) = a_W \omega Q^2 + b_W \omega^2 Q + c_W \omega^3 \qquad (3.10b)$$

The mass flow rate through all seven paths can be determined implicitly with given node static pressures, fan speeds and damper commands using Equations (3.1) to (3.4) and (3.6) to (3.8). Then the mass conservation can be applied at three nodes, including the relief air plenum, the mixed air plenum, and the room.

$$\begin{bmatrix} -Q_{ra}(P_{RM},P_{RE},\omega_{RF}) + Q_{rel}(P_{RE},\theta_{RLD}) + Q_{rec}(P_{RE},P_{MA},\theta_{RCD}) \\ -Q_{oa}(P_{MA},\theta_{OAD}) - Q_{rec}(P_{RE},P_{MA},\theta_{RCD}) + Q_{sa}(P_{RM},P_{MA},P_{TB},\omega_{SF}) \\ -Q_{sa}(P_{RM},P_{MA},P_{TB,STP},\omega_{SF}) + Q_{ra}(P_{RM},P_{RE},\omega_{RF}) + Q_{ex}(P_{RM}) + Q_{inf}(P_{RM}) \end{bmatrix} = \begin{bmatrix} 0 \\ 0 \\ 0 \end{bmatrix}$$

(3.11)

In summary, ten governing equations are available, including seven path characteristic functions, defined by Equations (3.1) to (3.4) and (3.6) to (3.8), and three node mass conservation functions, defined by Equation (3.11).

3.2. Damper Position-Command Relationship

As discussed previously, the three dampers are interlinked completely or partially and controlled by a damper command (D). A RLD command (R) is also required for BPP and BPA control methods. The relationships between the damper positions and damper commands are associated with an airflow-pressure control method. Table 1 summarizes each control loop defined by its controlled variable as well as its corresponding control input for five different airflow-pressure control methods. For each decoupled RLD method, there are two sub-methods, including BPP and BPA depending on how the pressure static pressure is controlled.

Table 3.1 Airflow-pressure control methods

No.	Method	Operation	Control Type	Controlled Variable		
				Building Static Pressure	Outdoor Airflow Rate	Relief Plenum static Pressure
1	Traditional	-	-	RF speed	OAD, RCD, and RLD	-
2	OAD open	Overlapping	-	RF speed	RCD and RLD	-
3	OAD open	Sequenced	-	RF speed	RCD or RLD	-
4	Decoupled RLD	Overlapping	BPP	RLD	OAD and RCD	RF speed
			BPA	RF speed	OAD and RCD	RLD
5	Decoupled RLD	Sequenced	BPP	RLD	OAD and RCD	RF speed
			BPA	RF speed	OAD and RCD	RLD

For the traditional control method (Method 1), all the dampers are interlinked completely.

$$\theta_{OAD} = D \tag{3.12a}$$

$$\theta_{RCD} = 1 - D \tag{3.12b}$$

$$\theta_{RLD} = D \tag{3.12c}$$

For the overlapping control method with the OAD fully open (Method 2), the RCD and RLD are interlinked with an overlapping action controlled by the damper command (D), while the OAD is fully open.

$$\theta_{OAD} = 1 \tag{3.13a}$$

$$\theta_{RCD} = 1 - D \tag{3.13b}$$

$$\theta_{RLD} = D \tag{3.13c}$$

For the sequenced control method with the OAD fully open (Method 3), the RCD and RLD are interlinked with a sequenced action controlled by the damper command (D), while the OAD is fully open.

$$\theta_{OAD} = 1 \tag{3.14a}$$

$$\theta_{RCD} = \begin{cases} 1 & D < 0.5 \\ 2(1-D) & D \geq 0.5 \end{cases} \qquad (3.14b)$$

$$\theta_{RLD} = \begin{cases} 2D & D < 0.5 \\ 1 & D \geq 0.5 \end{cases} \qquad (3.14c)$$

For the decoupled-overlapping BPP and BPA control methods (Method 4), the OAD and RCD are interlinked with an overlapping action controlled by the damper command (D), while the RLD has a direct action with the RLD command (R).

$$\theta_{OAD} = D \qquad (3.15a)$$

$$\theta_{RCD} = 1 - D \qquad (3.15b)$$

$$\theta_{RLD} = R \qquad (3.15c)$$

For the decoupled-sequenced BPP and BPA control method (Method 5), the OAD and RCD are interlinked with a sequenced action controlled by the damper command (D), while the RLD has a direct action with the RLD command (R).

$$\theta_{OAD} = \begin{cases} 2D & D < 0.5 \\ 1 & D \geq 0.5 \end{cases} \qquad (3.16a)$$

$$\theta_{RCD} = \begin{cases} 1 & D < 0.5 \\ 2(1-D) & D \geq 0.5 \end{cases} \qquad (3.16b)$$

$$\theta_{RLD} = R \qquad (3.16c)$$

3.3. Applications of Nonlinear Network Model

As mentioned earlier, different objectives have a different set of independent and dependent variables and to simulate these cases separate procedures need to be developed. This section of the chapter defines the applications of the network model and specifies the procedures for these applications.

3.3.1 To Select Airflow-Pressure Control Method

To select an airflow-pressure control method with fairly constant system gain, the outdoor air system gain and interactive disturbance inputs from outdoor air control are applied to evaluate the control performance. To achieve this objective the three independent control inputs are the SF speed (ω_{SF}), RF speed (ω_{RF}), OAD command (D) and RLD command (R) (in case of BPP and BPA control methods) while, the path airflows, and node pressures are calculated. The procedure developed to get these results is defined as Procedure A and discussed in next section.

To evaluate the energy performance under a given operating condition defined by an outdoor airflow rate, supply airflow, building static pressure and duct static pressure; SF and RF power need to be calculated. The SF and RF power is dependent on the SF and RF speed. The SF and RF speed for the given condition are calculated using Procedure B (for methods 1 to 3), Procedure C (for BPA) and Procedure D (for BPP).

3.3.2 To Recommend Building Pressure Control Method from BPP and BPA

To select a building pressure control from the two decoupled RLD control methods, BPP and BPA two procedures are used. These procedures consider the limiting cases of the damper position, specifically RLD.

To test the controllability of the BPA method the relief air plenum static pressure (P_{RE}) is to be maintained at its set point by calculating the RLD command value. The RF speed is to be determined from the setpoint value of $P_{RM.}$ Also, the OAD and RCD command (D), SF speed is to be calculated from the given OA and SA flows and the duct static pressure (P_{TB}). As the RLD reaches the fully open or fully closed position, P_{RE} cannot be maintained at its setpoint. To handle this case the procedure should consider P_{RE} as a

dependent variable and its value should be calculated for the limiting cases of RLD position. To simulate this case Procedure C is developed.

To test the controllability of the BPP method the building static pressure is to be maintained at its set point by calculating the RLD command value. Also, the OAD and RCD command (D), SF and RF speed are to be calculated from the given OA and SA flows and the pressure setpoints P_{TB} and P_{RE}. However, as the RLD reaches the fully open or fully closed position, the building static pressure cannot be maintained. In such case, P_{RM} becomes a dependent variable and the value is calculated for the limiting cases of RLD position. To simulate this case Procedure D is developed.

3.3.3 To Develop Control Method in Absence of Sensors

To develop and evaluate the performance of fixed damper position and return fan speed tracking method to control OA flow and building static pressure respectively two procedures are used.

To test the fixed OAD position method SF and RF speed are the dependent variable and for decoupled RLD method, RLD command is an additional dependent variable. The OA flow, SF, and RF speed are calculated from the OAD position, given SA flow and the setpoints P_{TB} and P_{RM}. The approach developed to solve the set of equations for the mentioned dependent variable is described as Procedure E in the next section.

To test return fan speed tracking for the three correlations offset, proportional, and linear between SF and RF speed, first, the set of RF speeds are calculated from the assumed correlation. Then the set of dependent and independent variables are same as that mentioned in the Procedure A.

3.3.4 Summary of Applications and Procedures

From above discussion, it is clear that for the three applications total five different set of dependent variables are present and for these applications, five different procedures need to be developed. These procedures are described in detail in next section. The applications and the procedures are summarized in the following table.

Table 3.2 Summary of the applications and procedures

Objectives	Applications	Procedures
Select Airflow-Pressure Control Method	Evaluate the control performance	A
	Evaluate the energy performance of Method 1 to 3	B
	Evaluate the energy performance of the BPA	C
	Evaluate the energy performance of the BPP	D
Recommend Building Pressure Control Method	Active (BPA)	C
	Passive (BPP)	D
Develop Control Method in Absence of Sensors	Fixed OAD position method	E
	Return fan speed tracking	A

3.4. Procedures

Following sub-sections describe the procedures in detail

3.4.1 Procedure A

The path airflow and node static pressure are controlled variables determined by control inputs such as the fan speeds and the damper commands. Due to disturbances and control instability, these controlled variables are not usually perfectly controlled at desired setpoints and thus their actual values are unknown. Since an AHU as well as air distribution ducts and conditioned spaces form a nonlinear network, the solutions for nonlinear networks have to be applied to obtain the path airflow and node static pressure.

This method has three independent control inputs, the SF speed (ω_{SF}), RF speed (ω_{RF}), and OAD command (D), for the traditional control, and add one more independent control input, the RLD command (R) for the BPP and BPA controls. The supply airflow rate is maintained by TB dampers based on the space cooling load conditions and is treated as an independent variable in this study. Therefore, three constraints for the traditional control and four constraints for the BPP and BPA controls need to be applied to determine the system performance. The constraints can be either controlled variables or/and given control inputs.

Meanwhile, the system performance variables include seven path airflows, Q_{sa}, Q_{ra}, Q_{rel}, Q_{rec}, Q_{oa}, Q_{ex}, and Q_{inf}, and three node pressures, P_{RE}, P_{MA}, and P_{RM}. Figure 3.2 represents the block diagram of this procedure. The variables on the left side of the block are independent variables and on the right side are the dependent variables. The independent variable, RLD command (R) is applicable only in case of BPP and BPA methods.
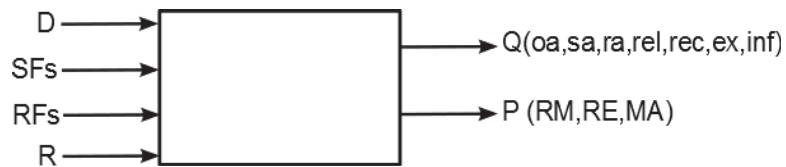
Figure 3.2 Dependent variables for Procedure A

A network must satisfy the laws of conservation of mass and energy. With an assumption of constant air density, the mass conversation is represented volume conversation. For each junction node, the entering mass flows should be balanced with leaving mass flows, while for each closed loop the net total static pressure drop along all paths within the loop should be zero (Mays, 1999; Boulos et al., 2006). A node equations solution (Boulos et al., 2006) is applied to obtain the airflow rate through each path and the static pressure at

each node. The node equations solution uses node static pressures as unknown variables, which automatically satisfies the conservation of energy. Then the mass flow rate through all seven paths can be determined implicitly with given node static pressures using Equations (3.1) to (3.4), (3.6) to (3.8) as well as the correlations between damper command and damper position i.e. Equations (3.12) to (3.16). The supply air Q_{sa} is calculated from the supply air duct static pressure, P_{TB}.

$$S_{TB} \cdot Q_{sa}^2 = P_{TB} \tag{3.17}$$

Next, the residual mass balance errors (E) at the relief air plenum, the mixed air plenum, and the room can be expressed as functions of three node static pressures:

$$\begin{bmatrix} E_{RE}(P_{RE}, P_{MA}, P_{RM}) \\ E_{MA}(P_{RE}, P_{MA}, P_{RM}) \\ E_{RM}(P_{RE}, P_{MA}, P_{RM}) \end{bmatrix} = \begin{bmatrix} -Q_{ra}(P_{RM}, P_{RE}) + Q_{rel}(P_{RE}) + Q_{rec}(P_{RE}, P_{MA}) \\ -Q_{oa}(P_{MA}) - Q_{rec}(P_{RE}, P_{MA}) + Q_{sa}(P_{RM}, P_{MA}) \\ -Q_{sa}(P_{RM}, P_{MA}) + Q_{ra}(P_{RM}, P_{RE}) + Q_{ex}(P_{RM}) + Q_{inf}(P_{RM}) \end{bmatrix}$$

$$\tag{3.18}$$

According to the conservation of mass, the residual mass balance errors at all nodes should be zero.

$$\begin{bmatrix} E_{RE}(P_{RE}, P_{MA}, P_{RM}) \\ E_{MA}(P_{RE}, P_{MA}, P_{RM}) \\ E_{RM}(P_{RE}, P_{MA}, P_{RM}) \end{bmatrix} = \begin{bmatrix} 0 \\ 0 \\ 0 \end{bmatrix} \tag{3.19}$$

Equation (3.19) demonstrates a nonlinear system of equations with three equations and three unknown node static pressures. For a nonlinear system, the unknown node static pressures can be solved very efficiently by the Newton-Raphson procedure (Mays, 1999; Boulos et al., 2006). The unknown node static pressures are adjusted iteratively in a direction that will reduce the residual mass balance errors.

Generally, a nonlinear system of equations in the node static pressure format, such as Equation (3.19), can be written in a linearized form with the node static pressure changes using a truncated Taylor series expansion:

$$\begin{bmatrix} \dfrac{\partial E_{RE}}{\partial P_{RE}} & \dfrac{\partial E_{RE}}{\partial P_{MA}} & \dfrac{\partial E_{RE}}{\partial P_{RM}} \\[2mm] \dfrac{\partial E_{MA}}{\partial P_{RE}} & \dfrac{\partial E_{MA}}{\partial P_{MA}} & \dfrac{\partial E_{MA}}{\partial P_{RM}} \\[2mm] \dfrac{\partial E_{RM}}{\partial P_{RE}} & \dfrac{\partial E_{RM}}{\partial P_{MA}} & \dfrac{\partial E_{RM}}{\partial P_{RM}} \end{bmatrix}_i \cdot \begin{bmatrix} \Delta P_{RE} \\ \Delta P_{MA} \\ \Delta P_{RA} \end{bmatrix}_i = - \begin{bmatrix} E_{RE} \\ E_{MA} \\ E_{RM} \end{bmatrix}_i \tag{3.20}$$

The node static pressure changes, which are required to reduce the residual mass balance errors, can be solved by Equation (3.20). Then the refined node static pressures (i+1) can be updated by adjusting the guessed node static pressures (i).

$$\begin{bmatrix} P_{RE} \\ P_{MA} \\ P_{RA} \end{bmatrix}_{i+1} = \begin{bmatrix} P_{RE} \\ P_{MA} \\ P_{RA} \end{bmatrix}_i + \begin{bmatrix} \Delta P_{RE} \\ \Delta P_{MA} \\ \Delta P_{RA} \end{bmatrix}_i \tag{3.21}$$

With finalized node static pressures, the airflow rate through each path can then be obtained using Equations (3.1) to (3.4) and (3.6) to (3.8).

3.4.2 Procedure B

A solution is developed to determine the desired speed of the SF and RF and the desired damper command (D) under perfectly-controlled building static pressures, duct static pressures, and outdoor airflow rates. The supply airflow rate (Q_{sa}) through all terminal boxes is an independent variable. This procedure is used to measure the energy performance of the first three methods in Table 3.1 i.e. except the BPA and BPP methods.

The space static pressure is maintained at its set point, P_{RM}. The supply air duct static pressure is maintained at its setpoint, P_{TB}. The outdoor air flow is controlled at a given

value, Q_{oa}, which is determined by outdoor air operation modes, economizer or non-economizer, and varies from a minimum airflow to the supply airflow.

With an assumption of perfect control, all control inputs are integrated to maintain all controlled variables at their setpoints interactively under a steady state regardless of the assignment of the control input and its controlled variable in each control loop. With the determined fan speeds, the SF and RF head and power can be calculated using Equations (3.10) and applied to evaluate the fan energy performance.

Figure 3.3 is the block diagram for this procedure. The variables on the left side of the block Q_{oa}, Q_{sa}, $P_{RM,}$ and P_{TB} are independent variables and on the right side the SF speed, RF speed, and damper command (D) are the dependent variables.

Figure 3.3 Dependent variables for Procedure B

The fan heads and powers can be solved using mass and energy conservation principles as follows:

1) Determine the space infiltration airflow (Q_{inf}) and exhaust airflow (Q_{ex}) based on the controlled space static pressure, P_{RM}, using Equations (3.1) and (3.8).

2) Determine the return airflow (Q_{re}), recirculating airflow (Q_{rec}), and relief airflow (Q_{rel}) using the mass conservation at three nodes, including a relief air plenum (RE), a mixed air plenum (MA), and a room (RM), with an assumption of constant air density.

$$Q_{ra} = Q_{sa} - Q_{ex} - Q_{inf} \qquad (3.22)$$

$$Q_{rec} = Q_{sa} - Q_{oa} \qquad (3.23)$$

$$Q_{rel} = Q_{ra} - Q_{rec} \qquad (3.24)$$

3) Determine the damper command (D) using energy conservation to ensure that the net total static pressure drop along the outdoor air, recirculating air, and relief air paths is zero by substituting Equations (3.12) to (3.14) depending on different airflow-pressure control methods into Equations (3.2) to (3.4). For the control methods other than the two BPP (overlapping and sequenced) control methods,

$$\Delta P_{rel}(D) + \Delta P_{oa}(D) - \Delta P_{rec}(D) = 0 \qquad (3.25)$$

4) Determine the head of the SF and RF using Equations (3.6) and (3.7), and then the fan speed and power using Equations (3.10a and 3.10b).

3.4.3 Procedure C

In this procedure supply airflow and setpoints determine required damper command, SF and RF speeds. This procedure is used to simulate the BPA methods from Table 3.1.

Figure 3.4 represents the block diagram of this procedure. The variables on the left side of the block Q_{oa}, Q_{sa}, P_{RM}, $P_{RE,}$ and P_{TB} are independent variables and on the right side SF speed, RF speed, RLD command (R) and damper command (D) are the dependent variables.

Figure 3.4 Dependent variables for Procedure C

In the application, the return fan speed is calculated by maintaining the building pressure constant and the RLD command (R) is calculated to maintain the relief air plenum static

pressure at the setpoint. At the limiting conditions of RLD command the relief plenum static pressure is calculated for the limiting conditions.

1) Determine the space infiltration airflow (Q_{inf}) and exhaust airflow (Q_{ex}) based on the controlled space static pressure, P_{RM}, which is controlled by the RF speed, using Equations (3.1) and (3.8).

2) Determine the return airflow (Q_{re}), recirculating airflow (Q_{rec}), and relief airflow (Q_{rel}) using the mass conservation at three nodes, including a relief air plenum (RE), a mixed air plenum (MA), and a room (RM), with an assumption of constant air density using equations (3.22) to (3.24).

3) The relief air plenum static pressure is controlled and is applied to determine the RLD command (R) by substituting Equation (3.19c) or (3.20c), in Equation (3-2),

$$P_{RE} = \Delta P_{rel}(R) \qquad (3.26a)$$

If the calculated RLD command (R) is either fully open or fully closed, the relief air plenum static pressure cannot be maintained at its setpoint and is determined by the RLD position, either fully open (R=1) or fully closed (R=0). For a fully open RLD, the relief air plenum static pressure is

$$P_{RE} = \Delta P_{rel}(R = 1) \qquad (3.26b)$$

For a fully closed RLD, the relief air plenum static pressure is

$$P_{RE} = \Delta P_{rel}(R = 0) \qquad (3.26c)$$

Figure 3.5 represents the independent and dependent variables in the limiting case discussed above.

Figure 3.5 Limiting case for Procedure C

4) Determine the damper command (D) using energy conservation to ensure that the net total static pressure drop along the outdoor air, recirculating air, and relief air paths is zero by substituting Equations (3.15) and (3.16) depending on different airflow-pressure control methods into Equations (3.2) to (3.4) and then applying the pressure loop summation equation (3.26a), (3.26b) and (3.26c) .

$$P_{RE} + \Delta P_{oa}(D) - \Delta P_{rec}(D) = 0 \qquad (3.27)$$

5) Determine the head of the SF and RF using Equations (3.6) and (3.7), and then the fan speed using Equations (3.10a and 3.10b).

3.4.4 Procedure D

In this procedure supply airflow and setpoints determine required damper command, SF and RF speeds. This procedure is used to simulate the BPP method. Figure 3.6 represents the block diagram of this procedure. The variables on the left side of the block Q_{oa}, Q_{sa}, P_{RM}, $P_{RE,}$ and P_{TB} are independent variables and on the right side SF speed, RF speed, RLD command (R) and damper command (D) are the dependent variables.
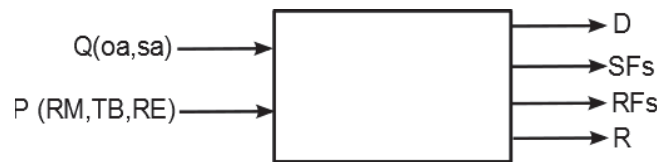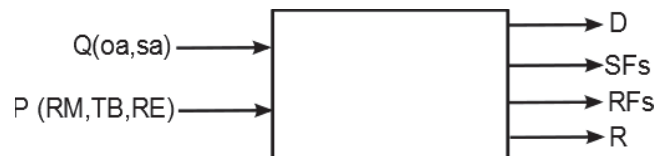

Figure 3.6 Dependent variables for Procedure D

In the application, the return fan speed is calculated by setpoint of the relief air plenum static pressure. Using the return fan head for the calculated return fan speed and the required building pressure the relief damper position is determined. If the calculated relief damper position is out of the range of normal operation then the building static pressure is calculated for the limiting conditions of the RLD. Figure 3.7 represents this limiting case in block diagram.

1) The relief air plenum static pressure is always controlled at its setpoint, P_{RE}, by the RF speed. The maximum and minimum relief air flow rates can be determined by the fully open (R=1) and fully closed (R=0) RLD derived from equation (3-2).

$$P_{RE} = [S_{rel} + S_{reld}(R = 1)] \cdot Q_{rel,max}^2 \qquad (3.28a)$$

$$P_{RE} = [S_{rel} + S_{reld}(R = 0)] \cdot Q_{rel,min}^2 \qquad (3.28b)$$

2) Determine the recirculating airflow (Q_{rec}) using the mass conservation at the node of a mixed air plenum (MA) with equation (3.22) for given OA airflow and SA airflow

3) Determine the space infiltration airflow (Q_{inf}) and exhaust airflow (Q_{ex}) based on the controlled space static pressure, P_{RM}, using Equations (3.1) and (3.8) and determine the return airflow (Q_{re}) and relief airflow (Q_{rel}) using the mass conservation at three nodes, including a relief air plenum (RE) and a room (RM), with equation (3.22) and (3.24).

4) If the calculated relief airflow is within the control range between $Q_{rel,min}$ and $Q_{rel,max}$ determined in step (1) the RLD command (R) can be determined by

$$P_{RE} = [S_{rel} + S_{reld}(R)] \cdot Q_{rel}^2 \qquad (3.29)$$

5) If the calculated relief airflow is out of the control range, the RLD is either the fully closed for less calculated relief airflow or the fully open for more calculated relief air flow. Under these conditions, the building static pressure cannot be maintained at its setpoint.

Figure 3.7 Limiting case for Procedure D

6) Determine the damper command (D) using energy conservation to ensure that the net total static pressure drop along the outdoor air, recirculating air, and relief air paths is zero using Equation (3.27) by substituting Equations (3.15) and (3.16) into Equations (3.2) to (3.4).

7) Determine the head of the SF using Equations (3.6) and then the fan speed using Equations (3.10a)

8) Determine the return airflow using equation (3.23) using the recirculation airflow, calculated in step (2)

9) If the calculated relief airflow is within the control range, the relief airflow and building static pressure can be controlled.

10) If the calculated relief airflow is out of the control range, the building pressure cannot be maintained. The space mass balance is applied to determine the space static pressure

$$Q_{ra} = Q_{sa} - Q_{ex}(P_{RM}) + Q_{inf}(P_{RM}) \qquad (3.30)$$

Where the return airflow is calculated in step (9), the supply airflow is given and the exhaust airflow and infiltration airflow are functions of the space static pressure, defined by equations (3.1) and (3.8)

11) Determine the head of the RF based on the relief plenum pressure and the space static pressure calculated in either step (9) or (10) using Equations (3.7) and then the fan speed using Equations (3.10b.)

3.4.5 Procedure E

For fixed OAD position following procedure is followed where setpoints given to determine SF and RF speeds. In this procedure building static pressure is maintained by RF therefore it covers only BPA method (and BPP method is not covered). Figure 3.8 represents the block diagram of this procedure. The variables on the left side of the block damper command (D), Q_{sa}, and $P_{RM,}$ are independent variables and on the right side SF speed, and RF speed are the dependent variables. For BPA method, P_{RE} is an additional independent variable which is used to determine the dependent variable, RLD command (R).
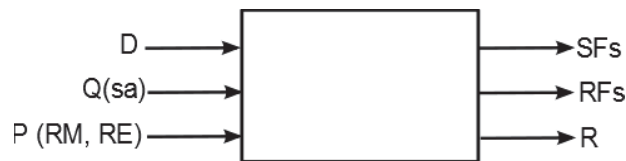
Figure 3.8 Dependent variables for Procedure E

1) Determine the space infiltration airflow (Q_{inf}) and exhaust airflow (Q_{ex}) based on the controlled space static pressure, P_{RM}, which is always controlled by the RF speed, using Equations (3.1) and (3.8).

2) Determine the return airflow (Q_{ra}), using the mass conservation at three nodes, including a relief air plenum (RE), a mixed air plenum (MA), and a room (RM), with equation (3.22).

3) The relief air plenum static pressure is controlled at P_{RE} for the BPA method and RLD command (R) is determined by substituting Equation (3.15) and (3.16) in Equation (3.2) for the given method.

4) For a given OAD position (D) to determine the OA flow rate using energy conservation to ensure that the net total static pressure drop along the outdoor air, recirculating air, and relief air paths is zero by substituting Equations (3.12) to (3.16) depending on different airflow-pressure control methods into Equations (3.2) to (3.4). For the control methods other than the two BPA (overlapping and sequenced) control methods,

$$\Delta P_{rel}(D, Q_{rel}) + \Delta P_{oa}(, Q_{oa}) - \Delta P_{rec}(D, Q_{rec}) = 0 \qquad (3.31)$$

For the two BPA methods,

$$P_{RE} + \Delta P_{oa}(D, Q_{oa}) - \Delta P_{rec}(D, Q_{rec}) = 0 \qquad (3.32)$$

Equations (3.31) can be solved with the mass conservation equation (3.23) and (3.24). In BPA method, Equation (3.32) can be solved with the mass conservation equation (3.23).

5) Determine the head of the SF and RF using Equations (3.6) and (3.7), and then the fan speed using Equations (3.10a and 3.10b).

Above procedures from section 3.4.1 to 3.4.5 are used for applications in chapter 4.

CHAPTER 4. RESULTS AND ANALYSIS

In earlier chapter, the nonlinear network method and the five procedures to achieve the objectives are discussed. In this chapter, a test case is developed. This test case is simulated with the code developed using the equations of nonlinear network model. This chapter describes the test case in detail. Later, the results of the simulation are discussed for each objective.

First, the results of outdoor air system gain and interactive disturbance inputs from outdoor air control are discussed to evaluate the control performance. Also the energy performance of the five damper control methods is evaluated by comparing the SF and RF head and power.

In the next section, results to select a building pressure control method from the two decoupled RLD control methods are discussed. The results are analyzed for the condition as the RLD reaches the fully open or fully closed position.

In the last section, the test case is simulated to develop and evaluate the performance of fixed damper position and return fan speed tracking method to control OA flow and building static pressure respectively.

4.1. AHU System Design

A single duct VAV AHU with economizer operation is designed using the equipment selection software of an AHU manufacturer (Trane, 2014). The design supply airflow rate is 18.8 m^3/s (40,000 CFM) and the design return airflow rate is 18.9 m^3/s (38,000 CFM). The design airflow rate difference between the supply air and return air is 0.9 m^3/s (2,000 CFM) for space pressurization at 12 Pa (0.05 inch of water) to balance with the

www.manaraa.com

design exhaust airflow rate of 0.7 m^3/s (1,500CFM) and the infiltration airflow rate of 0.2 m^3/s (500CFM).

The characteristic of each path is represented by the static pressure drop under a given airflow rate, which may not be the same as the design airflow rate of this path, and is listed in Table 4.1. The damper characteristic is for the fully open position. High-velocity dampers are selected to avoid stratification in the mixed air chamber. Terminal boxes always remain at a constant static pressure drop, which is equal to the supply air duct static pressure set point regardless of its airflow rate, under perfect control conditions.

Table 4.1 Characteristics of an AHU network

Path	Component	Static Pressure drop	Airflow
		Pa (inch.w)	m^3/s (CFM)
Infiltration	Envelope	12 (0.05)	0.2 (500)
Exhaust air	Duct	124 (0.5)	0.7 (1,500)
Supply air	Distribution	946 (3.8)	18.8 (40,000)
	Terminal box	374 (1.5)	-
Return air	Duct	473 (1.9)	17.9 (38,000)
Relief air	Duct	50 (0.2)	17.9 (38,000)
	Damper	71 (0.287)	17.9 (38,000)
Outdoor air	Duct	50 (0.20)	18.8 (40,000)
	Damper	79 (0.318)	18.8 (40,000)
Recirculating air	Duct	90 (0.363)	18.8 (38,000)
	Damper	71 (0.287)	18.8 (38,000)

The resistance factor for a partially open damper depends on the damper type and is calculated based on the inherent damper characteristic curves in Figure 4.1 provided by ASHRAE (2010c). Since high-velocity dampers are selected, the damper authority is relatively high for all three dampers and parallel blade dampers are chosen for all three dampers (ASHRAE, 2010c; Lizardos and Elovitz, 2000) in the simulation. Figure 4.1

also demonstrates that the flow change is quicker or the damper has faster flow response at a more open damper position than at a more closed damper position for the same damper position change.
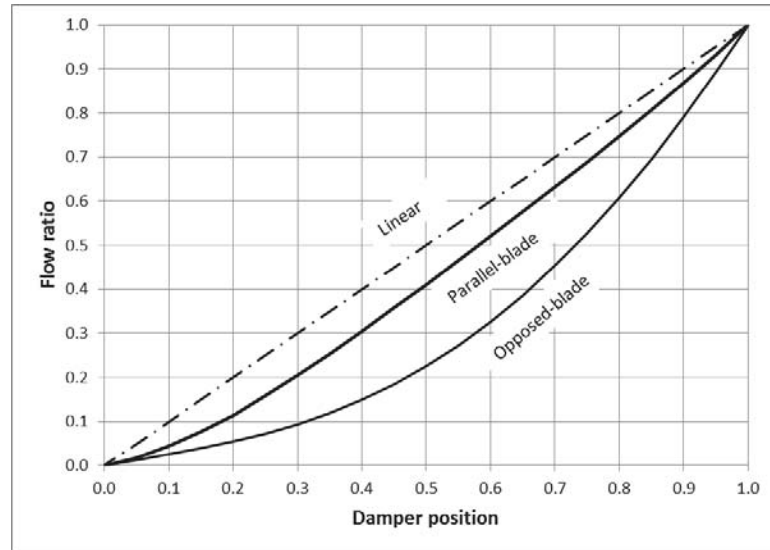
Figure 4.1 Inherent damper characteristic curves

Three fans, i.e., an SF, an RF, and an EF, are installed in the AHU and the building. The SF and RF have a VFD while the EF always operates at design speed. The fan head and power curves of the SF and RF under the design speed were provided by the same equipment selection software (Trane, 2014) and are shown in Figure 4.2. The EF is selected separately and the fan head curve for the EF is shown in Table 4.2 (Greenheck, 2011).
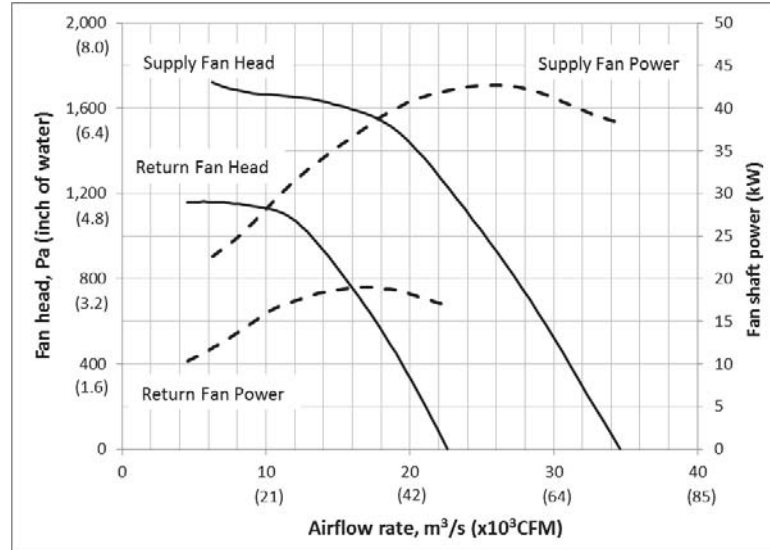
Figure 4.2 SF and RF head and power curves

Table 4.2 EF head data

Airflow rate		Fan head	
m³/s	CFM	PA	Inch of water
0.523	1108	163	0.652
0.629	1334	139	0.559
0.699	1482	116	0.466
0.755	1599	93	0.373
0.802	1699	70	0.280
0.842	1785	46	0.186
0.862	1826	35	0.140
0.882	1868	23	0.093
0.902	1911	12	0.047
0.922	1954	0	0.000

4.2. Selection of Airflow-Pressure Control Method

To achieve the first objective the energy performance of supply and return fan is evaluated. In addition to the energy performance evaluation of the SF and RF power, the outdoor air system gain and interactive disturbance inputs to/from outdoor air control are applied to evaluate the control performance.

The five airflow-pressure control methods discussed in chapter 2 are simulated for energy performance and control performance using the non-linear network model explained in chapter 3 and the results are discussed in following sections.

4.2.1 System Energy Performance

The simulation is performed with two supply airflow rates, the design airflow and 75% of the design airflow and outdoor airflow rate varying from the minimum (0.9 m^3/s or 2,000 CFM) to 100% under five different airflow-pressure control methods in order to identify impacts of supply airflow and outdoor airflow rates.

1) The duct static pressure was controlled at 374 Pa (1.5 inch of water);

2) The space static pressure was controlled at 12 Pa (0.05 inch of water).

3) The relief air plenum static pressure was controlled at a setpoint for two decoupled RLD control methods. Since high-velocity dampers were selected, the static pressure drop through the relief air path with the fully open damper was 121 Pa (0.487 inch of water) at the design supply airflow. Therefore, the set point was chosen at 120 Pa (0.5 inch of water) at the design airflow, which is higher than the value recommended by ASHRAE (2010c), and is linearly reset with the supply airflow ratio squared at partial supply airflow in order to reduce the relief air path static pressure drop for better RF energy performance.

Figure 4.3 shows the calculated damper command versus the outdoor airflow ratio varying from 5% to 100% using five different airflow-pressure control methods at two different supply airflows: 1) 18.8m^3/s (or 40,000 CFM), marked by (40), and 2) 14.1 m^3/s (30,000 CFM), marked by (30). The simulated damper command curves reveal that a

significant impact of the airflow-pressure control method on the system OA flow characteristic curve. While the traditional method (square) has the most linear outdoor airflow ratio versus the damper command curve, the overlapping method with OAD fully open (triangle) also has the more linear outdoor airflow ratio versus the damper command curve. However, the sequenced control with the OAD fully open (circle) and the DECOUPLED RLD-sequenced control (diamond) have the least linear curves with fast outdoor airflow ratio change under low and high damper command and slow outdoor airflow ratio change under medium damper command. The traditional and two overlapping methods control the outdoor airflow by at least two reverse-action dampers according to Equations (11), (12) and (14). As a result, the fast flow response of one damper at a more open position always goes along the slow flow response of another damper at a more closed position and consequently the outdoor airflow is approximately linear with the damper command. On the other hand, the two sequenced methods control the outdoor flow by only a single damper with other dampers at fixed positions according to Equations (13) and (15). Without compensation between two reverse-action dampers, the outdoor flow is determined by the flow response of the active damper. As a result, fast outdoor airflow change exists at the low and high damper command and slow outdoor airflow change exists at the medium damper command. Figure 4.3 also demonstrates that all outdoor airflow ratios versus damper command curves are consistent with the airflow-pressure control method regardless of the supply airflow. As a result, the outdoor airflow ratio has an inherent characteristic curve with the damper command for each airflow-pressure control method. In other words, the outdoor airflow

ratio can be determined by the damper command with a calibrated outdoor airflow vs command curve.
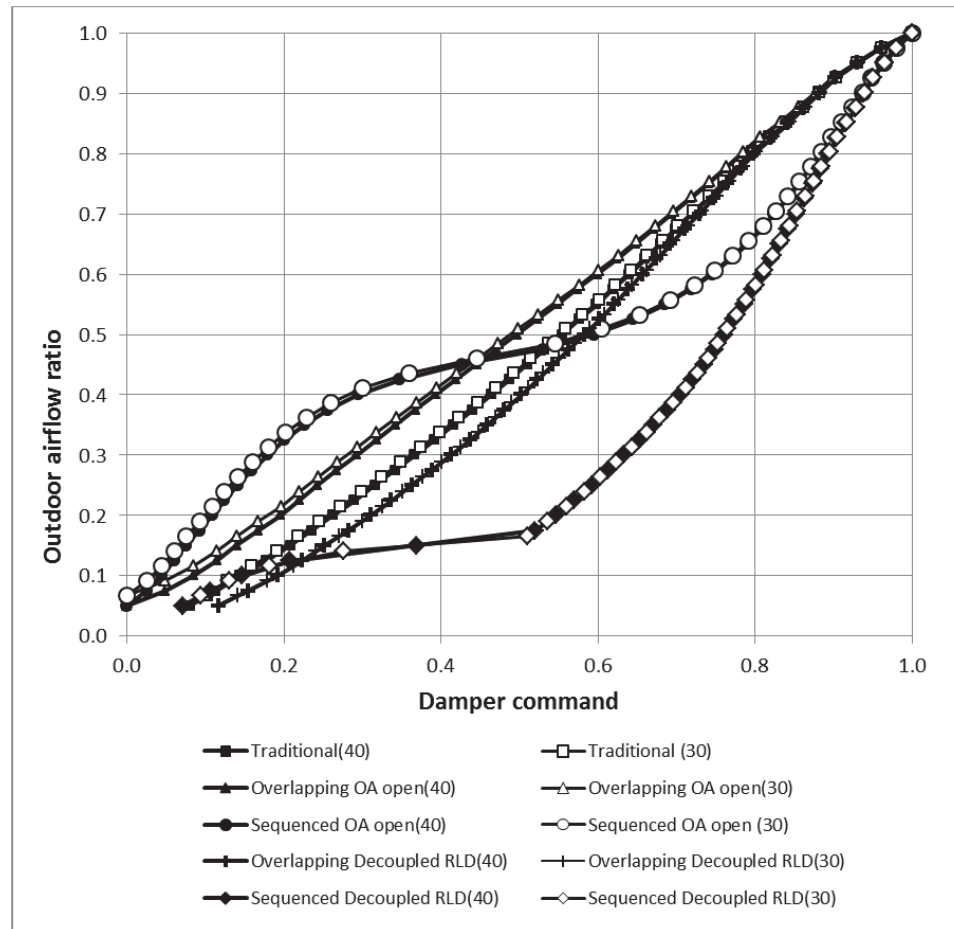
Figure 4.3 Outdoor airflow ratio versus desired damper command

Figure 4.4 shows the relative SF head based on its design SF head versus the outdoor airflow ratio at two different supply airflows. The airflow-pressure control methods with the OAD fully open have the best SF energy performance, presented by the same overlapped curves (triangle and circle), since the fully open OAD causes the least impact on the SF head. On the other hand, the traditional control (square) requires the highest SF head.
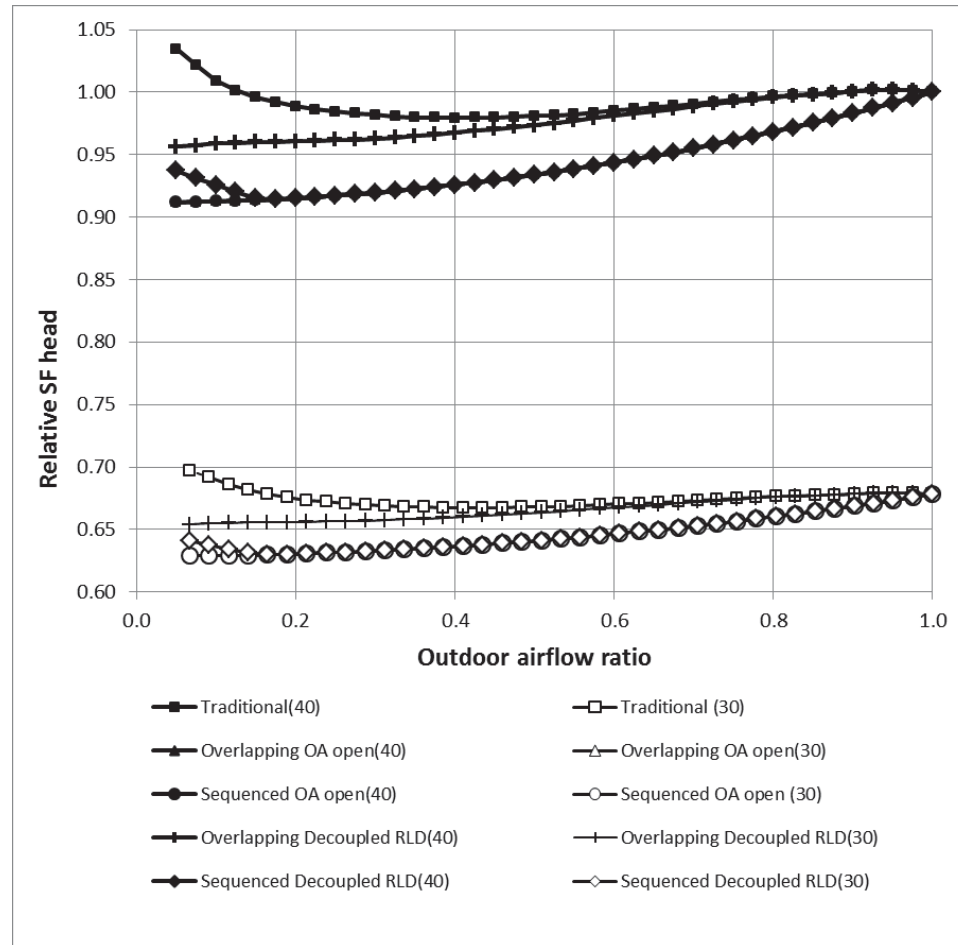
Figure 4.4 SF head versus outdoor airflow ratio

Figure 4.3 shows the relative RF head based on the design RF head versus the outdoor airflow ratio. The sequenced method with the OAD fully open (circle) has better RF energy performance than the overlapping method with the OAD fully open (triangle), and has the best RF energy performance in almost all outdoor airflow ratio ranges. Under a low outdoor airflow ratio, both the OAD and RCD are fully open and the RLD has to be closed more in order to force return air into the recirculating air path, which consequently causes an increased RF head. However, the SF head reduction will compensate for any RF head increase. Since the relief air plenum, static pressure is controlled for two decoupled RLD controls; the RF head (cross and diamond) remains the same regardless

of outdoor airflow ratio and has the worse RF energy performance. Figures 4.4 and 4.5 also show that the VFD can significantly improve the fan energy performance under partial supply airflow conditions.
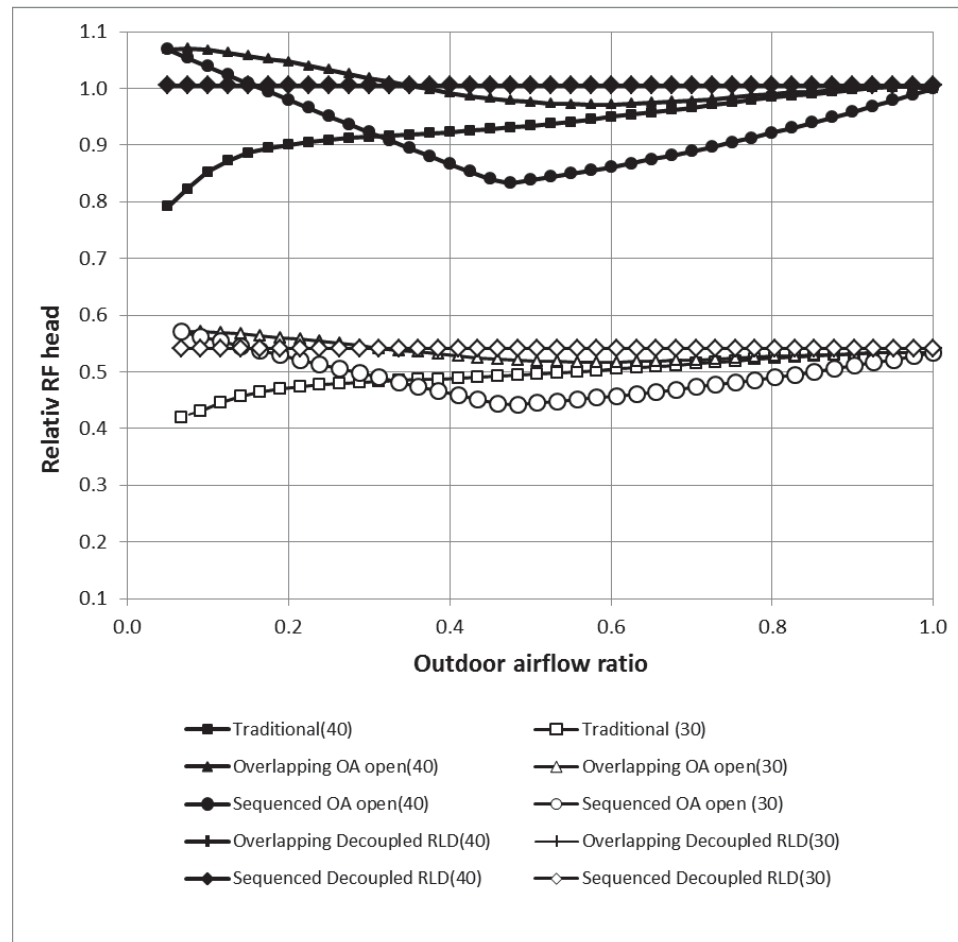
Figure 4.5 RF head versus outdoor airflow ratio

Figure 4.6 compares the relative total fan power based on the total design SF and RF power among different airflow-pressure control methods. It is evident that the overlapping method with the OAD fully open (circle) has better energy performance with a maximum 8% power reduction and an average 4% power reduction over the traditional method. On the other hand, more significant fan energy reduction, approximately 50%, is achieved by the VFD under partial supply airflow conditions.
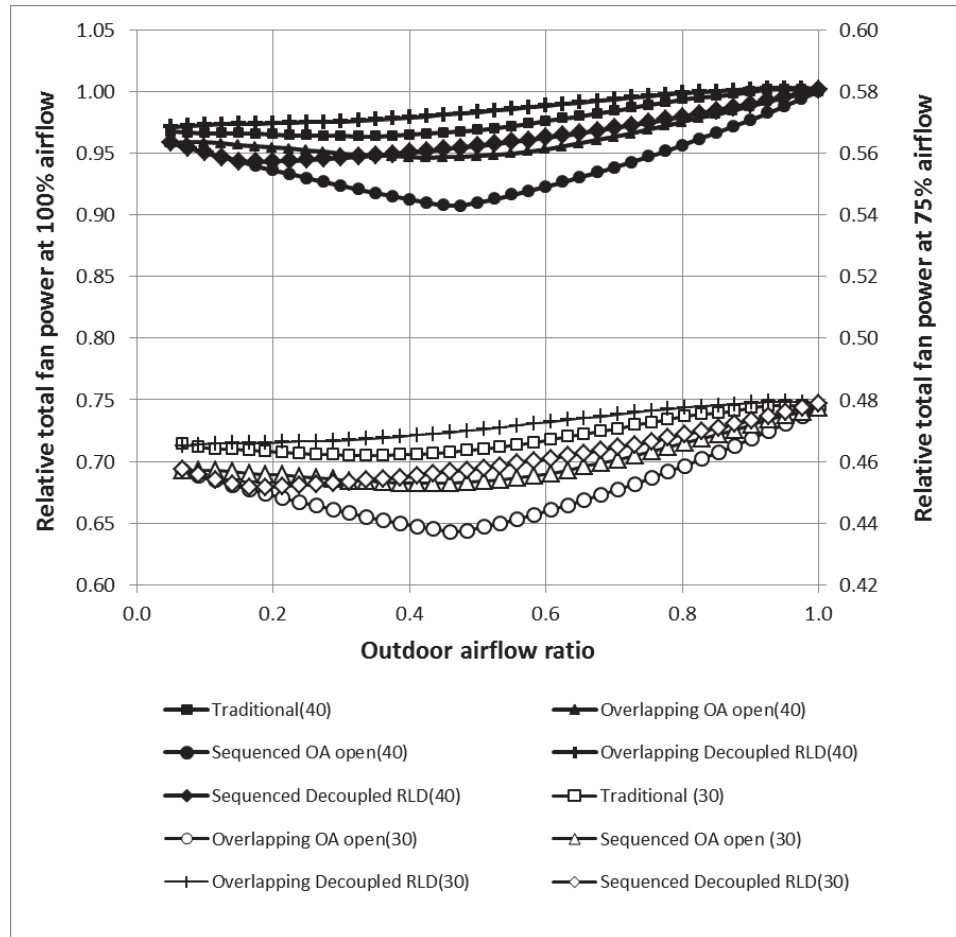
Figure 4.6 Total fan power versus outdoor airflow ratio

4.2.2 Nonlinearity in OA Control

A solution for the control performance evaluation is developed to determine the behavior of the controlled variables, including outdoor airflow, building static pressure, and duct static pressure, in response to its corresponding control input variations and other disturbances/noises.

The control performance evaluation is an essential part of this simulation as the network has a non-linear response. The non-linearity of the network is not only due to the damper and fan characteristics but the connected air paths in the network. The SF, the RF, and the three air dampers in an AHU, as well as the air distribution ducts and conditioned spaces,

form a network with air paths and nodes rather than simple integration of ideal duct-damper paths. In addition to nonlinear damper curves, the nodal differential static pressure has a nonlinear relationship with airflow for each path. Within a nonlinear network, the system gain, the derivative of a controlled variable to its corresponding control input, varies under different operating conditions. As a result, pre-tuned controller gains that work well at a full-load condition may not work for a partial load condition and vice versa. Based on control theory, an increased system gain tends to make the system unstable while a reduced system gain tends to have a slow transient response and an enlarged steady state error (Burns, 2001; Nise, 2011).

Moreover, any speed change of the SF and RF or any position change of the three air dampers affects the airflow rate through all paths and the static pressure at all nodes within the network. A damper command not only is a control input on the outdoor airflow but also creates disturbance inputs on both the building static pressure and supply air duct static pressure. On the other hand, the SF or RF speed is not only a control input for static pressure control but also creates a disturbance input on the outdoor airflow.

Since each control loop in PID controllers acts independently, a control action is represented by a change in one of these control inputs, which initiates changes in all controlled variables within the nonlinear network.

In a nonlinear system, a controlled variable actually responds nonlinearly to its control input. In other words, a system gain, the ratio of a controlled variable change to its control input change, varies with operating conditions, which is represented by supply airflow and outdoor airflow in an AHU system. In order to evaluate the outdoor air control performance, the outdoor air system gain is defined as the derivative of the

outdoor airflow ratio to the damper command, shown in Equation (3.26). The outdoor airflow ratio is the ratio of the outdoor airflow rate to the supply airflow rate. In an ideal control system, a constant system gain is preferred. In an actual outdoor air control within an AHU system, a smaller variation in outdoor air system gain presents better control performance.

$$K_{OA} = \frac{d(Q_{oa})/Q_{sa}}{dD}\bigg|_{Q_{oa},Q_{sa}} \qquad (4.1)$$

Within a network, a control input determines its controlled variable in the same control loop but also serves as a disturbance input for other controlled variables in other control loops. A damper command creates disturbance inputs on both the building static pressure and supply air duct static pressure, while the SF or RF speed creates a disturbance input on the outdoor airflow. Therefore, four interactive disturbance factors are defined and used to evaluate these interactive disturbance inputs. A disturbance on the duct static pressure causes supply airflow variations, which directly influence the space thermal conditions. Therefore, the disturbance input on the supply airflow is studied to substitute the disturbance input on the duct static pressure. For an ideal control system, no interactive disturbance factors are preferred. For an actual outdoor air control in an AHU network, a fewer number of interactive disturbance factors presents better control performance.

- The disturbance factor on the supply airflow by the damper command is defined as the derivative of the supply airflow to the damper command normalized by the initial supply airflow.

$$K_{sa-D} = \frac{d(Q_{sa})/Q_{sa}}{dD}\bigg|_{Q_{oa},Q_{sa}} \qquad (4.2)$$

- The disturbance factor on the space static pressure by the damper command is defined as the derivative of the space static pressure to the damper command normalized by the initial space static pressure.

$$K_{RM-D} = \left. \frac{d(P_{RM})/P_{RM}}{dD} \right|_{Q_{oa},Q_{sa}} \tag{4.3}$$

- The disturbance factor on the outdoor airflow by the SF speed is defined as the derivative of the outdoor airflow ratio to the SF speed.

$$K_{oa-SF} = \left. \frac{d(Q_{oa})/Q_{sa}}{d\omega_{SF}} \right|_{Q_{oa},Q_{sa}} \tag{4.4}$$

- The disturbance factor on the outdoor airflow by the RF speed is defined as the derivative of the outdoor airflow ratio to the RF speed.

$$K_{oa-RF} = \left. \frac{d(Q_{oa})/Q_{sa}}{d\omega_{RF}} \right|_{Q_{oa},Q_{sa}} \tag{4.5}$$

The control performance is evaluated at the determined system operating conditions in the energy performance evaluation, including the three damper positions and two fan speeds, as defined in Figures 4.3 to 4.5. A ±1% change is added to one of the control inputs, including the damper command, SF speed, and RF speed. The outdoor airflow rate, supply airflow rate, and building static pressure are then calculated using the nonlinear network solution discussed previously. Finally, the outdoor air control system gain and four interactive disturbance factors are calculated. It should be noted that the system gain is different from the curve slope in Figure 4.3, which is calculated with an assumption that the supply airflow rate and outdoor airflow are perfectly controlled.

Figure 4.7 compares the system gains of the outdoor airflow ratio controlled by the damper command versus the outdoor airflow ratio. The outdoor air control system gain varies with the outdoor airflow ratio almost regardless of the supply airflow rate and a

variation profile is unique to each airflow-pressure control method. The traditional method (square) and the overlapping method with the OAD fully open (triangle) have the least system gain variation over the outdoor airflow ratio range from 5% to 100%. The decoupled RLD sequenced method (diamond) has the most significant system gain variation, followed by the sequenced method with the OAD control (circle). As a result, these two sequenced methods have the worst control performance. For example, if the controller is tuned based on a system gain of 0.25 with an outdoor airflow ratio of 0.45, the system gain will increase to 2 if the outdoor airflow ratio increases to 0.9. The system will then tend to be unstable with a sudden increase in system gain by a factor of 8 by using the sequenced control with OAD fully open.
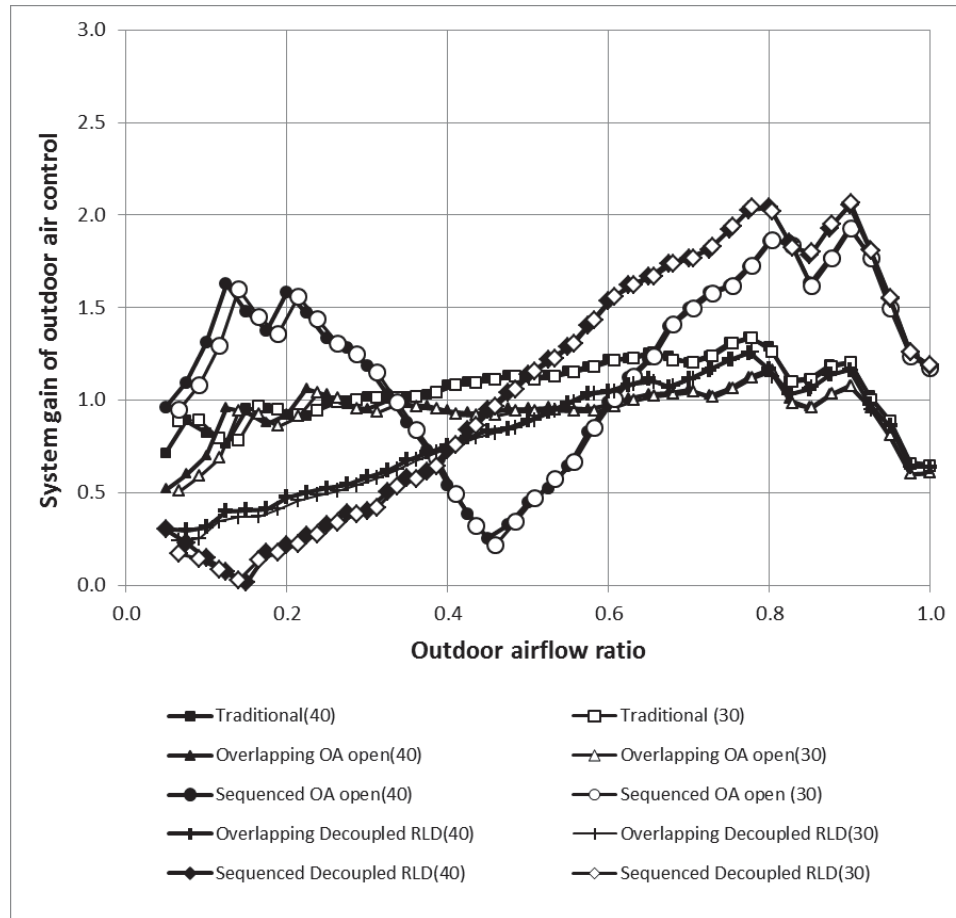
Figure 4.7 System gain of outdoor air control versus outdoor airflow ratio

Figure 4.8 shows the disturbance factor on the space static pressure by the damper command. Figure 4.9 shows the disturbance factor on the supply airflow rate by the damper command. Two decoupled RLD control methods (diamond and cross) and the sequenced method with the OAD fully open (circle) create the most significant disturbance on the building static pressure control loop. Two sequenced controls (diamond and circle) create the most significant disturbance on the supply airflow.
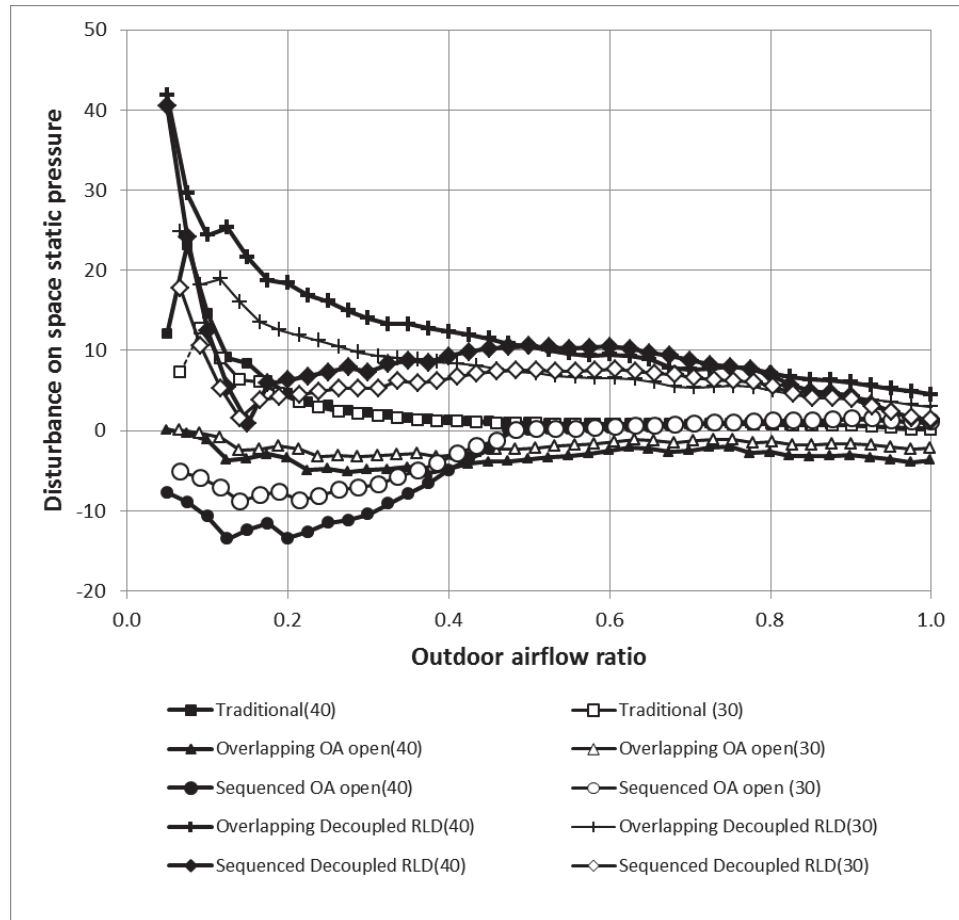
Figure 4.8 Disturbance on the space static pressure by the damper command
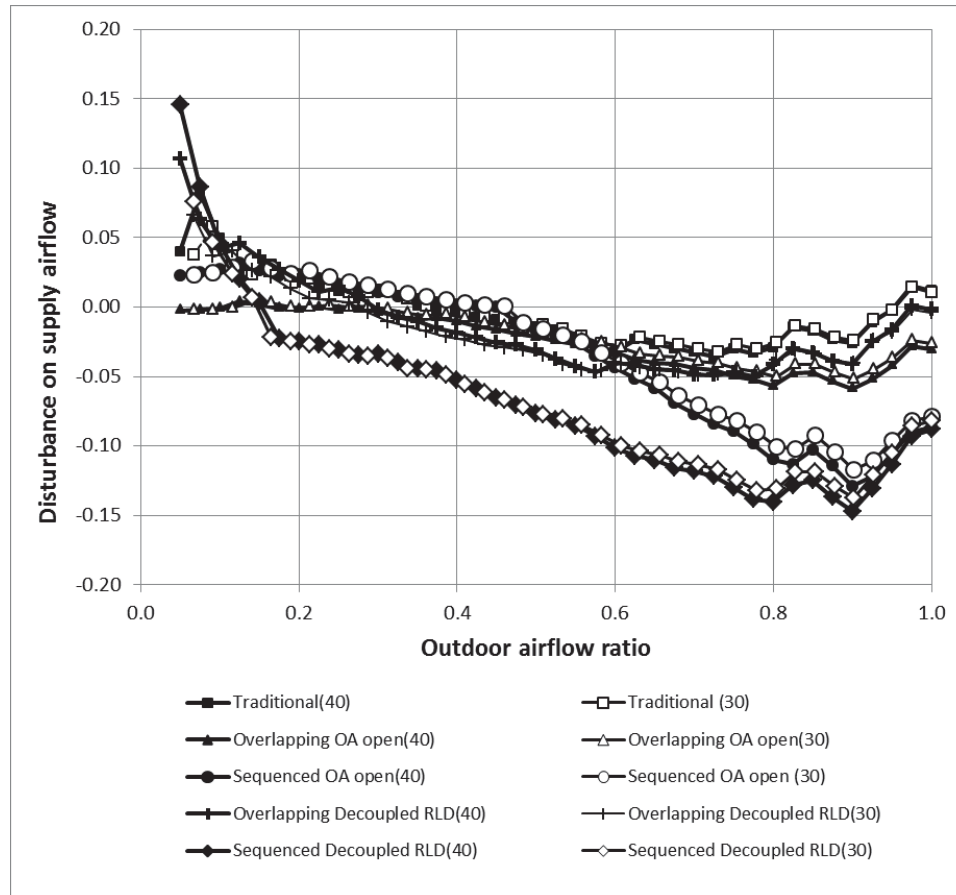
Figure 4.9 Disturbance on the supply airflow by the damper command

Figure 4.10 shows the disturbance factor on the outdoor air control by the SF speed, and

Figure 4.11 shows the disturbance factor on the outdoor air control by the RF speed. The

traditional method (square) has the least disturbance on the outdoor air control by the SF

and RF speed controls, especially under the minimum outdoor airflow range. Two

sequenced control methods (diamond and circle) have the most significant disturbance on

the outdoor air control when the fan speeds are modulated. The outdoor airflow ratio

varies by 10% of the SF speed change by using the traditional method (square), and by

35% to 55% of the SF speed change by using two sequenced control methods (diamond

and circle) at the minimum outdoor airflow range. The outdoor airflow ratio varies by

10% of the RF speed change by using the traditional method (square), and by 32% to

55% of the RF speed change by using two sequenced control methods (diamond and circle).
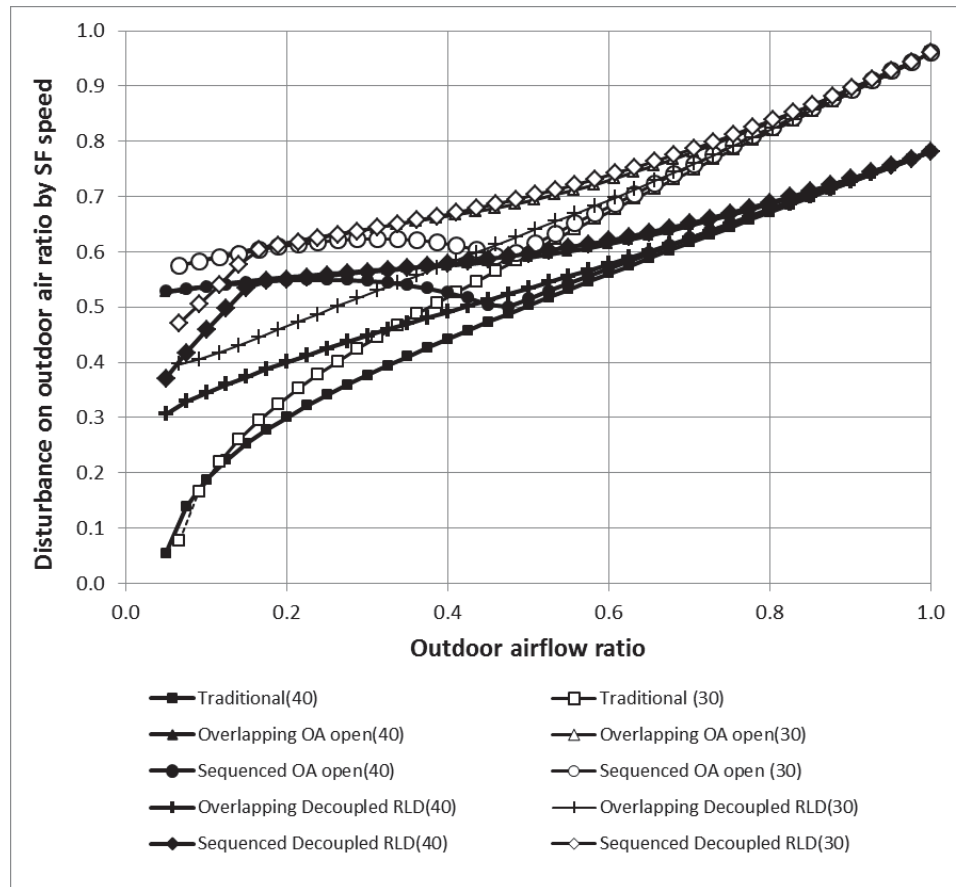
Figure 4.10 Disturbance on the outdoor airflow ratio by the SF speed
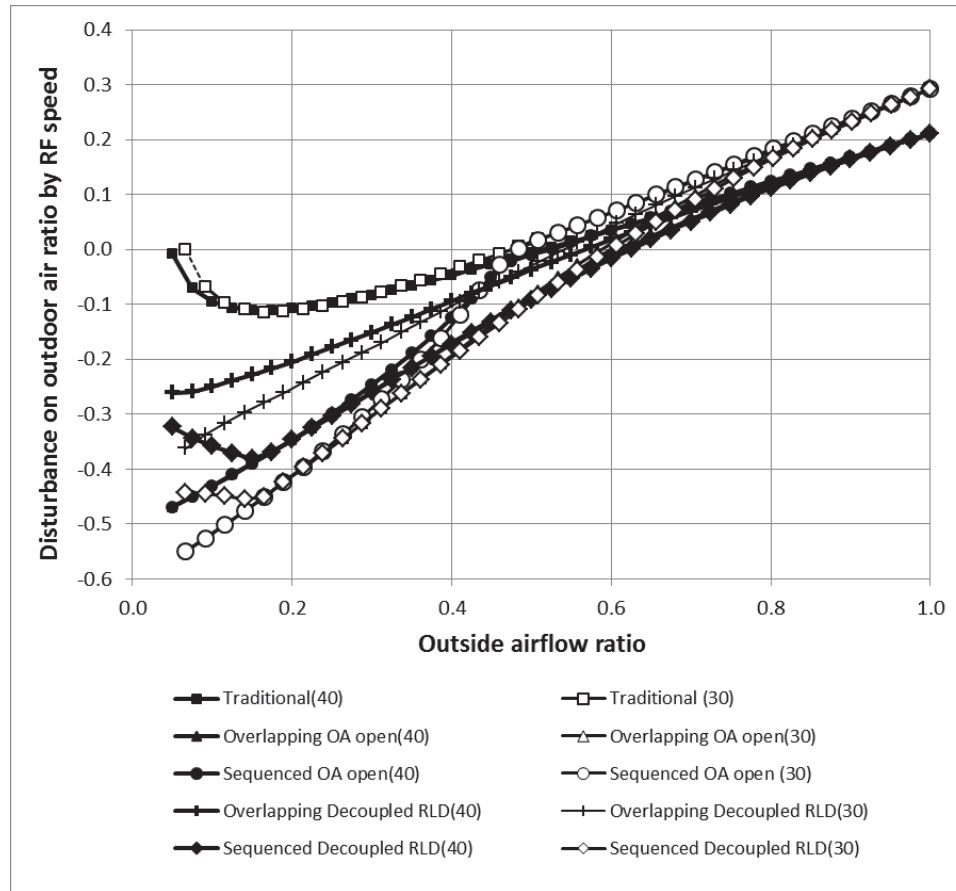
Figure 4.11 Disturbance on the outdoor airflow ratio by the RF speed

Table 4.3 summarizes the simulated energy and control performance of five different airflow-pressure control methods. The relative fan head and total fan power are averaged over the outdoor airflow ratio range, from the minimum outdoor airflow to 100%. The outdoor air control system gain ratio is defined as the ratio of the maximum system gain to the minimum system gain over the outdoor airflow ratio range. The disturbance factors on the space static pressure and supply airflow by the damper command, and the disturbance factors on the outdoor airflow ratio by the SF speed and RF speed are also averaged over the outdoor airflow ratio range.

Table 4.3 Summary of energy and control performance with the five methods

	Design Supply Airflow					75% of Design Supply Airflow				
Control	1	2	3	4	5	1	2	3	4	5
Relative SF head	0.99	0.94	0.94	0.97	0.94	0.68	0.65	0.65	0.66	0.65
Relative RF head	0.94	0.98	0.94	1.03	1.03	0.51	0.56	0.51	0.64	0.64
Relative total fan power	0.977	0.962	0.940	0.986	0.963	0.468	0.460	0.451	0.472	0.461
Power reduction (%)	0%	2%	4%	-1%	1%	0%	2%	4%	-1%	1%
K_{OA} ratio	2.1	2.3	7.6	4.2	137.9	2.1	2.3	8.9	14.8	19.5
K_{RM-D}	2.9	-3.3	-3.6	12.5	8.7	2.1	-1.9	-2.1	10.7	15.0
K_{sa-D}	0.00	0.02	0.04	0.01	-0.07	0.00	0.02	0.03	0.06	0.14
K_{oa-SF}	0.50	0.62	0.60	0.55	0.61	0.60	0.73	0.71	0.71	0.75
K_{oa-RF}	0.02	0.09	0.07	0.03	-0.09	0.05	0.08	0.06	0.07	0.10

In summary, the sequenced method with the OAD fully open has the best energy performance with 4% power reduction, but has poor control performance with averaged system gain ratios from 7.6 to 8.9. The DECOUPLED RLD-sequenced method has the worst control performance with averaged system gain ratios from 19.5 to 137.9. On the other hand, the traditional method has the best control performance with averaged system gain ratios of 2.1 and lowest disturbance factors. It is obvious that the traditional method has the best control performance, while the two sequenced control methods have the worst control performance even though they have the best energy performance. Nevertheless, the primary purpose of dampers in an AHU is to control airflow and static pressure, and the control performance seems more important than the energy performance. For control purposes, it is recommended that the traditional airflow-pressure control method with all three dampers completely interlinked be selected for the studied AHU.

4.3. Controllability of Building Pressure Control Method

To compare the controllability of fan and relief air damper on building pressure the same hypothetical AHU system discussed in section 4.1 considered. Same design conditions are used for design space cooling load, minimum outdoor airflow rate, and supply and return air duct static pressure drop. In order to evaluate the performance of the Building Pressure Passive (BPP) Control and Building Pressure Active (BPA) Control at the potential RLD fully closed and fully open positions, the system performance on this AHU is simulated at both low and high outdoor air ratio.

The resistance factor for a partially open damper depends on the damper type and is given based on the inherent damper characteristic curves. Since high-velocity dampers are selected, the damper authority is relatively high for all three dampers and parallel blade dampers are chosen for all three dampers (ASHRAE, 2010c; Lizardos and Elovitz, 2000) in the simulation. Figure 4.12 shows the inherent damper characteristic curves of parallel blade dampers, provided by ASHRAE (2010c), as well as installed damper curves for the OAD, RCD, and RLD based on their authorities. It can be seen that the installed damper curves have approximately linear relationship for all three dampers.
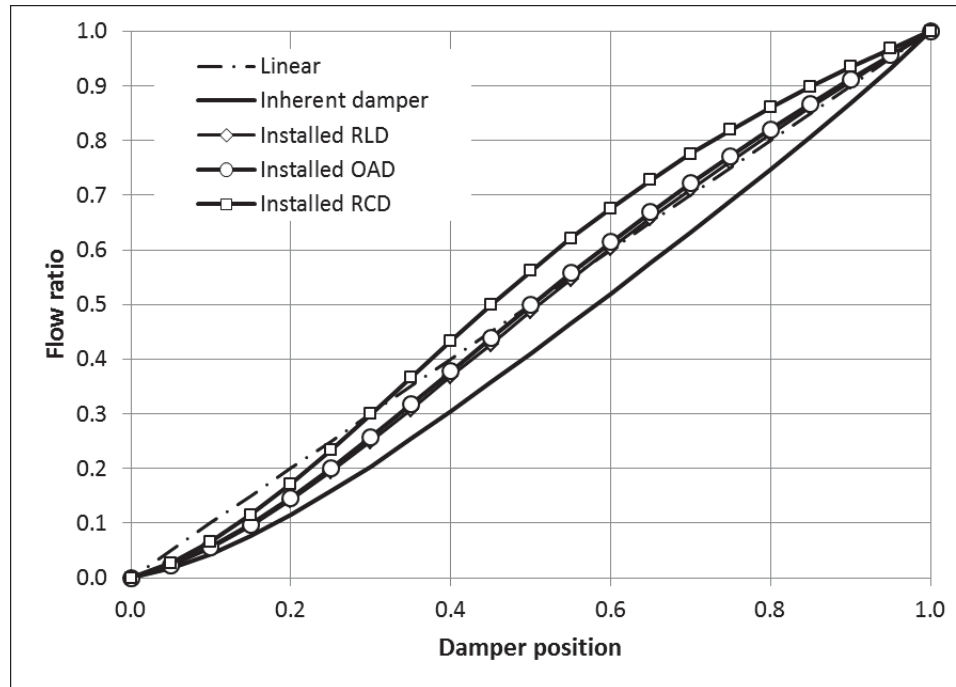
Figure 4.12 Inherent and installed damper characteristic curves

4.3.1 Required OAD Command for Minimum OA

In the traditional control, three control inputs, including the OAD command (D), the SF speed and the RF speed are determined based on three controlled variable setpoints. The duct static pressure setpoint is 374 Pa (1.5 inch of water), the space static pressure setpoint is 12 Pa (0.05 inch of water) and the outdoor airflow rate setpiont is 1.88 m^3/s (4,000CFM) when the supply airflow rate varies from 7.5 m^3/s (16,000 CFM) to 18.8 m^3/s (40,000CFM).

For the BPP and BPA controls, the relief air plenum static pressure control is added in order to determine the fourth control input, the RLD command (R). The relief air plenum static pressure setpoint is 25 Pa (0.1 inch of water).

Since the minimum outdoor airflow rate remains constant for IAQ control while the supply airflow rate varies with space cooling load, the outdoor airflow ratio and damper command should increase as the supply airflow rate decreases. Figure 4.13 demonstrates

that the required minimum OAD commands with square markers for the traditional control and diamond markers for two decoupled RLD controls increase as the supply airflow ratio, the ratio of the supply airflow rate to the design supply airflow rate (18.8 m^3/s or 40,000 CFM), decreases from 1 to 0.4 in order to maintain constant outdoor airflow rate. The two decoupled RLD controls have the same OAD command (D) curve since the dampers are within their control range between the fully open and the fully closed positions.
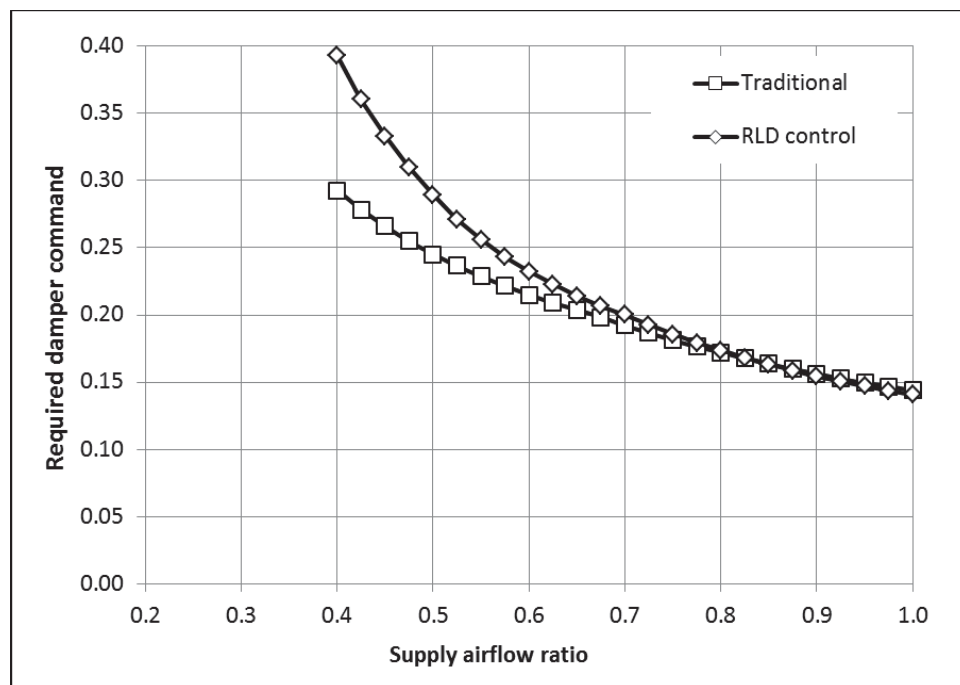
Figure 4.13 Required damper command for constant minimum outdoor airflow rate

Due to the lack of reliable airflow sensors, it is a common practice to use a fixed minimum OA damper position for minimum OA flow control in AHUs (Apte, 2006). The fixed minimum OAD position, which is calibrated at the design supply airflow, will cause the actual OAD position less than required as the supply airflow decreases. In addition to the fixed OAD position control, malfunctioning OA flow sensors also can cause the OAD below the required OAD position. In such conditions, the actual OA flow

rate is less than needed and the IAQ is severely affected. Moreover, less than needed outdoor air intake may also potentially lead to the reverse relief airflow and the negative building static pressure. To understand the impacts, it is worth investigating the system performance when the OAD commands are less than the required minimum OAD commands as defined in Figure 4.13.

4.3.2 OAD Command Less than the Required

In this section, the required OAD command is first determined to maintain a minimum outdoor airflow rate at given supply airflow rates. Then, the OAD is forced to reduce below the required position to 40% of the required position in order to make the OAD gradually approach to the closed position and that result in lower outdoor airflow ratio than needed.

The system performance is simulated with the OAD command varying from 40% to 100% of the required minimum OAD command. In practice, the system only operates at the design condition for a short period in a year, therefore, the supply airflow rate is kept at lower value than the design airflow rate and the simulation is conducted when the supply airflow ratio is 80% i.e., in this case, the supply airflow rate of 15.0 m^3/s (32,000 CFM). The required OAD command for the traditional control is 0.172 and that for the BPP and BPA controls is 0.173. In earlier simulation case, the required OAD commands were calculated to keep constant OA flow rate. In this section, the system performance, including the outdoor airflow, is evaluated when the OAD is kept at a position lower than the required OAD positions.

In the traditional (interlinked dampers) control, precise control over the duct static pressure and building static pressure is achieved and respective setpoints are met as these controlled variables are controlled by active components i.e. the SF and RF.

The building static pressure in BPA control and the relief plenum pressure in BPP control always meet their setpoint along with the duct static pressure through active controls by modulating fan speeds. However, the building static pressure in the BPP control and the relief air plenum static pressure in the BPA control are controlled by the decoupled RLD, and may not always meet the setpoint if the RLD reaches limits of its operation i.e. either the fully open or the fully closed position. In this case, the limit of the RLD position (either the fully open or the fully closed position), acts as a constraint forcing the building static pressure to deviate from the setpoint in the BPP control and the relief air plenum static pressure in the BPA control.

Figure 4.14 demonstrates the simulated outdoor airflow rate ratio (a), which is defined as the ratio of the outdoor airflow rate to the actual supply airflow rate (15.0 m^3/s or 32,000 CFM), RLD position (b), building static pressure (c) and relief air plenum static pressure (d) versus the relative OAD command, which is normalized by the required OAD command shown in Figure 4.13. Based on the actual supply airflow rate, the required outdoor air ratio is 0.125 for IAQ control. As shown in Figure 4.14(a), outdoor airflow is less than the required for three controls due to the OAD position is less than the required. It is obvious that the IAQ will not be guaranteed in this case.

By the traditional control with square markers, the outdoor airflow decreases (shown in Figure 4.14(a)) and the RLD is closed (shown in Figure 4.14(b)) continuously as the OAD is closed. Since the building static pressure is always maintained at its setpoint by

the RF speed, shown in Figure 4.14(c), the relief airflow decreases as the outdoor airflow decreases and finally flows in a reverse direction to make up the insufficient outdoor airflow when the outdoor airflow is below the summation of the building infiltration and exhaust airflow. As a result, the relief air plenum static pressure gradually decreases to a negative value as the OAD is closed below 60% of the required OAD position, shown in Figure 4.14(d). Therefore, negative pressure and reverse relief airflow are the problems associated with the tradition control when the OAD is operated below the required damper position.

The system performance is presented with diamond markers for the BPP control and with circle markers for the BPA control. The RLD in the decoupled RLD controls is impacted by the relief air plenum static pressure, directly in the BPP control and indirectly in the BPA. From Figure 4.14(b) it can be observed that the RLD approaches closing position much faster as compared to the OAD command when the RLD is decoupled from the control, and as a result, the RLD is fully closed when the OAD command is below 60% of the required command. From Figure 4.14(c) and 4.14(d) it can be observed that both the relief air plenum and building static pressure are well controlled at their setpoints before the RLD is fully closed or when OAD command is above 60% of the required command. Since the BPP and BPA controls share the same governing equations along with the same controlled variable setpoints, the system performance, including the RLD position as shown in Figure 4.14(b), is the same before the RLD is fully closed. However, the system performance tends different after the OAD damper drops below 60% of the required positon and the RLD is fully closed. The building static pressure loses control and eventually becomes negative in the BPP control, shown in Figure 4.14(c), while the

relief air plenum static pressure loses control and eventually becomes negative in the BPA control, shown in Figure 4.14(d).
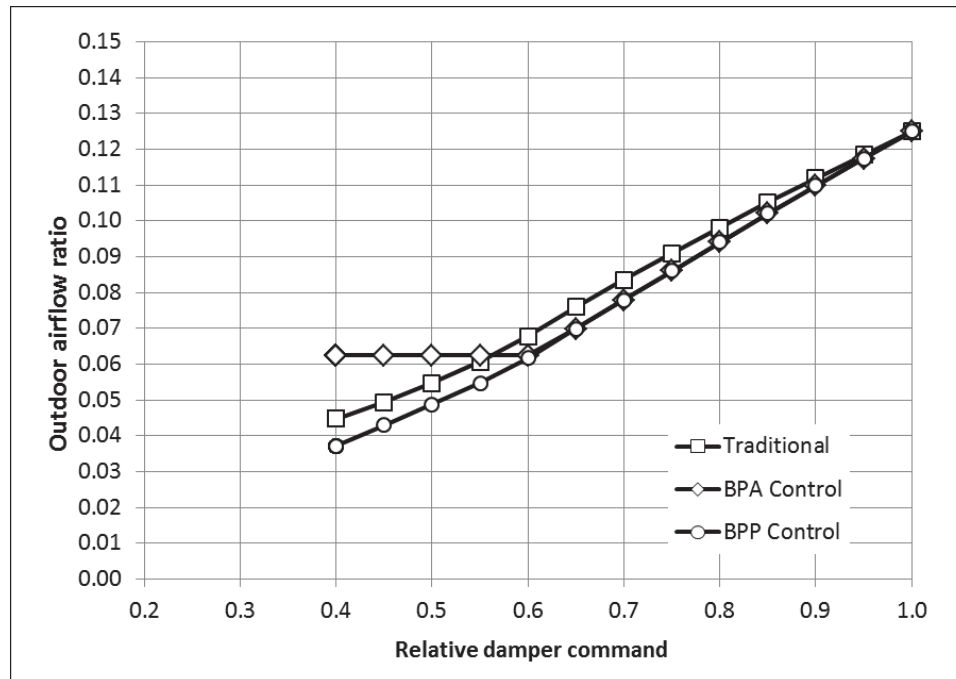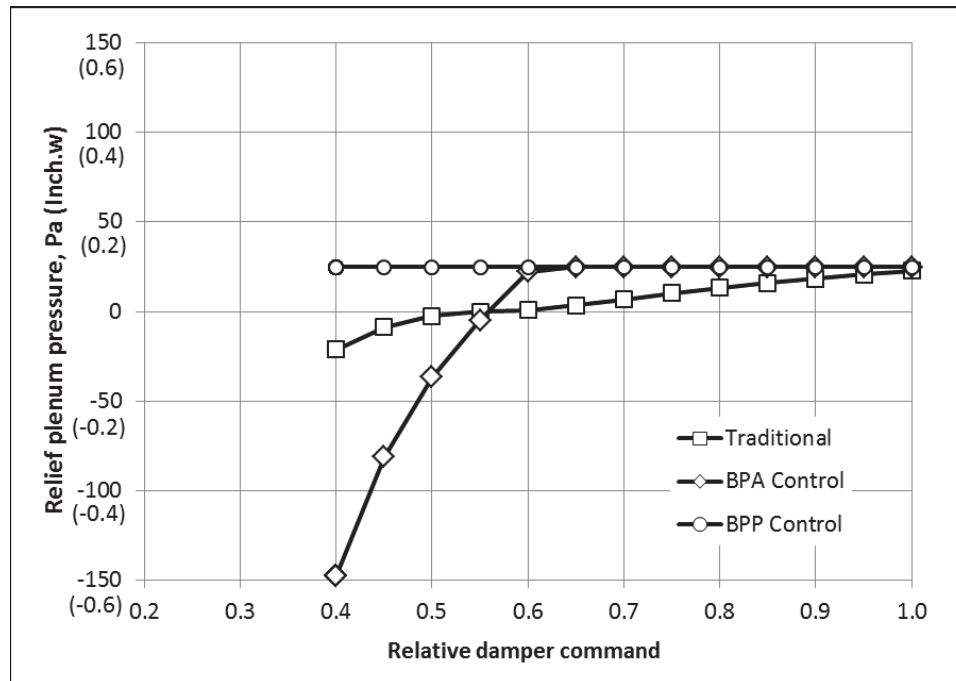

(a) Outdoor airflow rate
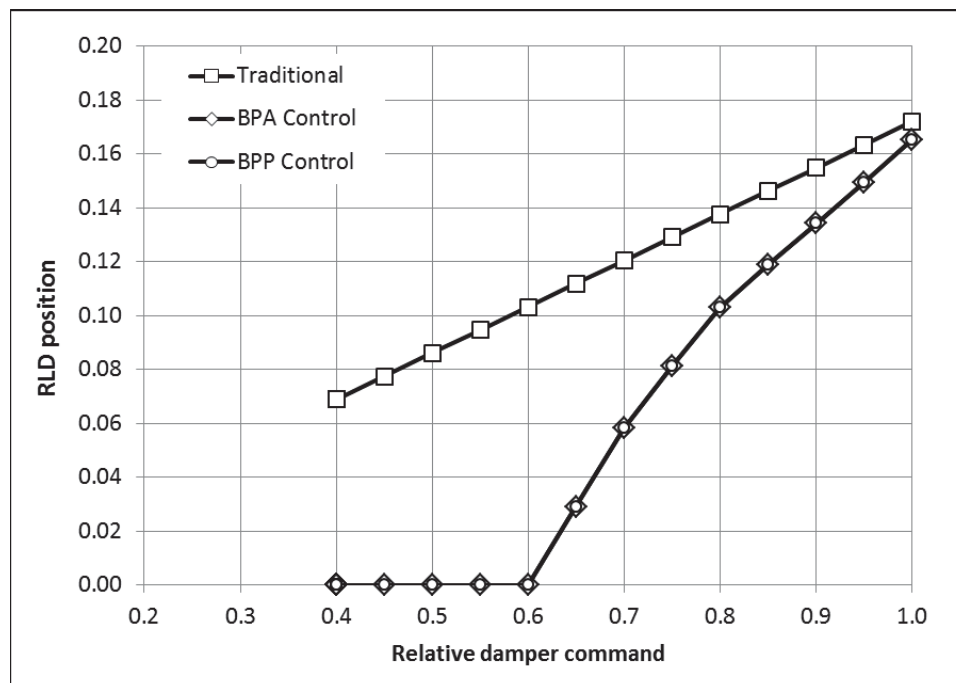
(b) RLD position
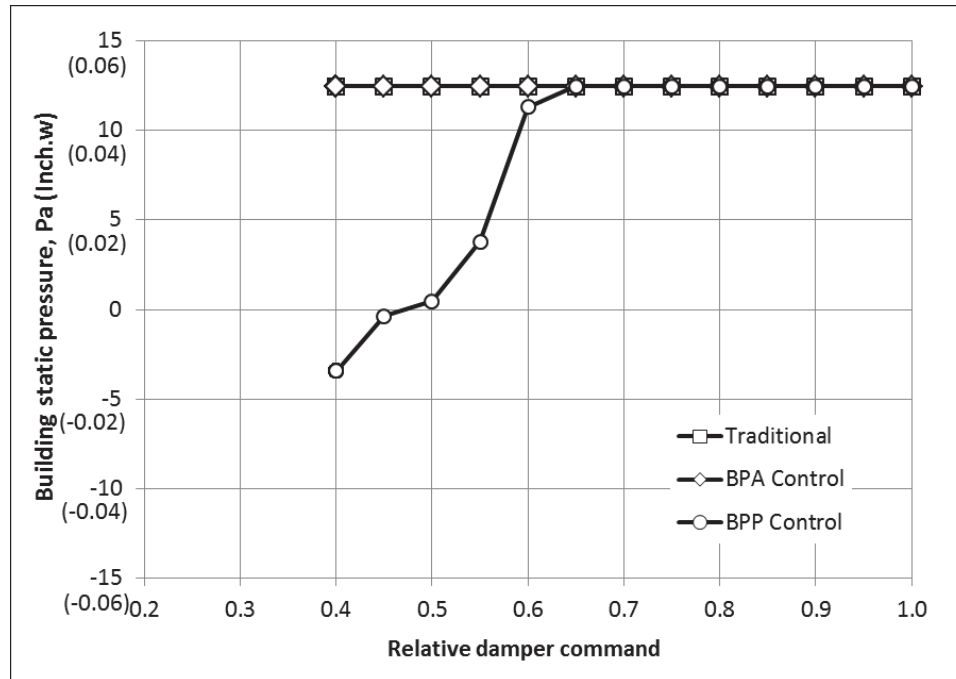
(c) Building static pressure

(d) Relief plenum pressure

Figure 4.14 Performance with less open OAD

In the BPA control, the negative relief air plenum static pressure demands the fully

closed RLD damper and consequently avoids the reverse relief airflow. Since the

building static pressure is maintained at its setpoint by the RF, the building does not have outside air infiltration. Figure 4.14(a) also shows a constant outdoor airflow, which is balanced with as the building exhaust and infiltration airflow, when the RLD is fully closed.

On the other hand, in the BPP control, the RF always can maintain the positive relief air plenum static pressure, shown in Figure 4.14(d). Since the negative building static pressure demands the fully closed RLD damper, the relief airflow is positive and insignificant. However, the negative building static pressure results in uncontrolled outdoor air infiltration, which is balanced with the insufficient outdoor airflow shown in Figure 4.14(a), when the RLD damper is fully closed.

In summary, both the BPA and BPP controls can well prevent the reverse relief airflow at lower outdoor airflow ratio. However, the BPP control results in negative building static pressure while the BPA control can well maintain the positive building static pressure.

4.3.3 OA Ratio Higher than Minimum Required

Earlier section simulated the case where OAD command is less than the required command with low outdoor air ratio. This section will cover the system performance with the OA flow ratio up to 100%.

The relief airflow should increase as the outdoor airflow increases in order to maintain the building static pressure setpoint. In the BPP and BPA control, the maximum capacity of the relief air path with the fully open RLD increases as the relief air plenum static pressure setpoint increases. The lower static pressure setpoint may limit the relief air capacity and result in the excessive positive building static pressure when the outdoor airflow ratio is close to 100%. On the other hand, the higher static pressure setpoint will

lead to higher RF energy consumption. Therefore, the system performance, including the RF speed and the building static pressure, is simulated at the controlled outdoor airflow ratio from 0.1 to 1.0 when the supply airflow is 15.0 m³/s (32,000 CFM) or 80% of the design supply airflow. Two different relief air plenum static pressure setpoints, 25 Pa (0.1 inch of water) and 75 Pa (0.3 inch of water), are selected in the simulation to present the low and high limits given by ASHRAE (2010c). Besides the outdoor airflow ratio and relief air plenum static pressure, other two controlled variables, the duct static pressure and the building static pressure have the same setpoints as in the previous simulation. The duct static pressure setpoint is 374 Pa (1.5 inch of water) and the building static pressure setpoint is 12 Pa (0.05 inch of water).

Figure 4.15 shows that the RLD position (a), RF speed (b), building static pressure (c) and relief air plenum static pressure versus the outdoor airflow ratio, in the BPP and BPA controls.

To maintain the building static pressure, the relief airflow increases as the outdoor airflow increases. As a result, the RLD is open more as the outdoor airflow ratio increase, shown in Figure 4.15(a). As a control input, the RLD has an identical position with four identical controlled setpoints between the BPP and BPA controls. Therefore, two controls share a same RLD position curve under a same relief air plenum static pressure setpoint. On the other hand, the lower relief air plenum static pressure forces the RLD is open more in order to maintain relief airflow required by outside airflow. The RLD positon under the relief air plenum static pressure of 25 Pa (0.1 inch of water) with circle markers is more open than the curve under the relief air plenum static pressure of 75 Pa (0.3 inch of water) with cross markers. As a result, the lower relief air plenum static pressure

forces the RLD to quick reach the fully open position at the outdoor airflow ratio of 0.6 and finally lose the control on its controlled variable when the outdoor airflow ratio is above 0.6.

According to Equation (3.7), the RF head increases as the relief air plenum static pressure increases. Therefore, the RF speed under the relief air plenum static pressure of 75 Pa (0.3 inch of water) with cross markers is higher than one under the static pressure of 25 Pa (0.1 inch of water), shown in Figure 4.15(b). Since the RLD is entirely within the controllable range under the higher relief air plenum static pressure and the return airflow is constant at supply airflow of 15.0 m^3/s (32,000 CFM), the BPP and BPA controls share a same higher constant RF speed curve. With the same principle, the RF runs at a lower constant speed with the lower static pressure setpoint below the outdoor airflow ratio of 0.6 when the RLD still is within the controllable range. However, the RF speed curve splits to curves, with square markers for the BPP control and circle markers for the BPA control, when the outdoor airflow ratio is above 0.6.

With higher relief air plenum static pressure, the RLD is always within a controllable range in both controls. Therefore, the building static pressure is maintained at its setpoint of 12 Pa (0.05 inch of water), represented with cross markers in Figure 4.15(c) and the relief air plenum static pressure is maintained at its setpoint of 75 Pa (0.3 inch of water) with cross markers in Figure 4.15(d). With lower relief air plenum static pressure, the building static pressure and relief air plenum static pressure are also maintained at their setpoint before the outdoor airflow ratio reached 0.6 and the RLD reaches the fully open position. However, when the RLD reaches the fully open position, its controlled variable loses control. In the BPP control, the relief air plenum static pressure with square markers

in Figure 4.15(d) is well controlled by the RF speed. On the other hand, the relief airflow remains constant because of the fully opened RLD as the outdoor airflow increases. As a result, the building static pressure with square markers in Figure 4.15(c) significantly increases. In the BPA control, the building static pressure with square markers in Figure 4.15(c) is well controlled by the RF speed. On the other hand, the RLD cannot open more to reduce the relief air plenum static pressure. As a result, the relief air plenum static pressure with circle markers in Figure 4.15(d) increases from 25 Pa (0.1 inch of water) to almost 75 Pa (0.3 inch of water).
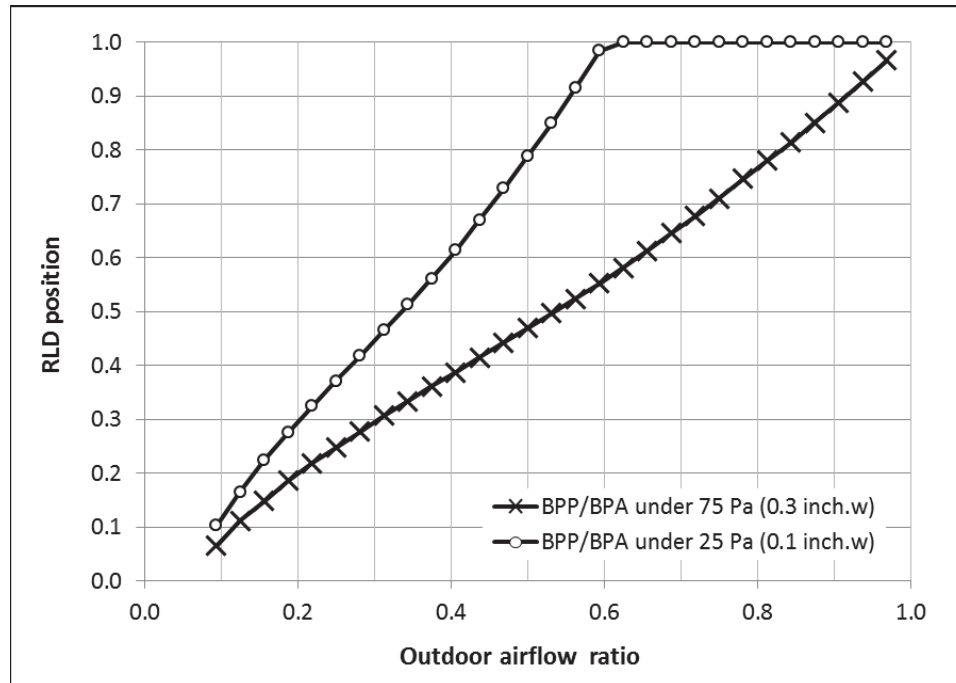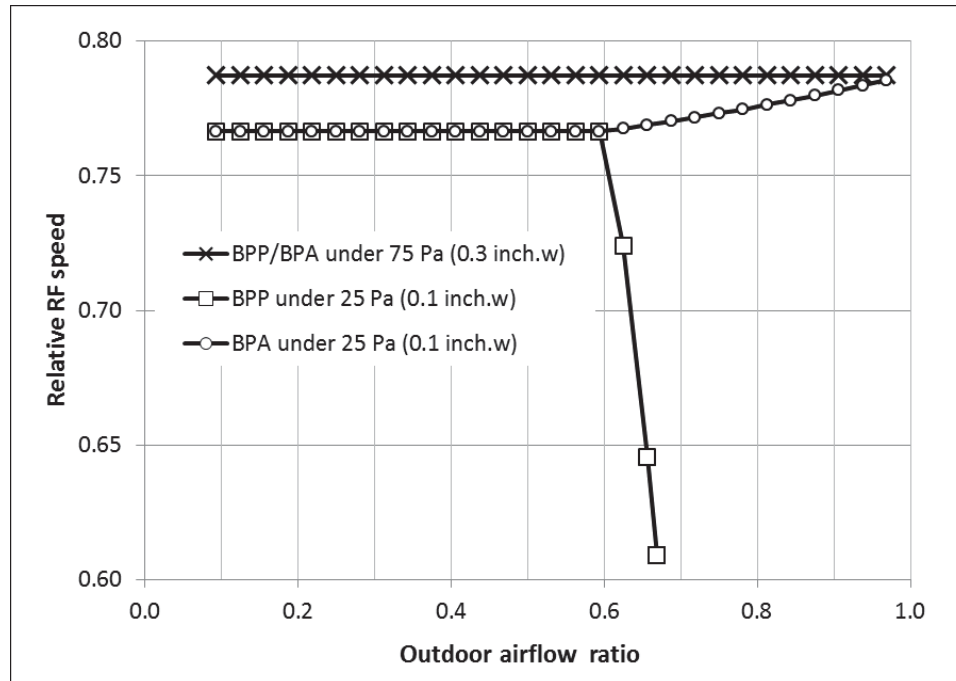

(a) RLD position.
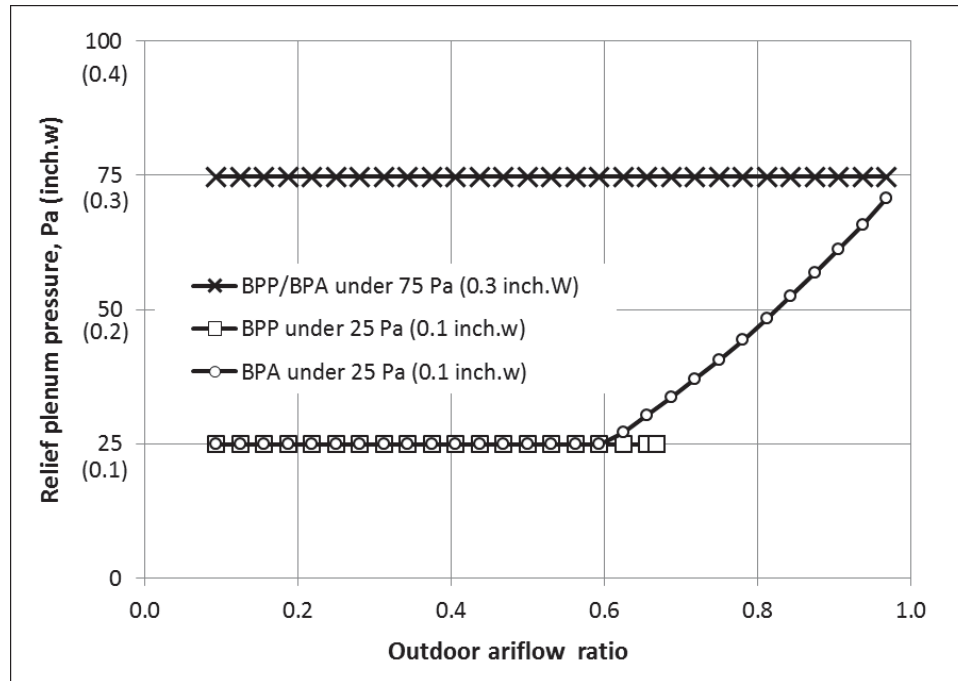
(b) RF speed
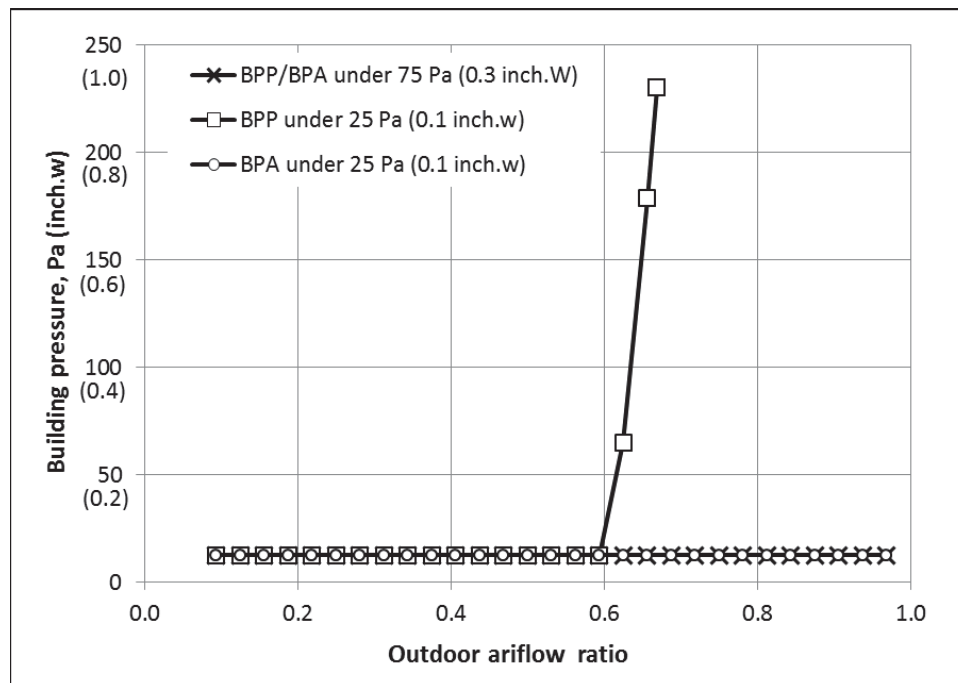
(c) Building static pressure.

(d) Relief plenum pressure

Figure 4.15 Performance with more outdoor air intake

In summary, the BPP control will cause the high RF speed as well as high RF power under the high relief plenum pressure setpoint and lose the building static pressure control under the low relief plenum pressure setpoint when the outdoor airflow ratio is close to 100%. Meanwhile, the BPA control can well control the building static pressure with low RF power by setting a low relief air plenum static pressure setpoint even though the relief air plenum static pressure is higher than its setpoint.

4.4. Lack of Sensors

First, a hypothetical AHU system is designed based on design space cooling load, minimum outdoor airflow rate, and supply and return air duct static pressure drop first. Then the system performance of the AHU with the fixed damper positions but with the perfect RF speed control is simulated in order to cover the AHUs that do not have the outdoor airflow sensor but do have either an accurate pressure sensor or two accurate

supply and return airflow sensors. Next, the system performance of the AHU with the integration of the fixed damper position method and the RF speed tracking method is simulated to cover the AHU that does not have the outdoor airflow sensor as well as the building static pressure and supply airflow and return airflow sensors.

4.4.1 Fixed Damper Positions for Minimum Outdoor Air Control

In this simulation, it is assumed that the studied AHU does not have the outdoor airflow sensor but building static pressure is perfectly controlled by a building static pressure sensor or supply and return airflow sensors. The perfect building static pressure setting is also intended to identify the required correlation between the RF and SF fan speeds. When the outdoor airflow sensor is not available in an AHU, the fixed damper position method is applied to maintain the minimum outdoor air intake for the IAQ control.

Two simulation steps are designed to evaluate the system performance for all five damper connections. The first step is to determine the required damper command (D) in order to maintain a fixed minimum outdoor airflow ratio, the ratio of the minimum outdoor airflow rate to the supply airflow rate, at 0.15, which is the same as the outdoor airflow ratio, the ratio of the design minimum outdoor airflow, 2.8 m^3/s (6,000 CFM), to the design supply airflow, 18.8 m^3/s (40,000 CFM), under the design condition. The second step is to calculate actual outdoor airflow ratio when the minimum damper command (D) is set at the required command calibrated under the design minimum outdoor airflow, 2.8 m^3/s (6,000 CFM), and the design supply airflow 18.8 m^3/s (40,000 CFM), in the first step.

Besides the constraint on the outdoor airflow ratio in the first simulation or the damper command in the second simulation, the duct static pressure setpoint is 374 Pa (1.5 inch of

water) to control the SF speed while the space static pressure setpoint is 12.5 Pa (0.05 inch of water) to control the RF speed. The relief plenum pressure is set at 50 Pa (0.2 inch of water) to control the RLD command with the two decoupled RLD connections. During the simulation, the supply airflow ratio, the ratio of the supply airflow rate to the design supply airflow rate, varies from 1.0 to 0.4.

Figure 4.16 demonstrates the required damper command to maintain the minimum outdoor airflow ratio of 0.15. The two decoupled RLD connections have a biggest variation of the required damper command, which increases from 0.14 to 0.70 with the sequenced action and from 0.21 to 0.45 with the overlapping action as the supply airflow ratio decreases from 1.0 to 0.4. The two OAD open connections have a less variation of the required damper command, which decreases from 0.08 to 0.04 with the sequenced action and from 0.14 to 0.05 with the overlapping action as the supply airflow ratio decreases from 1.0 to 0.4. The traditional connection has an approximately constant damper command of 21% regardless of the supply airflow ratio.
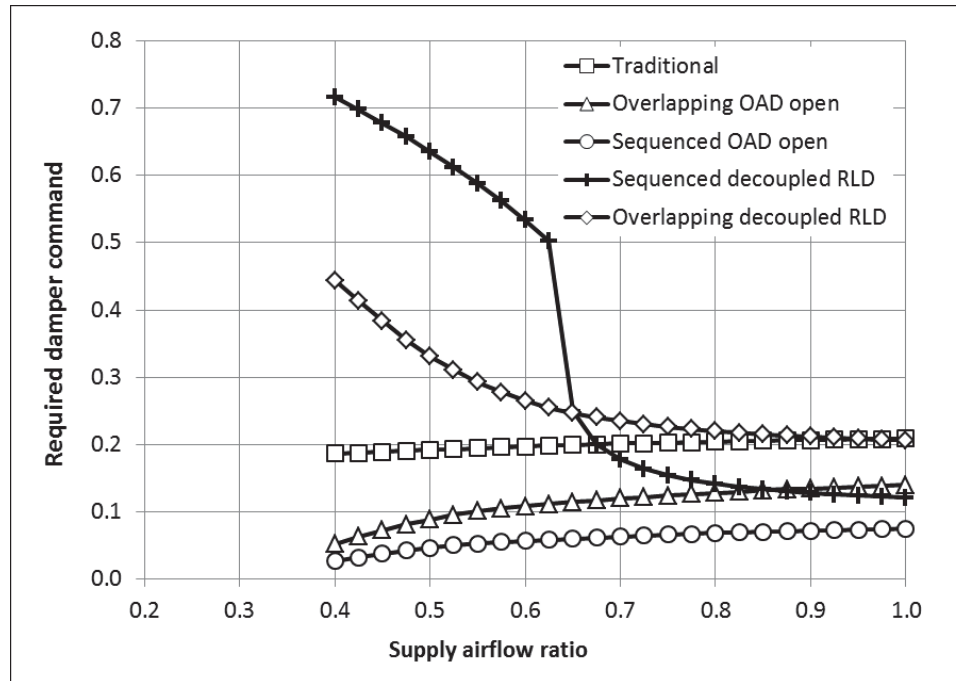
Figure 4.16 Required damper command to maintain 15% outdoor airflow ratio

In order to understand how the RF and SF fan speed correlate each other in perfect controls, the required RF speed versus SF speed curves are drawn in Figure 4.17 for the traditional damper connections and the two OAD fully open connections. It is obvious that the RF speed, which is modulated to maintain the constant building static pressure, does not have either a proportional relationship or an offset relationship with the SF speed. However, Figure 4.17 does show an approximately linear relationship between the RF and SF speeds.
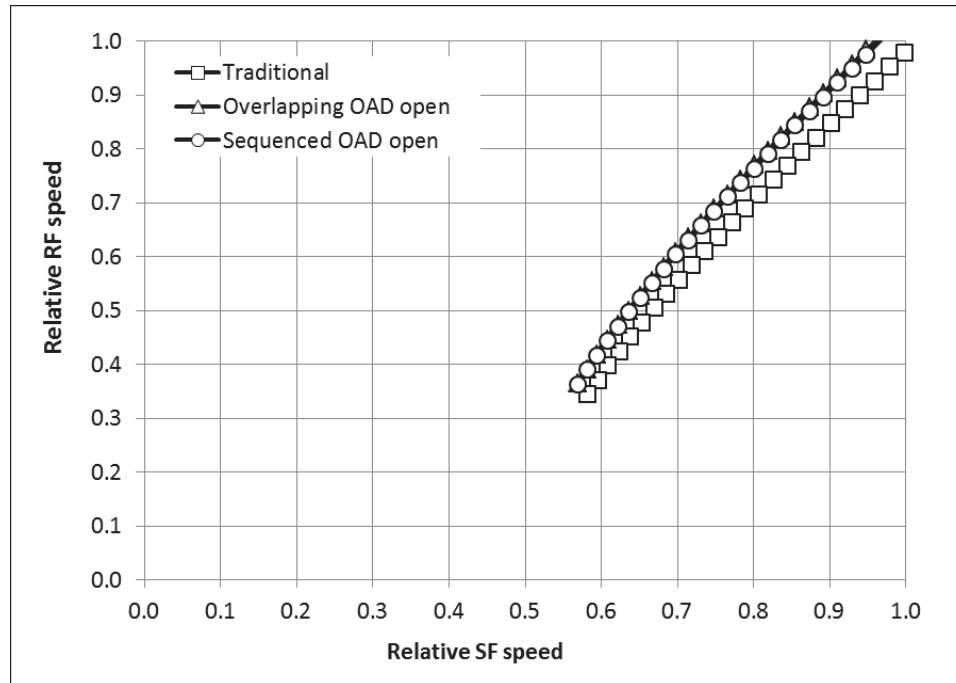
Figure 4.17 RF speed versus SF speed

Figure 4.18 shows the actual minimum outdoor airflow ratio when the damper command is always fixed at the minimum value, which is calibrated at the design minimum outdoor airflow and design supply airflow rates and listed within the parentheses, for all five damper connections. The large variation is obviously found for the two decoupled RLD connections and two OAD fully open connections. The smallest outdoor airflow ratio variation with the traditional connection is about 2% from 0.15 to 0.17 over the entire supply airflow range if the building static pressure is perfectly controlled at its setpoint, 12.5 Pa (0.05 inch of water). Therefore, the outside airflow ratio versus damper command curve can be calibrated regardless of the supply airflow if the traditional damper connection is chosen.

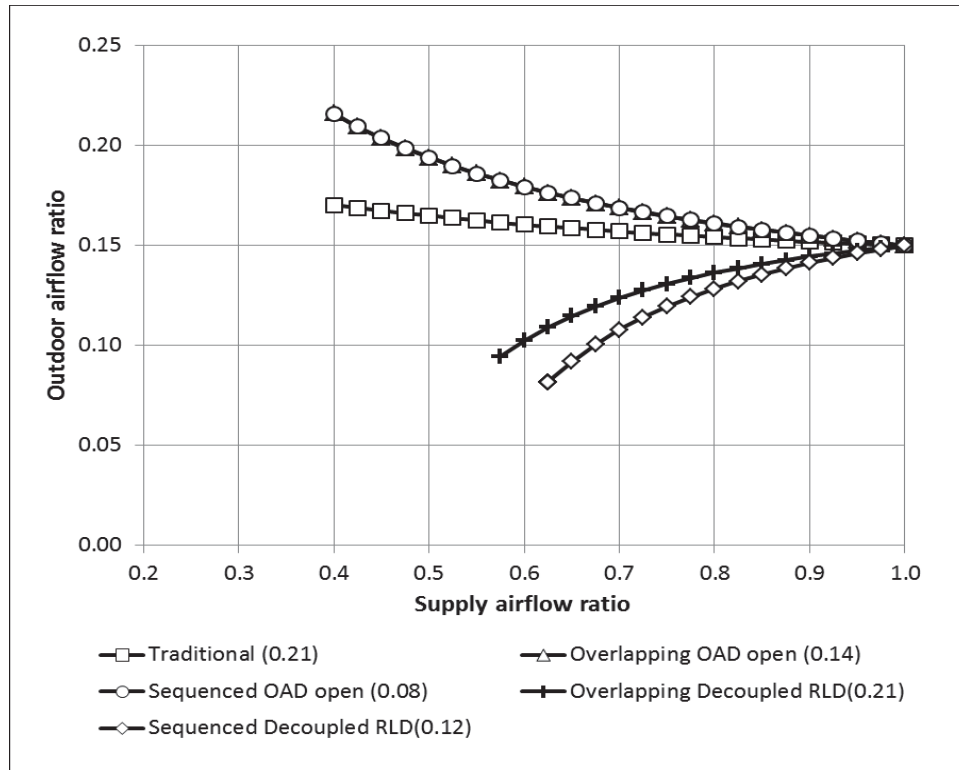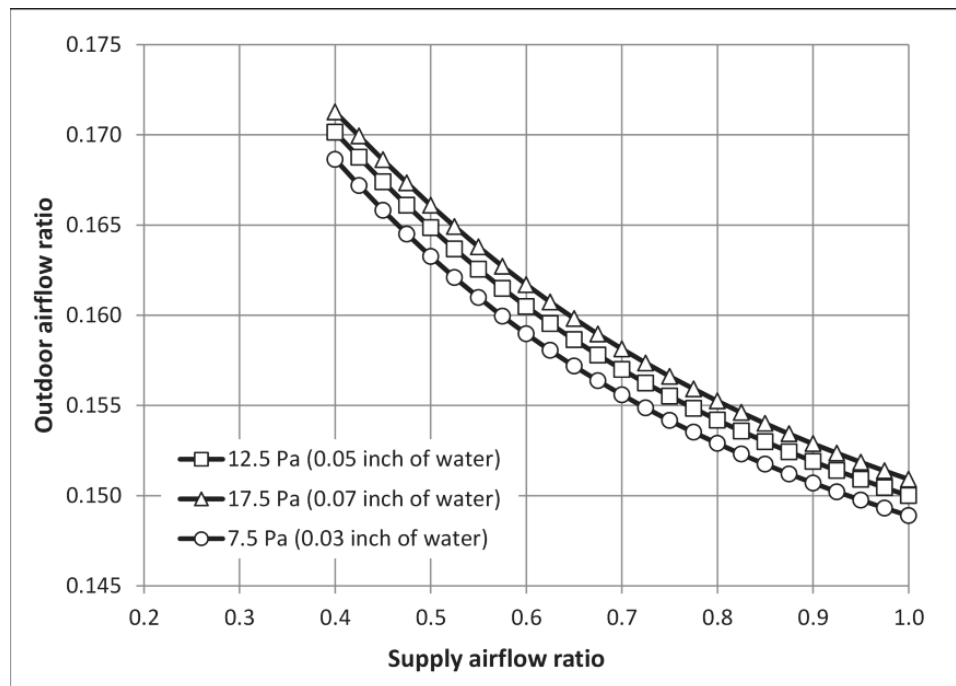**Figure 4.18 Outdoor airflow ratio versus supply airflow with a fixed damper command**

Figure 4.19 Outdoor airflow ratio under different building static pressure with the traditional control

The AHU control is a dynamic process, the actual building static pressure can vary around its setpoint. To identify the impact of the building static pressure, the correlation between the outdoor airflow ratio and damper position with traditional control is simulated with same damper position as in Figure 4.18 under different building static pressure and plotted in Figure 4.19. Figure 4.19 shows that ±40% change in building static pressure results in less than ±0.2% change in outdoor air ratio.

To verify the correlation between the outdoor airflow ratio and the damper command is not impacted by supply air flow ratios in the traditional OAD connection, the actual outdoor airflow ratio is also simulated with different supply airflow ratios and different damper commands. Figure 4.20 shows the simulated outdoor airflow ratio with respect to the supply airflow ratio from 1.0 to 0.4 under five different damper position commands, 0.15, 0.20, 0.25, 0.30 and 0.35. Figure 4.21 shows the simulated outdoor airflow ratio with respect to the damper command from 0.1 to 0.35 under three supply airflow ratio, 1.0, 0.8 and 0.6. It can be observed that the outdoor airflow ratio has a consistent relationship with the damper command and is approximately independent of the supply airflow ratio.
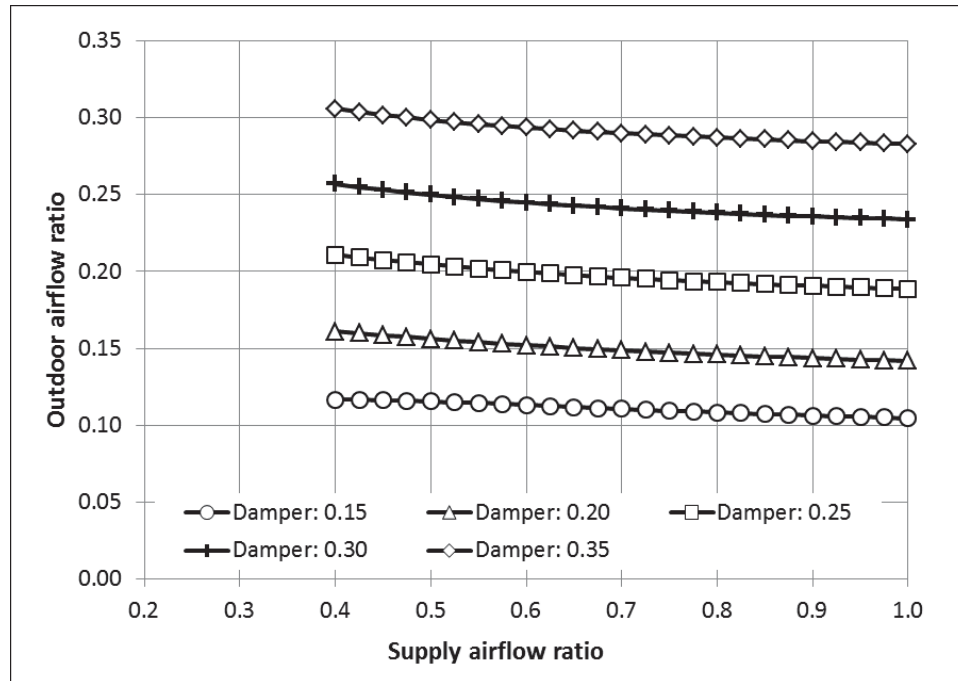
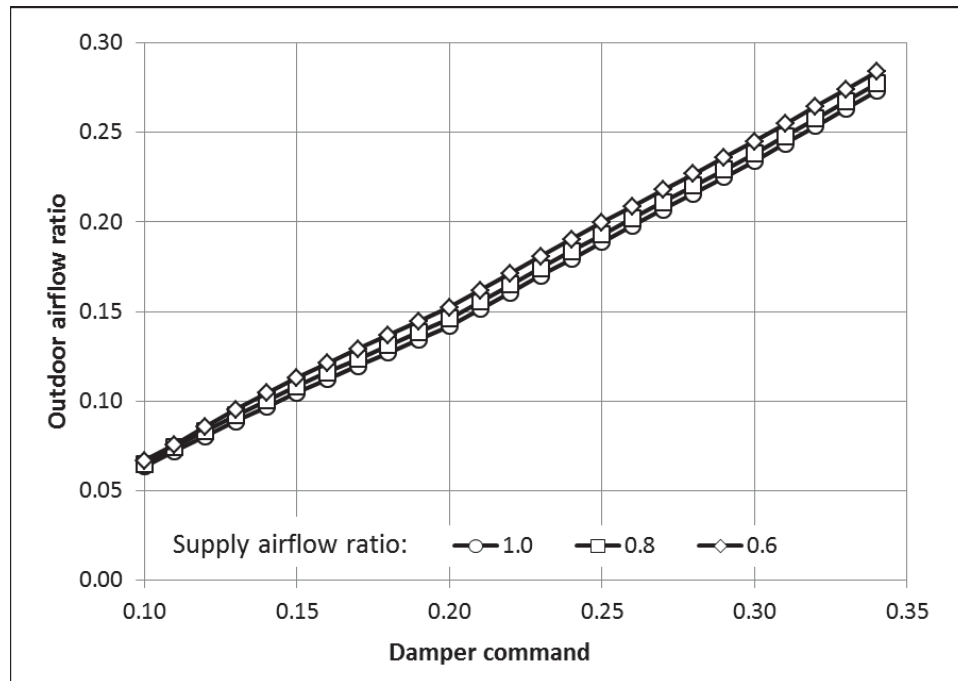**Figure 4.20 Outdoor airflow ratio versus supply airflow ratio with different damper commands**

Figure 4.21 Outdoor airflow ratio versus damper command with different supply airflow ratios

4.4.2 Fixed Damper Position with Return Fan Speed Tracking

In addition to the lack of the outdoor airflow sensor, space limitations, and expensive installation costs may prohibit physical supply and return airflow sensor installations while the thermal and wind effect may result in unacceptable errors of building static pressure measurement. As a result, the fixed damper position method has to be applied for the minimum outdoor airflow control and the RF speed tracking has to be applied on the building static pressure speed control. In general, the relief air plenum static pressure is not controlled if the RF speed tracking control is applied. Therefore, the two decoupled RLD connections are not discussed with this alternative control.

The damper command is fixed at the minimum value, which is calibrated under the design minimum outdoor airflow and supply airflow rates and is listed in Figure 4.19. Three RF speed tracking methods are evaluated, including offset tracking, proportional tracking, and linear tracking, for the traditional connection, overlapping OAD open connection and sequenced OAD open connection by simulating the system performance, including the outdoor airflow ratio and building static pressure.

- Offset tracking: The RF speed equals the SF speed subtracting a constant value. Here two constants, 0.06 and 0.12, are applied.

- Proportional tracking: The RF speed equals the SF speed multiplying a constant fraction. Here two fractions, 0.9 and 0.8, are applied.

- Linear tracking; the RF speed is a linear function of the SF speed. The linear functions are regressed based on the simulated RF and SF speed under the perfect control with reliable airflow and pressure sensors installed at the AHU, shown in Figure 4.17. Equations (4.6 to 4.8) represent the regressed functions

for the traditional connection, overlapping OAD open connection and sequenced OAD open connection respectively.

$$\omega_{RF} = 1.5819\omega_{SF} - 0.5148 \tag{4.6}$$

$$\omega_{RF} = 1.5853\omega_{SF} - 0.5090 \tag{4.7}$$

$$\omega_{RF} = 1.4411\omega_{SF} - 0.4485 \tag{4.8}$$

Figures 4.22 and 4.23 demonstrate the simulated outdoor airflow ratio and building static pressure with the proportional tracking method. Huge variation in the building static pressure from -50Pa to 250Pa (from -0.2 to 1 inch of water) is observed when the supply airflow ratio varies from 50% to 100% even though the outdoor airflow ratio insignificantly varies by 0.07.

Figure 4.22 Outdoor airflow ratio with RF speed proportional tracking

Figure 4.23 Building static pressure with RF speed proportional tracking

Figures 4.24 and 4.25 demonstrate the simulated outdoor airflow ratio and building static pressure with the offset tracking method. It can be seen that the building static pressure varies from -50Pa to 200Pa (from -0.2 to 0.8 inch of water) when the supply airflow ratio varies from 50% to 100% even though the outdoor airflow ratio insignificantly varies by 0.05. Therefore, both the proportional and offset tracking methods can maintain approximately constant outdoor air ratio but cannot maintain a constant positive building static pressure.

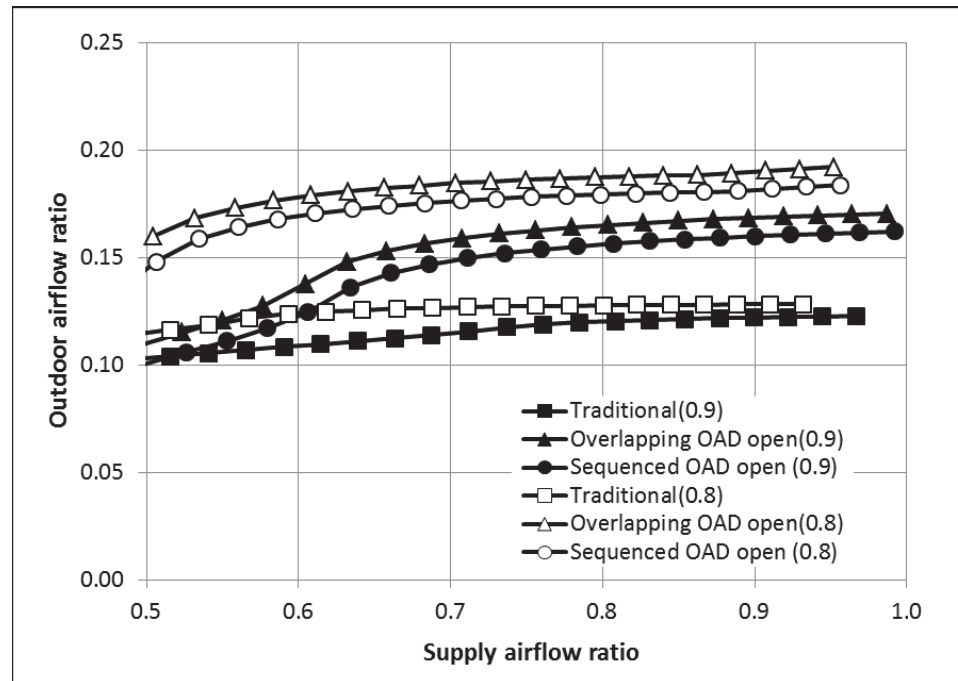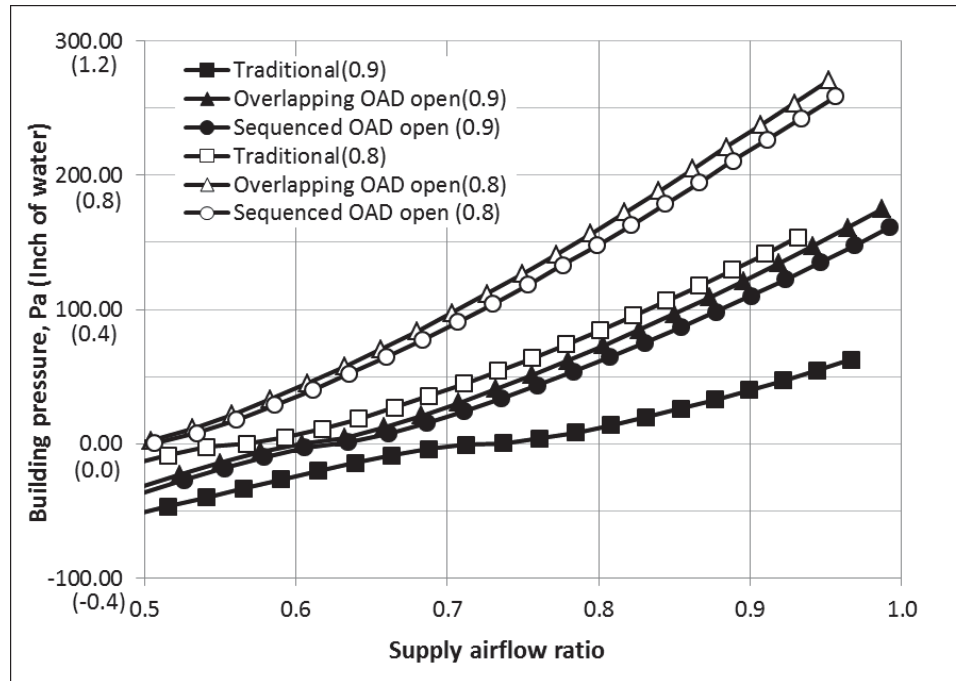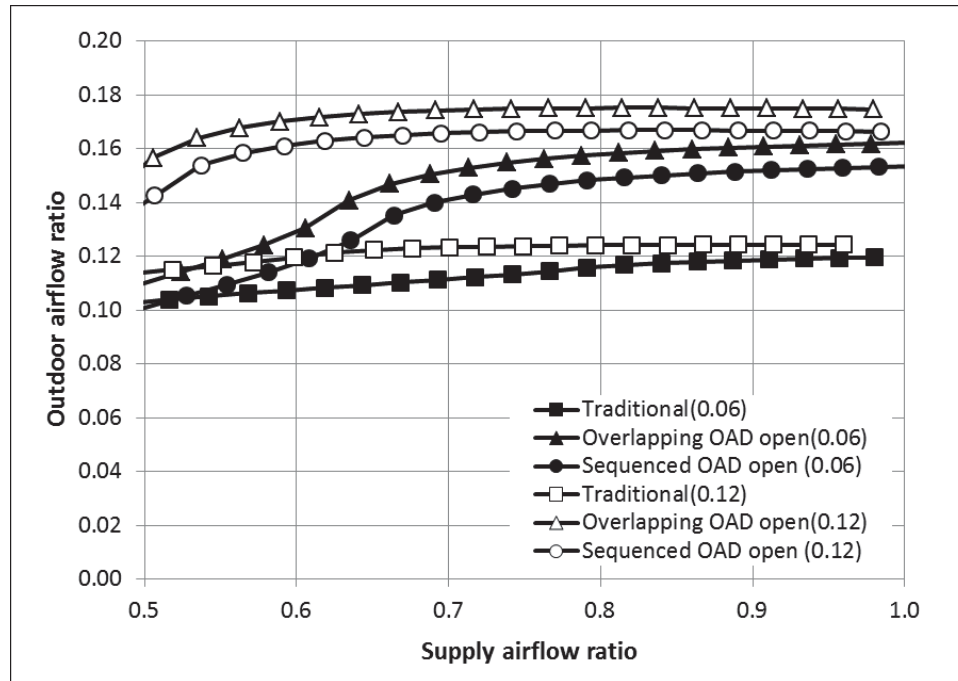**Figure 4.24 Outdoor airflow ratio with RF speed offset tracking**
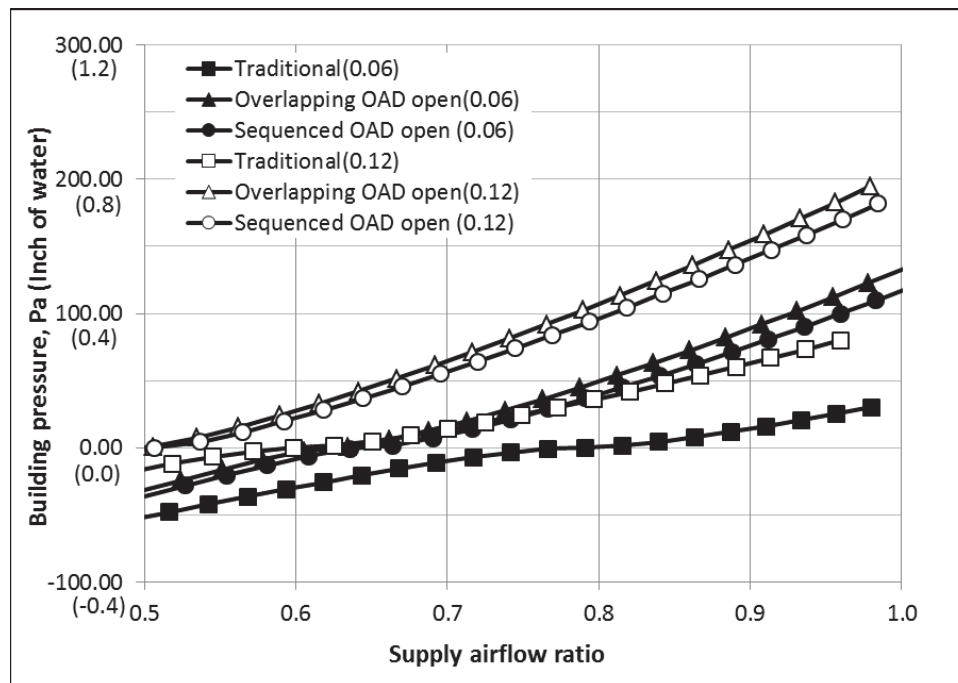
Figure 4.25 Building static pressure with RF speed offset tracking

Figures 4.26 and 4.27 show the simulated outdoor airflow ratio and building static pressure with the linear tracking method. The building static pressure is controlled at

positive pressure with relatively small variation, from 5 to 23Pa (from 0.02 to 0.09 inch of water) for the two OAD open connections and from 0 to 7 Pa (from 0 to 0.03 inch of water) for the traditional connection when the supply airflow varies from 50% to 100%. Also, the outdoor airflow ratio shows small variation, from 0.12 to 0.17 for the two OAD open connections and from 0.11 to 0.13 for the traditional connection. Therefore, the linear tracking method may provide a simple engineering solution for the airflow-pressure control for AHUs with the lack of airflow and pressure sensors. Even though the linear relationship between the RF and SF speeds need to be calibrated, the measurements for the calibration only need to be conducted at two different operating points in order to determine two constants in the linear expression.
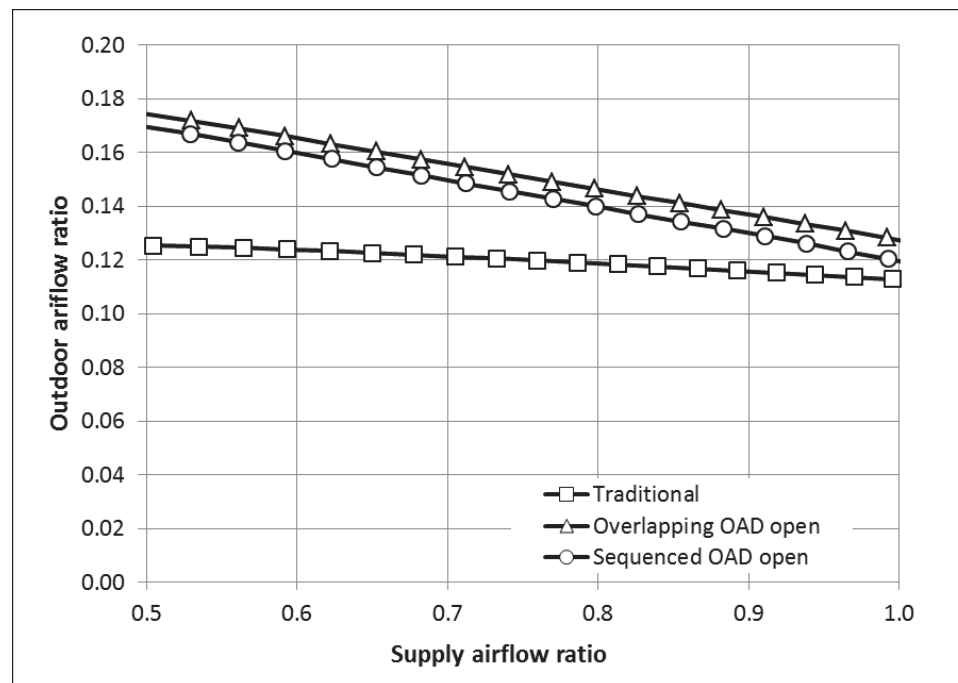
Figure 4.26 Outdoor airflow ratio with RF speed linear tracking
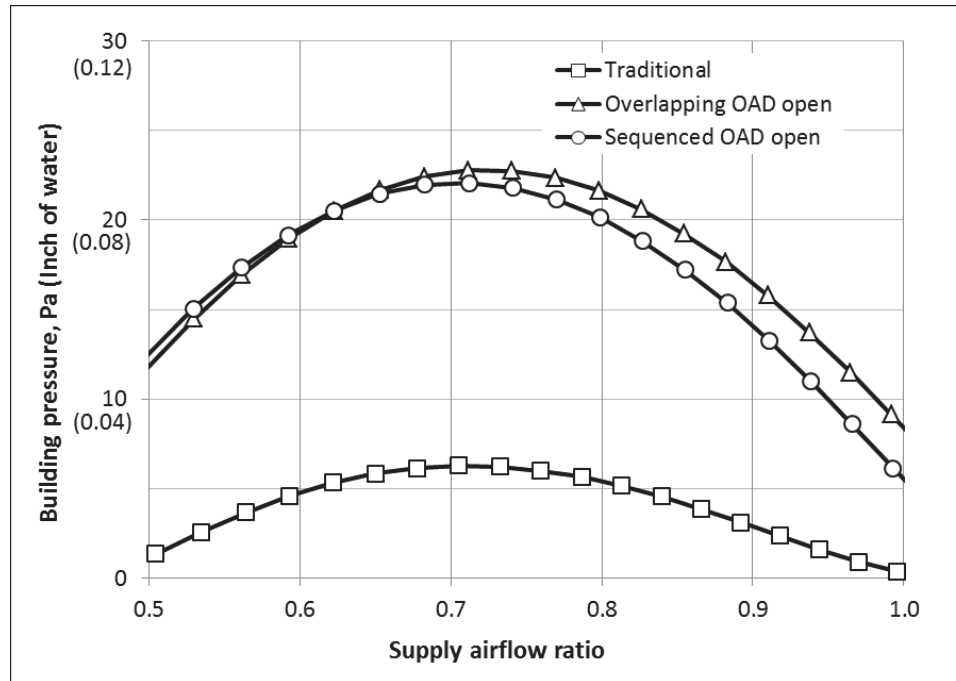
Figure 4.27 Building static pressure with RF speed linear tracking

From above results, it is clear that the fixed damper position with the RF speed linear tracking method maintains a positive building static pressure when all the dampers are interlinked. The steady state simulation shows that the linear tracking maintains the OA ratio constant than the proportional or offset tracking. The variation in building static pressure is relatively small with the traditional connection. The RF linear tracking method may provide an alternative solution to maintain a slightly positive building static pressure with the lack of airflow and pressure sensors in AHUs.

CHAPTER 5. CONTROL THEORY FOR HVAC SYSTEM

This chapter discusses the basic control theory for the HVAC system. It will involve derivation of transfer function equation for each component involved in the HVAC control loop under consideration. The transfer function is derived assuming linearization, therefore, equation for gains and time constants are derived. Using the transfer functions and the block diagrams open loop transfer function for the system is derived. These open loop transfer functions are used to study the stability of the system.

5.1. Cascade Control and Root Locus Analysis

To achieve the last objective of the research Cascade control is used to improve the stability of the control system and root locus analysis is used to demonstrate the results of the dynamic response.

5.1.1 Cascade Control

Cascade control is often considered as an adaptive and robust type of control method and widely used with PI controllers (Haugen, 2004; Marlin, 2000). A cascade control loop is constructed, by adding a secondary control loop inside the primary loop. In this type of control method, two controllers are used. The additional controller uses an intermediate measured variable as a reference to determine the corrected value of the independent variable.

For example, with cascade control in SZ AHU, for the space temperature control, the first controller will compare the space air temperature with the set-point and provide a feedback to the second controller, which then compares the signal with supply air temperature to correct the valve signal.

5.1.2 Root Locus Analysis

Root locus analysis is a graphical representation of the open loop roots of a system and the curves indicate the change in closed loop as the system gain changes. The dynamic response of a closed-loop system can completely be determined by the position of the roots (poles and zeros) in the s-plane (Kraisuntronlertphop & Gunpanich, 2012) and the curves. Poles are the roots of the polynomial in the denominator of the transfer function whereas; zeros are the roots of the polynomial in the numerator.

The s-plane plot of the system shows if the system response is stable or oscillatory. As long as the variation of the roots stay on the left side of the imaginary axis the system is completely stable. However, as the closed loop roots cross the imaginary axis and enter on the right side imaginary axis on the s-plot then the system shows oscillatory behavior for the value of the system gains corresponding to the section of the curve in the right side of the imaginary curve. Chapter 6 provides the root locus plots of the systems under consideration. In this chapter, the transfer functions required to determine the roots are derived.

5.2. Return Fan Control

In this section, a single duct VAV system is under consideration. In following subsections, equations for steady state gains are derived along with room time constant. These gains and time constants are used to derive the plant transfer functions. Later each control is discussed after applying corresponding feedback control to the basic plant block diagram. For each of these control methods, a transfer function is derived in the respective subsection.

5.2.1 The System Description

Figure 5.1(a) shows the basic schematic of the system under consideration and Figure 5.1(b) is a representative block diagram of the system. For model simplicity, we assume that the return plenum is at constant pressure. Supply and exhaust flow from the supply and exhaust fans are two disturbance inputs. Building static pressure is controlled by a control input, the return fan speed. The infiltration (Q_{inf}) is dependent on envelope resistance factor (S_{inf}), which is an envelope characteristic and building static pressure (P_{RM}).

$$P_{RM} = S_{inf} \cdot Q_{inf}^2 \tag{5.1}$$

In steady state, if the pressure is constant the return airflow can be determined using the mass conservation.

$$Q_{RA} = Q_{SA} - Q_{EX} - Q_{inf} \tag{5.2}$$

The return fan head is demanded by the return air duct pressure loss and the building static pressure.

$$H_{RF} + P_{RM} = S_{RA} \cdot Q_{RA}^2 \tag{5.3}$$

This return airflow from above equation along with required return fan head from return duct resistance factor, determine the required return fan speed.

$$H_{RF} = a\, Q_{RA}^2 + b\, Q_{RA}\, \omega + c\, \omega^2 \tag{5.4}$$
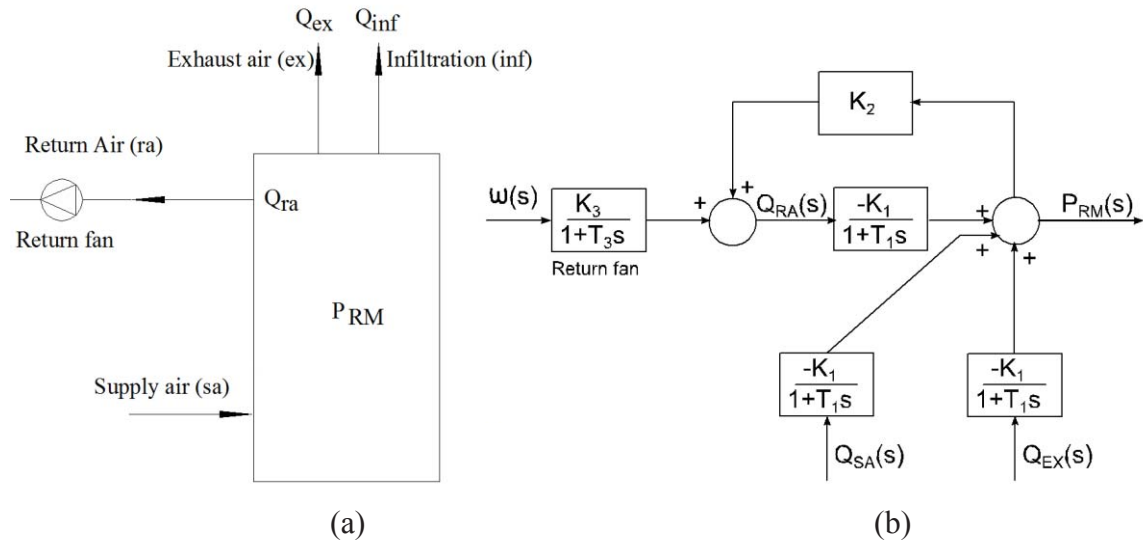
Figure 5.1 (a) Network schematic of a single duct VAV system and (b) block diagram for a single duct VAV system

5.2.2 Steady State Gains and Time Constant

In the derivation of the plant equations, the model is assumed to be linear. The change in building static pressure (P_{RM}) is a function of the change in supply, exhaust and return airflow.

Building static pressure can be calculated as,

$$P_{RM} = S_{inf}(Q_{SA} - Q_{EX} - Q_{RA}) \tag{5.5}$$

$$dP_{RM} = 2\,S_{inf}(Q_{SA} - Q_{EX} - Q_{RA})\,(dQ_{SA} - dQ_{EX} - dQ_{RA}) \tag{5.6}$$

Comparing it with the linear equation,

$$dP_{RM} = K_1\,(dQ_{SA} - dQ_{EX} - dQ_{RA}) \tag{5.7}$$

$$K_1 = 2\,S_{inf}(Q_{SA} - Q_{EX} - Q_{RA}) \tag{5.8}$$

Also, the change in return airflow is function of change in return fan speed and building pressure,

$$dQ_{RA} = K_2 dP_{RM} + K_3 d\omega \qquad (5.9)$$

The steady state gains K_1, K_2 and K_3 represent the change in magnitude. However, physical systems have a time constant due to inertia. Here inertia of motor shaft, fan blades and the time delay of VFD is lumped in a single time constant T_3. The value of T_3 is often assumed to be less than 5s (Karunakaran, 2009). The time constant T_1 is due to the room or building volume and its derivation is discussed further. The time constant for the pressure sensor and flow meters is selected from the specification datasheet of sensor manufacturers.

From equation (5.1)-(5.6) the steady-state gains are calculated as,

$$aQ_{RA}{}^2 + bQ_{RA}\omega + c\omega^2 = S_{RA}Q_{RA}{}^2 - P_b \qquad (5.10)$$

After differentiating the equation (5.10),

$$(2aQ_{RA} + b\omega)dQ_{RA} + (bQ_{RA} + 2c\omega)d\omega = 2S_{RA}Q_{RA}dQ_{RA} - dP_b \qquad (5.11)$$

Rearranging the equation (5.11),

$$\therefore dQ_{RA} = \left(\frac{1}{2S_{RA}Q_{RA}-2aQ_{RA}-b\omega}\right)dP_b + \left(\frac{bQ_{RA}+2c\omega}{2S_{RA}Q_{RA}-2aQ_{RA}-b\omega}\right)d\omega \qquad (5.12)$$

Comparing equation (5.12) with (5.9),

$$K_2 = \left(\frac{1}{2S_{RA}Q_{RA}-2aQ_{RA}-b\omega}\right) \qquad (5.13)$$

$$K_3 = \left(\frac{bQ_{RA}+2c\omega}{2S_{RA}Q_{RA}-2aQ_{RA}-b\omega}\right) \qquad (5.14)$$

The volume of the building provides a delayed response in building static pressure to the change in any of the flow rate in or out of the volume.

$$P_{Bldg}V_{Bldg} = m_{Bldg}RT \qquad (5.15)$$

Differentiating the equation with respect to time,

$$\frac{dP_{Bldg}}{dt} V_{Bldg} = \frac{dm_{Bldg}}{dt} RT \tag{5.16}$$

Change in mass flow rate in terms of volumetric airflow is,

$$\frac{dm_{Bldg}}{dt} = \rho\left(Q - Q_{inf}\right) \tag{5.17}$$

Where,

$$Q = Q_{SA} - Q_{RA} - Q_{EX} \tag{5.18}$$

Substituting equation in (5.17) in (5.16)

$$\frac{dP_{Bldg}}{dt} V_{Bldg} = \rho\left(Q - Q_{inf}\right) RT \tag{5.19}$$

Considering the building static pressure constant,

$$P_{Bldg} - P_{ATM} = S_{Bldg} \, Q_{inf}^{\,2} \tag{5.20}$$

Substituting equation (5.20) in (5.19),

$$V_{Bldg} \frac{dP_{Bldg}}{dt} = \rho RT \left(Q - \sqrt{\frac{P_{Bldg}-P_{ATM}}{S_{Bldg}}} \right) \tag{5.21}$$

Considering a small change in Q,

$$V_{Bldg} \frac{d\Delta P_{Bldg}}{dt} = \rho RT \left(\Delta Q - \frac{1}{2} \frac{1}{\sqrt{\frac{P_{Bldg}-P_{ATM}}{S_{Bldg}}}} \frac{P_{Bldg}}{S_{Bldg}} \right) \tag{5.22}$$

Equation (5.20) can be written as,

$$Q_{inf} = \sqrt{\frac{P_{Bldg}-P_{ATM}}{S_{Bldg}}} \tag{5.23}$$

Substituting equation (5.23) in (5.22),

$$V_{Bldg} \frac{d\Delta P_{Bldg}}{dt} = \rho RT \left(\Delta Q - \frac{1}{2} \frac{1}{Q_{inf}} \frac{\Delta P_{Bldg}}{S_{Bldg}} \right) \tag{5.24}$$

Building gauge pressure can be written as,

$$P = P_{Bldg} - P_{ATM} \tag{5.25}$$

Therefore, in this case the building pressure is the differential pressure,

$$\therefore \Delta P = \Delta P_{Bldg} \tag{5.26}$$

Substituting equation (5.26) in (5.24)

$$\therefore V_{Bldg} \frac{d\Delta P}{dt} = \rho RT \left(\Delta Q - \frac{\Delta P}{2Q_{inf} S_{Bldg}} \right) \tag{5.27}$$

Taking Laplace transform on both sides,

$$V_{Bldg} \, s \, P(s) = \rho RT \left[Q(s) - \frac{P(s)}{2Q_{inf} S_{Bldg}} \right] \tag{5.28}$$

Rearranging the equation (5.28),

$$P(s) \left(\frac{V_{Bldg}}{\rho RT} s + \frac{1}{2Q_{inf} S_{Bldg}} \right) = Q(s) \tag{5.29}$$

Writing the equation in transfer function format,

$$\frac{P(s)}{Q(s)} = \frac{1}{1 + \frac{2Q_{inf} S_{Bldg} V_{Bldg}}{\rho RT} s} \left(\frac{1}{2Q_{inf} S_{Bldg}} \right) \tag{5.30}$$

First order transfer function for relation between flow and pressure is,

$$\frac{P(s)}{Q(s)} = \frac{K_1}{1 + t_{Bldg} s} \tag{5.31}$$

Comparing equation (5.30) and (5.31),

$$\therefore t_{Bldg} = \frac{2Q_{inf}S_{Bldg}}{\rho}\frac{V_{Bldg}}{RT} \tag{5.32}$$

Using equation (5.15), $$t_{Bldg} = \frac{2Q_{inf}S_{Bldg}}{P_{Bldg}}\frac{m_{Bldg}}{\rho} \tag{5.33}$$

By the mass, volume and density correlation,

$$t_{Bldg} = \frac{2Q_{inf}V_{Bldg}}{P_{Bldg}}S_{Bldg} \tag{5.34}$$

Using equation (5.20), $$t_{Bldg} = \frac{2Q_{inf}V_{Bldg}}{P_{Bldg}}\frac{(P_{Bldg}-P_{ATM})}{Q_{inf}{}^2} \tag{5.35}$$

Rearranging equation (5.35), $$t_{Bldg} = \frac{2V_{Bldg}}{Q_{inf}}\frac{(P_{Bldg}-P_{ATM})}{P_{Bldg}} \tag{5.36}$$

Therefore, the time constant T_1 can be given as:

$$T_1 = \frac{2V_{RM}}{Q_{inf}}\left(1 - \frac{P_{ATM}}{P_{ATM}+P_{RM}}\right) \tag{5.37}$$

From Figure 5.1(b) following transfer functions can be derived. These functions are used to the open loop transfer function in each control method.

$$P_{RM}(s) = [Q_{RA}(s) + Q_{SA}(s) + Q_{EX}(s)]\left(\frac{-K_1}{1+T_1 s}\right) \tag{5.38}$$

$$Q_{RA}(s) = \frac{K_3}{1+T_3 s}\omega(s) + K_2 P_{RM}(s) \tag{5.39}$$

Traditionally, two control methods are used in the practice; direct pressure control and volumetric pressure control (Taylor 2014a). These methods are discussed in following subsections.

5.2.3 Direct Pressure Control
In the case of direct pressure control, a feedback loop from building static pressure is added. The building static pressure is measured by a differential pressure sensor with a

time constant T_{S1}. The measured building static pressure is then compared with a reference value i.e. the building static pressure setpoint (R_P) and based on the difference the controller with gain K_{C1} calculates corrected return fan speed (ω) to maintain the building static pressure (P_{RM}). Figure 5.2 is a block diagram for direct pressure control method.
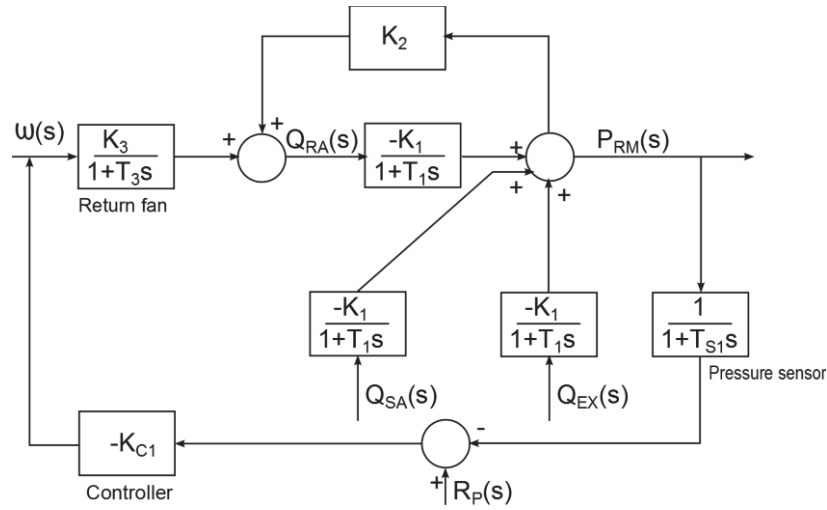
Figure 5.2 Direct pressure control

From the direct pressure control block diagram, we can write,

$$P_{RM}(s) = \left[\frac{K_3}{1+T_3 s}\omega(s) + K_2 P_{RM}(s)\right]\left(\frac{-K_1}{1+T_1 s}\right) \tag{5.40}$$

$$\therefore P_{RM}(s) = \frac{-K_1 K_3}{(1+T_3 s)(1+T_1 s+K_1 K_2)}\,\omega(s) \tag{5.41}$$

$$\omega(s) = \left[P_{RM}(s)\frac{(-1)}{1+T_{s1}s} + R_P(s)\right](-K_{C1}) \tag{5.42}$$

The closed loop transfer function for the system,

$$\frac{\omega(s)}{R_P(s)} = \frac{-K_{C1}}{1+\frac{K_1 K_3 K_{C1}}{(1+T_{S1}s)(1+T_3 s)(1+T_1 s+K_1 K_2)}} \tag{5.43}$$

Therefore the open loop transfer function for the direct pressure control,

$$G_D(s) = \frac{K_1 K_3 K_{C1}}{(1+T_{S1}s)(1+T_3s)(1+T_1s+K_1K_2)} \tag{5.44}$$

$$\therefore G_D(s) = \frac{K_1 K_3}{(1+K_1K_2)} \frac{1}{(1+T_{S1}s)(1+T_3s)\left(1+\frac{T_1}{1+K_1K_2}s\right)} K_{C1} \tag{5.45}$$

5.2.4 Volume Tracking Control

In volume tracking control, no feedback from building static pressure is used to control the return fan speed. Supply and return flows are measured with airflow meters with a time constant of T_{S2}. This difference is then compared with differential airflow setpoint (R_{dQ}). This setpoint is often determined at the time of commissioning or by a rule of thumb rule 0.05 to 0.15 cfm/ft^2 (Taylor, 2014a) for typical buildings. The controller with gain K_{C2} determines the return fan speed (ω) to maintain the difference in supply and return air. Figure 5.3 is a block diagram for volume tracking control method.
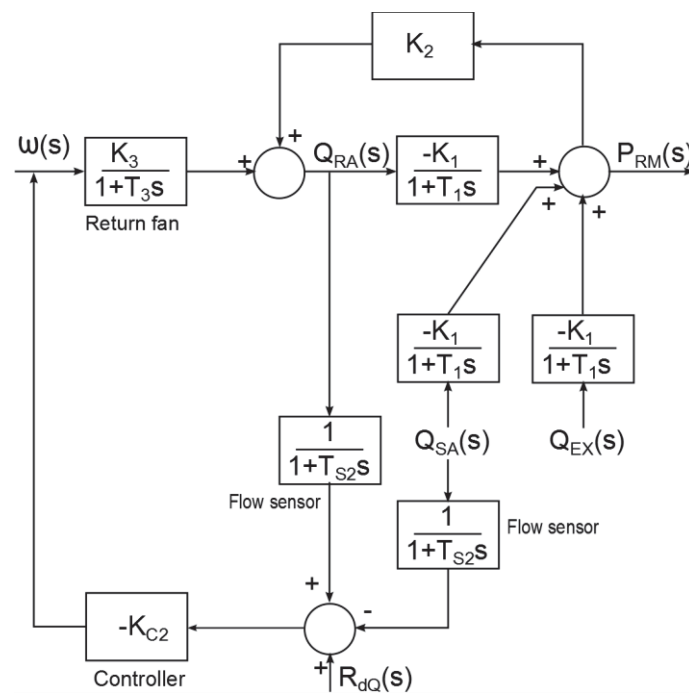

Figure 5.3 Volume tracking control

The transfer function for return fan speed with volume tracking control,

$$\omega(s) = \left[\left(\frac{K_3}{1+T_3 s}\omega(s) + K_2 P_{RM}(s)\right)\frac{1}{1+T_{s2}s} + R_P(s)\right](-K_{C2}) \tag{5.46}$$

Substituting $P_{RM}(s)$ from Equation (5.41) and rearranging the equation we get the closed loop system gain,

$$\frac{\omega(s)}{R_P(s)} = \frac{-K_{C2}}{1+\frac{K_3 K_{C2}}{(1+T_{s2}s)(1+T_3 s)} - \frac{K_1 K_2 K_3 K_{C2}}{(1+T_{s2}s)(1+T_3 s)(1+T_1 s+K_1 K_2)}} \tag{5.47}$$

The open loop transfer function for the volume tracking control is,

$$G_V(s) = \frac{K_3 K_{C2}}{(1+T_{s2}s)(1+T_3 s)} - \frac{K_1 K_2 K_3 K_{C2}}{(1+T_{s2}s)(1+T_3 s)(1+T_1 s+K_1 K_2)} \tag{5.48}$$

$$\therefore G_V(s) = \frac{K_3 K_{C2}(1+T_1 s)}{(1+T_{s2}s)(1+T_3 s)(1+T_1 s+K_1 K_2)} \tag{5.49}$$

$$\therefore G_V(s) = \frac{\frac{K_3}{1+K_1 K_2}(1+T_1 s)}{(1+T_{s2}s)(1+T_3 s)\left(1+\frac{T_1}{1+K_1 K_2}s\right)} K_{C2} \tag{5.50}$$

5.2.5 Cascade Control

In cascade control, feedback from building static pressure as well as the difference in supply and return airflow is used to control the return fan speed. The building static pressure is measured with a differential pressure sensor with time constant T_{S1}. The measured building static pressure is then compared with the building static pressure setpoint (R_P) and from the difference; a reference value for differential airflow is determined by the first controller. This reference is then compared with the difference in supply and return flows measured with airflow meters with a time constant of T_{S2}. The second controller with gain K_{C2} then determines the return fan speed (ω) to maintain the building static pressure. Figure 5.4 is a block diagram for cascade control method.
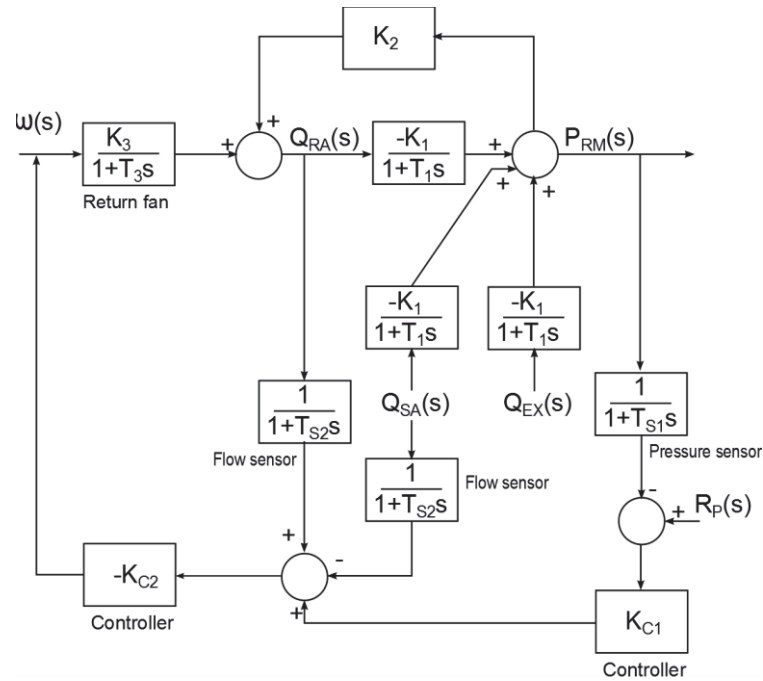
Figure 5.4 Cascade control

The return fan speed equation in this case is,

$$\omega(s) = \left[\left(\frac{K_3}{1+T_3 s}\omega(s) + K_2 P_{RM}(s)\right)\frac{1}{1+T_{s2}s} + \left(P_{RM}(s)\frac{(-1)}{1+T_{s1}s} + R_P(s)\right)K_{C1}\right](-K_{C2}) \qquad (5.51)$$

Substituting $P_{RM}(s)$ from Equation (5.41) and rearranging the equation we get the closed loop transfer function,

$$\frac{\omega(s)}{R_P(s)} = \frac{-K_{C1}K_{C2}}{1+\frac{K_3 K_{C2}}{(1+T_{s2}s)(1+T_3 s)} - \frac{K_1 K_2 K_3 K_{C2}}{(1+T_{s2}s)(1+T_3 s)(1+T_1 s+K_1 K_2)} + \frac{K_1 K_2 K_3 K_{C2}}{(1+T_{s1}s)(1+T_3 s)(1+T_1 s+K_1 K_2)}} \qquad (5.52)$$

The open loop transfer function for cascade control,

$$G_C(s) = \frac{K_3 K_{C2}}{(1+T_{s2}s)(1+T_3 s)} - \frac{K_1 K_2 K_3 K_{C2}}{(1+T_{s2}s)(1+T_3 s)(1+T_1 s+K_1 K_2)} + \frac{K_1 K_2 K_3 K_{C2}}{(1+T_{s1}s)(1+T_3 s)(1+T_1 s+K_1 K_2)}$$

$$(5.53)$$

$$\therefore G_C(s) = \frac{\left[(1+K_1 K_{C1})+(K_1 K_{C1}T_{s2}+T_{s1}+T_1)s+T_{s1}T_1 s^2\right]}{(1+T_{s1}s)(1+T_{s2}s)(1+T_3 s)\left(1+\frac{T_1}{1+K_1 K_2}s\right)}\frac{K_3}{1+K_1 K_2}K_{C2} \qquad (5.54)$$

5.3. Cooling Coil Valve Control

In following subsections equations for steady state gain constants are derived along with coil, duct and room time constant. These gains and time constants are used to derive the plant transfer functions. Later, each control is discussed after applying corresponding feedback control to the basic plant block diagram as shown in Figure 5.6(b). For each of these control methods, transfer functions are derived in the respective subsections.

5.3.1 System Description

Figure 5.5 shows the basic schematic of the system under consideration and Figure 5.6 is block diagram for the system. For simplicity of the model, only dry cooling coil is considered however, the results of this study can also be extended for heating coil. The time delay and temperature change due to the fan are neglected. The zone air is assumed to be well mixed and at a uniform temperature. The supply airflow assumed to be constant.
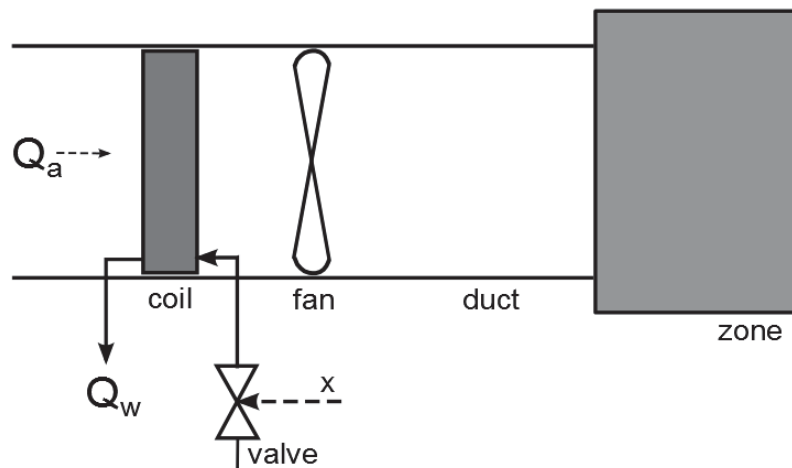

Figure 5.5 SZ AHU system schematic
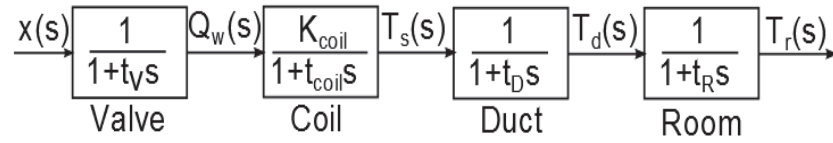
Figure 5.6 SZ AHU system block diagram

The model is assumed to be linear as shown in Figure 5.6 and transfer functions for SZ AHU can be written as,

$$T_r(s) = \left(\frac{1}{1+t_V s}\right)\left(\frac{K_{coil}}{1+t_{coil}s}\right)\left(\frac{1}{1+t_D s}\right)\left(\frac{1}{1+t_R s}\right)x(s) \tag{5.55}$$

For the chilled water flow, a valve with constant time delay is selected using manufacturer specification data (EnTech 1998). The time delay for duct (t_D) and room air (t_R) is calculated using equation (5.56) and (5.57) where L length of the duct, v_d average air velocity in the duct, V_R volume of the room, Q_a is the supply airflow.

$$t_D = \frac{L}{v_d} \tag{5.56}$$

$$t_R = \frac{V_R}{Q_a} \tag{5.57}$$

To derive the coil gain equation control volume for the coil is shown in Figure 5.7. The equations for coil gain (K_{coil}) and time delay (t_{coil}) are derived using heat transfer equations (5.58) and (5.59) on water and air side. C_C and C_{air} are the heat capacity rate of the coil (including water inside) and air.

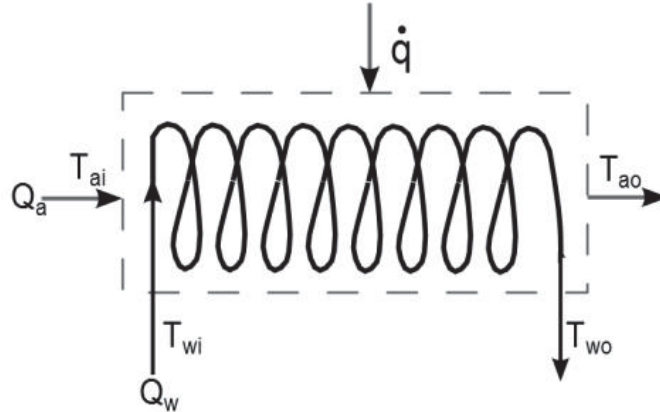**Figure 5.7 Coil control volume**

$$C_c \frac{dT_{wo}}{dt} = \dot{q} + C_{pw}\rho_w Q_w(T_{wi} - T_{wo}) \tag{5.58}$$

$$C_{air} \frac{dT_{ao}}{dt} = -\dot{q} + C_{pa}\rho_a Q_a(T_{ai} - T_{ao}) \tag{5.59}$$

Average of inlet ant outlet temperatures are assumed for the heat transfer between the two fluids.

$$\dot{q} = UA\left(\frac{T_{ai}+T_{ao}}{2} - \frac{T_{wi}+T_{wo}}{2}\right) \tag{5.60}$$

It is assumed that the water inlet temperature to the coil (T_{wi}) and air inlet temperature (T_{ai}) is at constant and the C_{air} term is very small compared to the other terms in equation (5.60). After simplifying, combining equation (5.58) and (5.59), substituting $\dot{C_a} = C_{pa}\rho_a Q_a$ and $\dot{C_w} = C_{pw}\rho_w Q_w$ and using Laplace transform for the resulting equation,

$$T_{wo}(s) = -\frac{\dot{C_a}}{C_c s+\dot{C_w}}T_{ao}(s) - \frac{\dot{C_w}}{C_c s+\dot{C_w}}\frac{(T_{wo}-T_{wi})}{Q_w}Q_w(s) \tag{5.61}$$

and,

$$T_{wo}(s) = T_{ao}(s)\left(1 + \frac{2\dot{C_a}}{UA}\right) \tag{5.62}$$

After combining equations (5.61) and (5.62),

$$T_{ao}(s) = -\left(\frac{(T_{wo}-T_{wi})\dot{C_w}UA}{Q_w(UA\dot{C_w}+2\dot{C_a}\dot{C_w}+\dot{C_a}UA)}\right)\frac{1}{\left(\frac{UAC_c+2\dot{C_a}C_c}{UA\dot{C_w}+2\dot{C_a}\dot{C_w}+\dot{C_a}UA}\right)s+1}Q_w(s) \tag{5.63}$$

$$T_{ao}(s) = -\frac{K_{coil}}{t_{coil}s+1}Q_w(s) \tag{5.64}$$

5.3.2 Conventional Control

Figure 5.8 (a) show a schematic of SZ AHU system with conventional control method where the zone temperature measured by the thermostat is compared with a reference temperature (R) i.e. the setpoint temperature. Figure 5.8 (b) is block diagram for the conventional control method of SZ AHU zone temperature. The output of the controller is then used to control the valve position and therefore the water flow through the coil (Q_w). The closed loop transfer function for the conventional method,

$$\frac{x(s)}{R(s)} = \frac{K_C}{1+\frac{K_{coil}K_C}{(1+t_Vs)(1+t_{coil}s)(1+t_Ds)(1+t_Rs)(1+t_ss)}} \tag{5.65}$$

Therefore the open loop transfer function for the SZ AHU conventional system is,

$$\therefore G_1(s) = \frac{K_{coil}K_C}{(1+t_Vs)(1+t_{coil}s)(1+t_Ds)(1+t_Rs)(1+t_ss)} \tag{5.66}$$

(a)

(b)
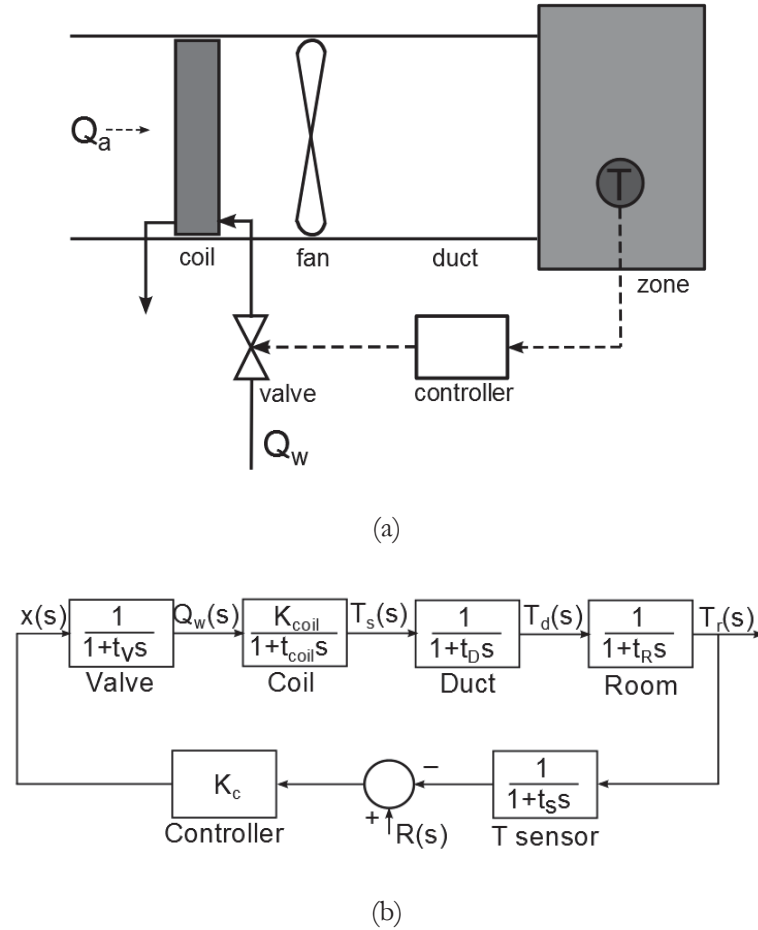
Figure 5.8 Conventional control (a) schematic and (b) block diagram of a SZ AHU system

5.3.3 Cascade Control

In cascade control method, Figure 5.9 (a) zone temperature and supply air temperature is measured to control the valve position. The zone temperature is compared with the setpoint temperature and the first controller determines the reference temperature for the supply air. From the changes in the supply air temperature, the second controller corrects the signal for the valve position. Figure 5.9 (b) shows block diagram for SZ AHU with cascade control method.

The closed loop transfer function for the cascade control method,

$$\frac{x(s)}{R(s)} = \frac{K_C}{1 + \frac{K_{coil}K_{C2}}{(1+t_Vs)(1+t_{coil}s)(1+t_Ss)}\left(\frac{K_{C1}}{(1+t_Ds)(1+t_Rs)} + 1\right)} \tag{5.67}$$

Therefore the open loop transfer function for the SZ AHU cascade control is,

$$\therefore G_2(s) = \frac{K_{coil}K_{C2}\ [K_{C1}+(1+t_D s)(1+t_R s)]}{(1+t_V s)(1+t_{coil}s)(1+t_D s)(1+t_R s)(1+t_s s)} \tag{5.68}$$
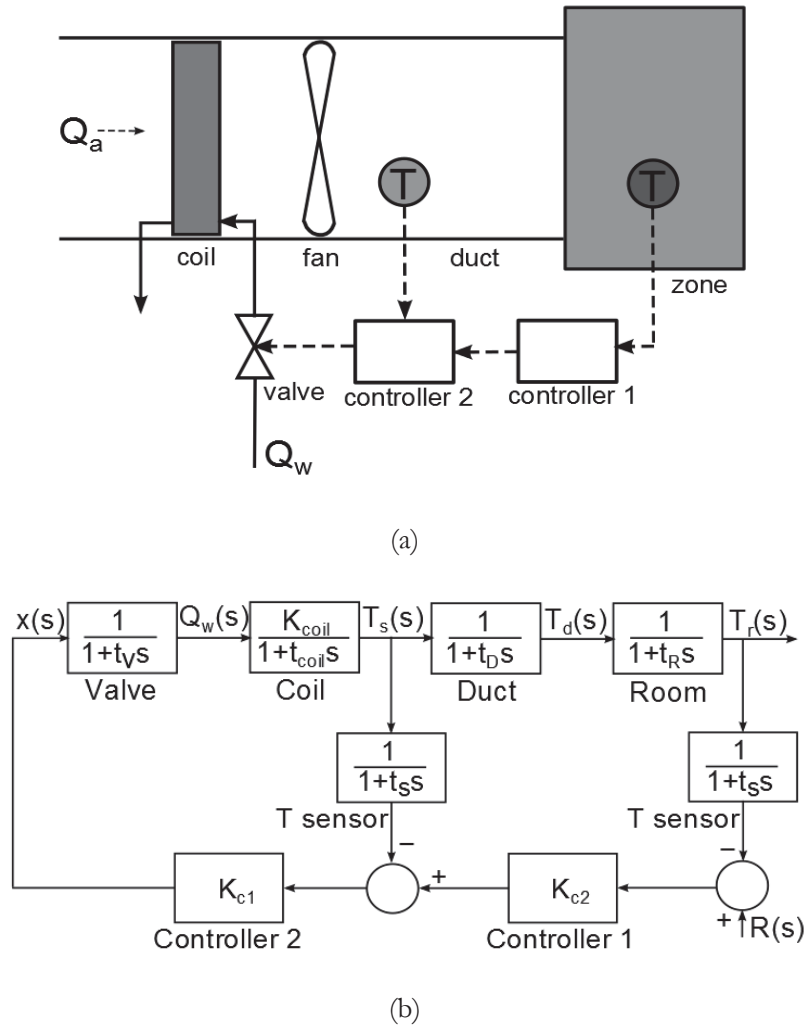

(a)

(b)

Figure 5.9 Cascade control (a) schematic and (b) block diagram of a SZ AHU system

The transfer functions in equations (5.45), (5.50), (5.54), (5.66) and (5.68) are checked

for stability in the Chapter 6 by considering test cases. The gains are assumed to be

constant and roots of above mentioned equations are plotted and analyzed with root locus

method.

CHAPTER 6. IMPROVEMENT IN RETURN FAN AND COOLING COIL VALVE CONTROL

To analyze the systems discussed in the earlier chapter the gain values need to be calculated. This is done by considering two test cases for the two systems under consideration i.e. return fan speed control and cooling coil valve control. After calculation of the gains, the roots are plotted on s-plot for root locus analysis. These plots provide an insight about the stability of the systems discussed in the earlier chapter.

6.1. Test Case for Return Fan Control

To test the stability of return fan control with direct building pressure control, volume tracking control and cascade control a single duct VAV AHU is designed using the equipment selection software of an AHU manufacturer (Trane, 2014).

The design supply airflow rate is 18.8 m^3/s (40,000 CFM) and the design return airflow rate is 17.9 m^3/s (38,000 CFM). The design airflow rate difference between the supply air and return air is 0.9 m^3/s (2,000 CFM) for space pressurization at 12.5 Pa (0.05 inch of water) to balance with the design exhaust airflow rate of 0.7 m^3/s (1,500CFM) and the infiltration airflow rate of 0.2 m^3/s (500CFM). Equation (6.1) is a normalized head-flow fan curve for the return fan.

$$\frac{H_{RF}}{H_{RF_D}} = -0.733 \left(\frac{Q_{RA}}{Q_{RA_D}}\right)^2 + 0.744 \frac{Q_{RA}}{Q_{RA_D}} \omega + 0.989 \omega^2 \qquad (6.1)$$

Using mentioned design values and equation (5.8), (5.13), (5.14), and (5.37) values of K$_1$, K$_2$, K$_3$ and T$_1$ are determined. At design condition,

www.manaraa.com

$$K_1 = 105.6\frac{Pa}{\frac{m^3}{s}},\ K_2 = 0.01365\frac{\frac{m^3}{s}}{Pa},\ K_3 = 17.59\frac{m^3}{s},\ T_1 = 11.80\ s$$

6.2. Root Locus Plot for Return Fan Control Methods

Root locus analysis of a system provides an insight into the stability of the system. With equations (5.45), (5.50), (5.54) and above calculated gains and time constant, root locus analysis is performed for direct pressure control, volume tracking control and cascade control. Figure 6.1 shows root locus plot of the direct pressure control.

Equation (5.45) is the open loop system gain for the direct pressure control. The AHU with feedback of direct pressure control is modeled in Simulink and the controller is tuned. The tuned controller gain of 0.005 is substituted for K_{C1} in equation (5.45) for the root locus analysis. At design condition the plant gain is, $\frac{K_1K_3}{(1+K_1K_2)} = 760.7$ and the system gain is $K_{C1} * \frac{K_1K_3}{(1+K_1K_2)} = 3.7$.
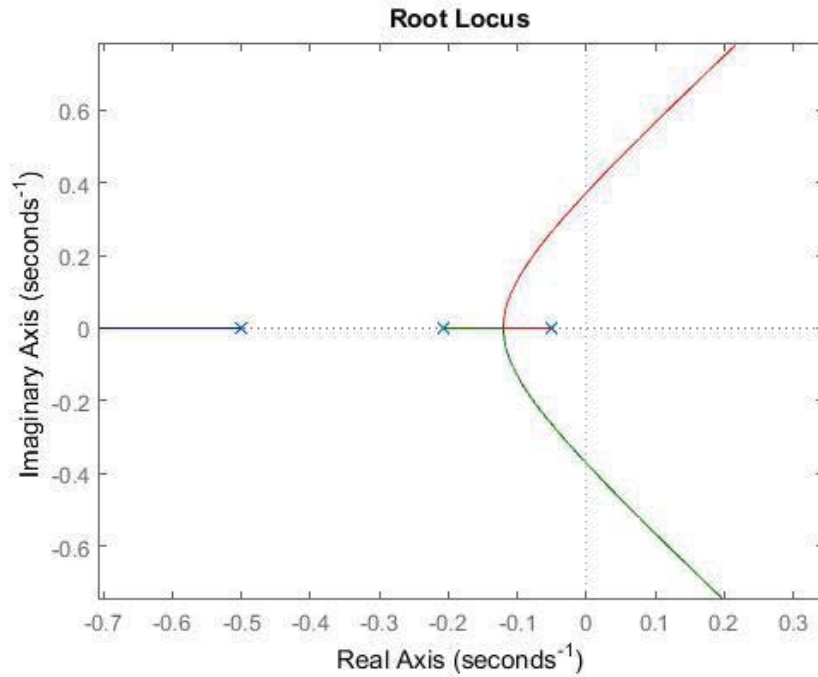
Figure 6.1 Root locus analysis of direct pressure control

From equation (5.45) it is clear that the direct pressure control will have three poles and no zeros. Same is observed in root locus analysis in Figure 6.1. The curve extends in the right-hand side of imaginary (y) axis. This indicates that the system can be unstable for higher absolute gain values. For the tuned controller the system gain is 3.7 in which the controller gain is constant however the plant gain can vary. Figure 6.2 shows the expanded part of Figure 6.1 with two points showing the system gain values. The design condition lies in the range of the two points shown. As the system gain exceeds 5.1 it is evident that the system will be unstable. Therefore it is important to check the variation in the plant gain with respect to change in operating condition.
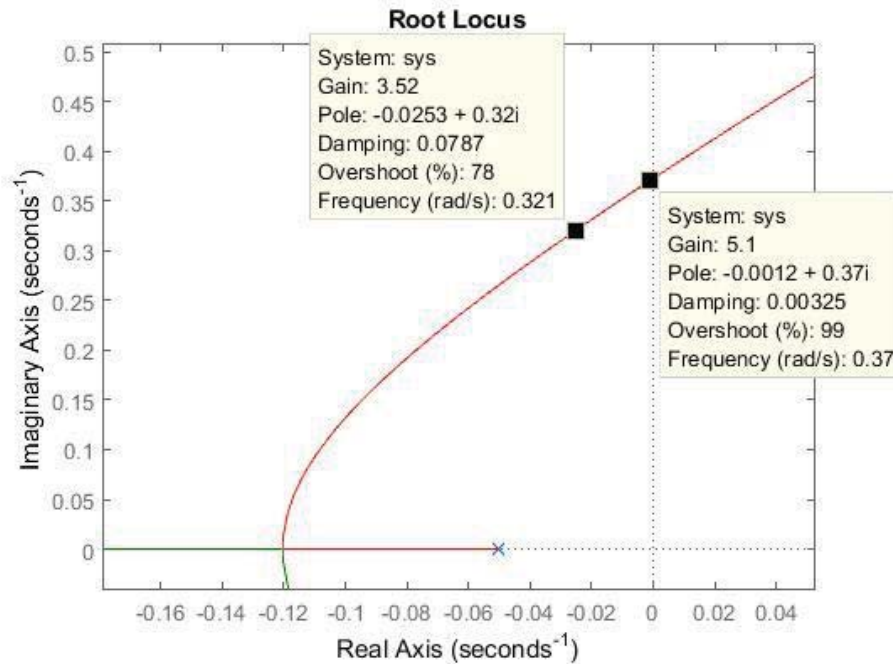
Figure 6.2 Expanded view of root locus analysis of direct pressure control

Building static pressure is one of the variables which is easily affected by the wind and thermal effect and opening and closing of the doors and windows as it is kept slightly above the atmospheric pressure. It is observed from the plot in Figure 6.3 that the system gain increases sharply from 2 to 4.5 as the building static pressure changes from 1 Pa (0.004 inwg) to 50 Pa (0.2 inwg). However, the system gain reaches its maximum value of 4.7 at about 100 Pa (0.4 inwg) and then it starts dropping. This shows that the system stays stable for any variation in the building pressure. However, this conclusion is based on a perfectly tuned controller.

$$K_{C1} * \frac{K_1 K_3}{(1 + K_1 K_2)}$$
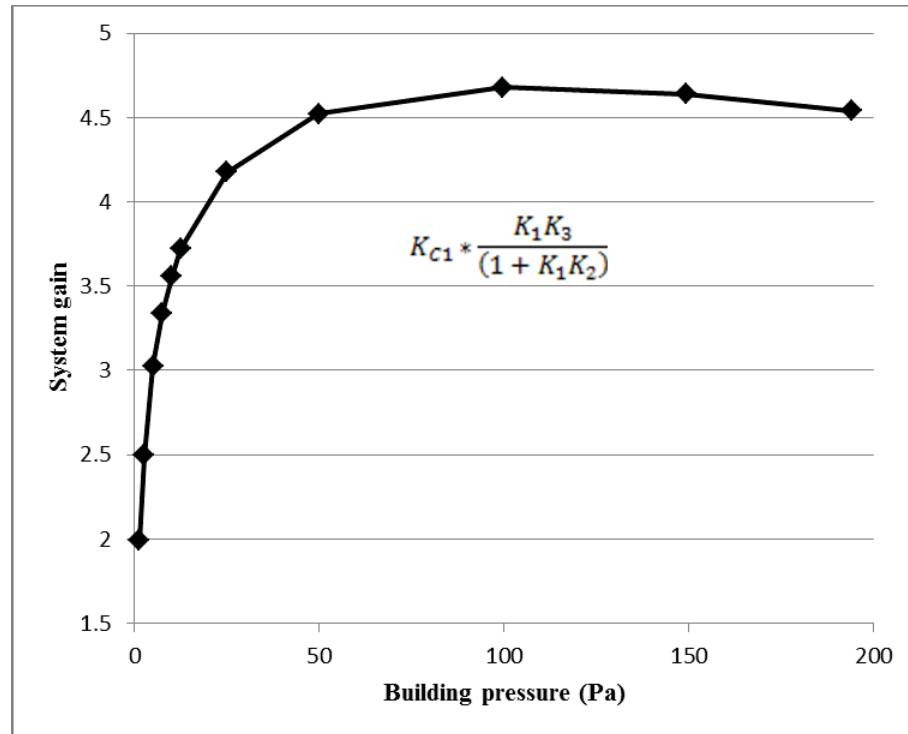
Figure 6.3 System gain variation with change in building pressure

The controller gain for root locus analysis in Figure 6.1 and 6.2 is 0.005 if the controller is not properly tuned then even for controller gain of 0.0065 the system will be unstable at 15 Pa (0.06 inwg) building pressure. Fluctuations of ±20 Pa (0.08 inwg) in building static pressure setpoint of 12.5Pa (0.05 inwg) is not uncommon. This suggests that the system stability is very sensitive to controller gain and building pressure. This may encourage setting the controller gain at a low value which may ensure the stability but will slow down the system response.

Form equation (5.50) it is evident that the root locus analysis of volume tracking control will have three poles and one zero. This addition of a zero provides excellent stability to the system. Figure 6.4, shows that the system curve at design condition which never enters the positive quadrants of the real axis. This ensures stability at all the system gains.

The zero introduced in the plot is due the room time constant T_1 which increases with increase in building pressure. Also, one of the poles due to the $\frac{T_1}{1+K_1K_2}$ term changes the position of the pole due to non-linearity of the system. This will change the shape of the curve at different operating conditions. Figure 6.5 and 6.6 are the root locus analysis of the volume tracking control at high and low building static pressure respectively. Even with the change in the position of a zero and pole the system appears extremely stable at all system gains. In fact the factor affecting the system gain $\frac{K_3}{1+K_1K_2}$ drops with increase in the building pressure. This suggests that the volume tracking control is extremely stable system.

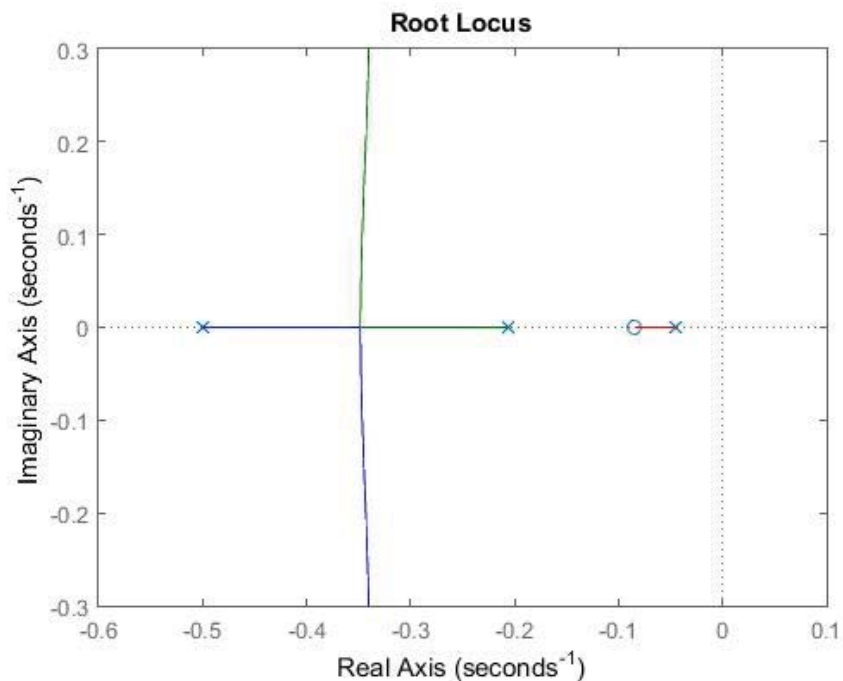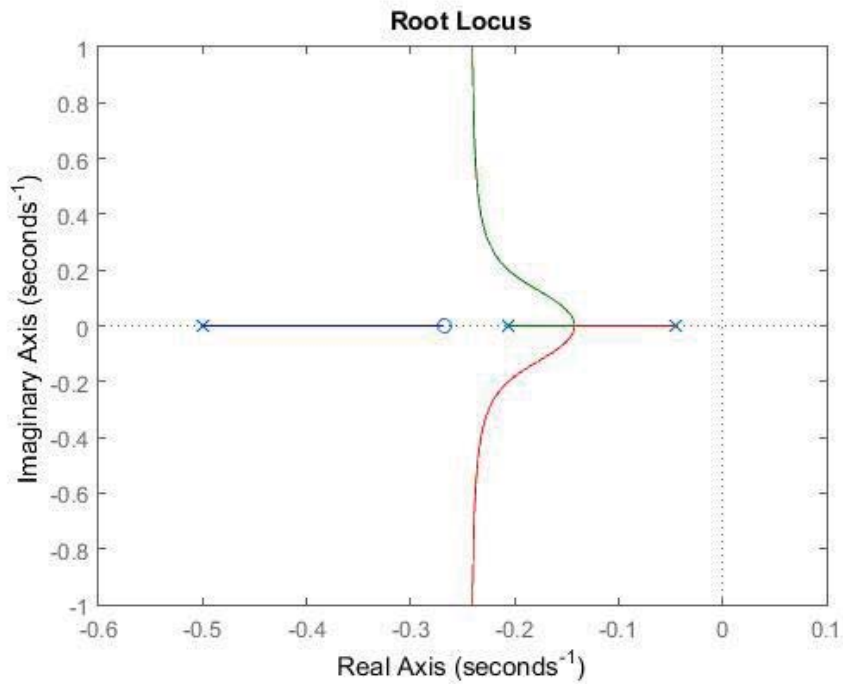**Figure 6.4 Root locus analysis of volume tracking control**

Figure 6.5 Root locus analysis of volume tracking control at high building pressure
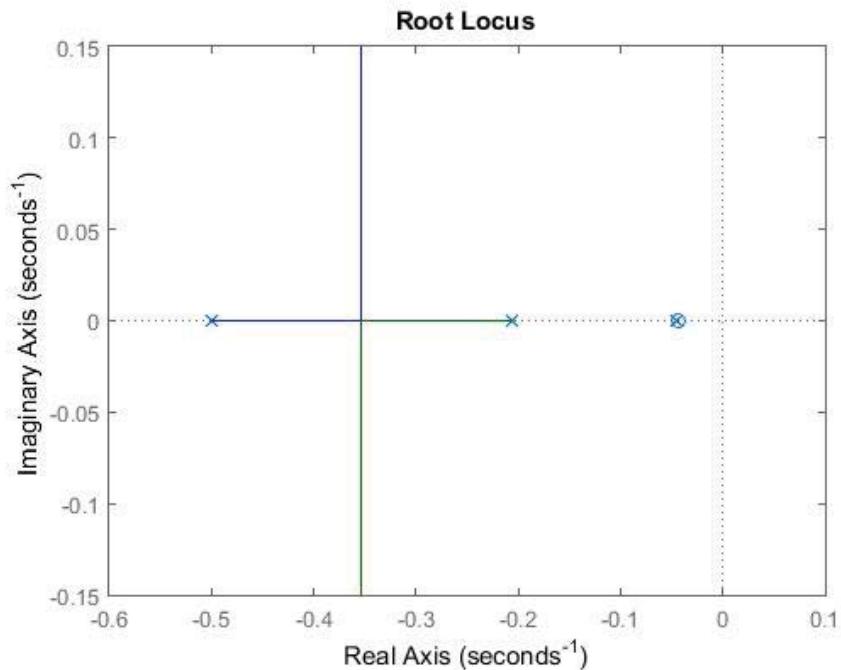
Figure 6.6 Root locus analysis of volume tracking control at low building pressure

However, this system relies on the difference in supply and return airflow and does not take a feedback from building pressure. The building static pressure can get affected by

infiltration due to opening and closing of windows and doors, and exhaust airflow. Volume tracking control does not take into consideration these variations. In fact when windows are open the building can get negatively pressurized allowing unconditioned air to enter the conditioned space. Also this control heavily relies on reading of airflow meters which often have high range of inaccuracy.

Equation (5.54) suggests there are four poles and two zeros in the root locus analysis and the controller gain K_{C2} affects the overall gain of the system. Figure 6.7 confirms that the system is highly stable for all the values system gain as the curve stays on the left-hand side of the imaginary (y) axis. Therefore fine tuning for controller 2 is not required.

Figure 6.7 Root locus analysis of cascade control

The tuned controller gains from direct pressure control and volume tracking control are used for the root locus plot in Figure 6.7. From equation (5.54) it is evident that the controller gain of the controller 1 (K_{C1}) will affect the shape of the curve along with room

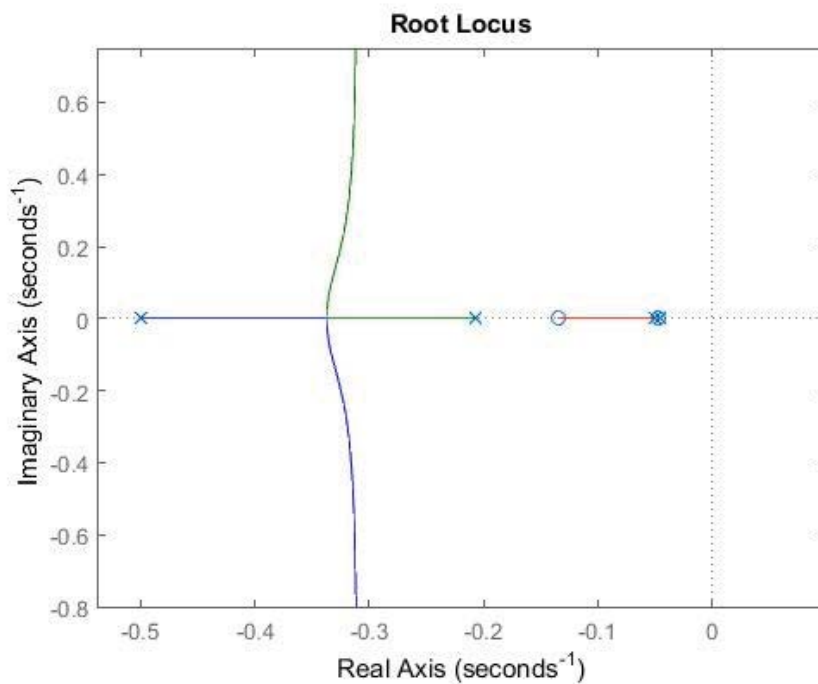time constant T_1 and K_1. From the earlier discussion in direct pressure control, the system stability was highly sensitive to K_{C1} as it was directly affecting the system gain. In cascade control even though K_{C1} does not affect the system gain directly it changes the location of zeros that can affect the shape of the curve. To check the stability for the high value of K_{C1} the earlier controller gain value of 0.005 from the direct pressure control is increased 10 times to 0.05 to approximately match the K_{C2} value of 0.05 from volume tracking control. Figure 6.8 shows the root locus analysis with increased K_{C1} value. Figure 6.8 indicates that the system is stable for all values of K_{C2}. As discussed earlier the factor affecting the system gain $\frac{K_3}{1+K_1K_2}$ drops with increase in the building pressure. Therefore K_{C1} provides first level of safety that gives the scope to set the value of K_{C2} and also allows the plant gain to vary making the system stable for changing in operating conditions. Even though cascade control reduces the sensitivity of the system to the controller gain K_{C1}, we do not recommend unrealistic or extremely high value for controller gain. Cascade control allows a good range to vary the controller gain to apply the engineering judgment.
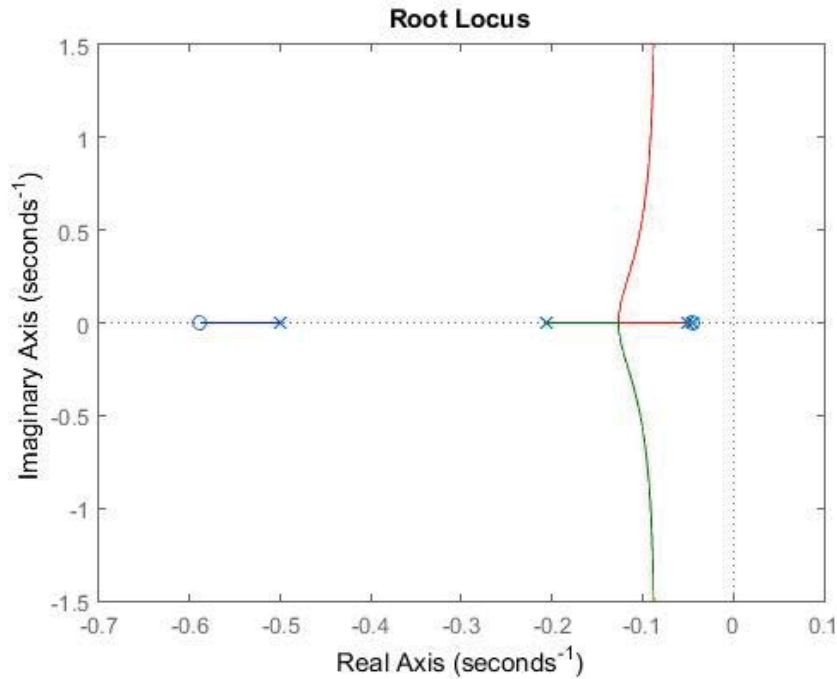
Figure 6.8 Root locus analysis of cascade control high KC1

The cascade control takes a feedback from the building pressure sensor, therefore, any change in the building static pressure due to infiltration, the wind or thermal effect is also corrected and right feedback is provided to return fan.

6.3. Test Case for Valve Control

For the simulation a SZ AHU cooling system for a 743 m^2 (8,000 sqft) zone is designed; fan and cooling coil is selected using the equipment selection software of an AHU manufacturer (Trane, 2014). The design supply airflow rate for the zone is 3.78m3/s (8,000 CFM). The cooling coil with 102 kW (347.9MBH or 29 ton) total cooling capacity and 70 kW (240MBH or 20 ton) sensible cooling capacity is selected for the design air dry bulb and wet bulb temperature from the mixing box 27°C (80F) and 20°C (64F). The design supply chilled water temperature is 7°C (45F). For the defined design conditions and the selected coil capacity, the calculated chilled water flow rate is 3.78m^3/s (57gpm)

and the design temperature of saturated air leaving the coil is 11.5°C (53F). At the design condition temperature of chilled water and air entering and exiting the cooling coil is known along with the cooling capacity of the coil. Using the data available the overall UA value (product of overall heat transfer coefficient and the heat transfer area) of the coil at design condition is calculated as 8.3kW/K (15.7 MBH/°F) and is assumed to be constant over the operational range. For simplification, dry coil condition is assumed. The equipment selection software used to design this test case provides the coil weight of 122 kg (270lb) and with water 162kg (357lb). Using these values overall heat capacity if the coil is calculated as 232kJ/K (122.2 Btu/°F).

Using test case and equation (5.63), the value of the K_{coil} and t_{coil} at design condition is calculated. The variation in gain and time delay of the cooling coil with a change in the chilled water flow rate is discussed in following sections. Based on the response time, control valves are classified from slow ($\tau=12s$) to very fast ($\tau=0.2s$) and for 80% of the cases control valve with one second time constant is suitable (EnTech 1998). Thermostat with time constant two seconds is selected. From equation (5.56) and (5.57) the time constant for the zone and the duct is calculated as 600s and 1.8s.

With equations (5.66) and (5.68), and above calculated gain and time constants, root locus analysis is performed for conventional control and cascade control method.

From equation (5.66) and (5.68), it is clear that the system gain is a function of coil gain. Also, the time delay of the coil has a strong effect on the shape of the curve in root locus analysis discussed further. Figure 6.9 shows the change in coil gain and time delay with respect to chilled water flow which is a function of valve position. As the chilled water flow decreases the coil gain increases. Therefore, if the controller is tuned at design

chilled water flow, during the part load operation the system can be unstable. From figure 6.9 it is clear that the coil response and therefore the system response are non-linear.
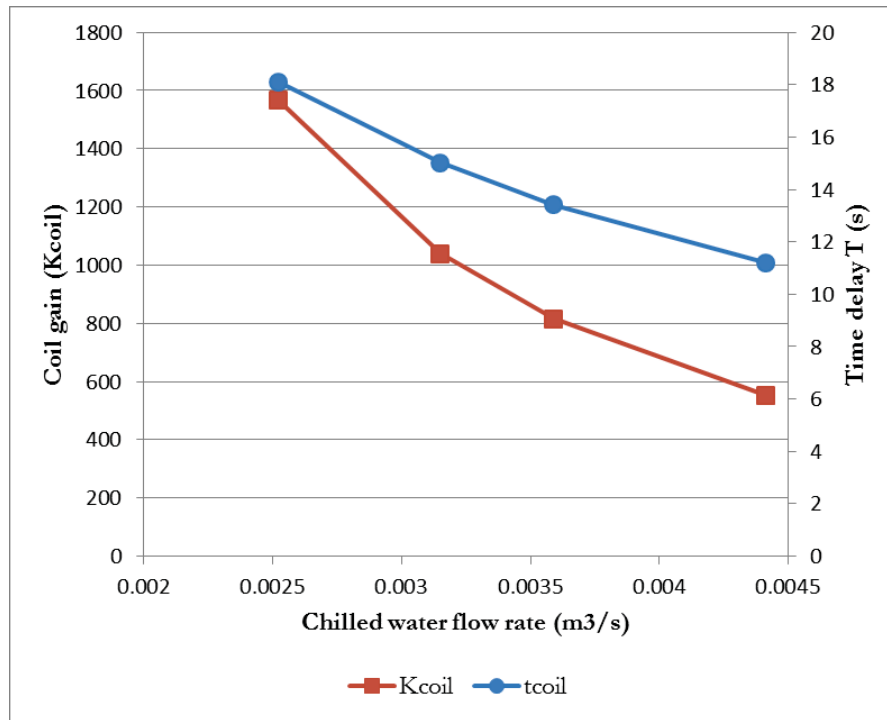
Figure 6.9 Coil gain and time delay

6.4. Root Locus Plot for Valve Control Methods

From equation (5.66) it is clear that the conventional control will have five poles and no zeros. Same is observed in root locus analysis in Figure 6.10(a). The curve extends in the right-hand side of imaginary (y) axis. This indicates that the system can be unstable for higher absolute gain values. Figure 6.9 shows that the coil gain increases with a decrease in the chilled water flow rate. From equation (5.66) it is clear that the system gain will change proportional to the coil gain. With a decrease in the cooling coil load, the coil gain will increase leading to increase in the system gain making the control loop unstable. This suggests that if the controller is tuned at design condition, in partial cooling load condition the control loop can enter the unstable region causing the control valve hunting.

Figure 6.10(a) shows the point with the gain value at which the system is just stable. As the system gain exceeds 0.0045, it is evident that the system will be unstable. From equation (5.68) it is clear that the controller gain of the controller 1 (K_{C1}) will affect the shape of the curve. From the earlier discussion in conventional control method, the system stability was highly sensitive to K_{C1} as it was directly affecting the system gain. In cascade control even though K_{C1} does not affect the system gain directly it changes the location of zeros that affects the shape of the curve. To check the stability for the high value of K_{C1} the earlier tuned controller gain value of 0.03 is increased to 0.1. Figure 6.10(b) shows the root locus analysis with increased K_{C1} value. Figure 6.10(b) indicates that the system is stable for system gain of 0.93. This is approximately 200 times higher than the conventional control gain value at which the system just becomes unstable. Therefore for the test case, the cascade control improved range for the stable control operation.
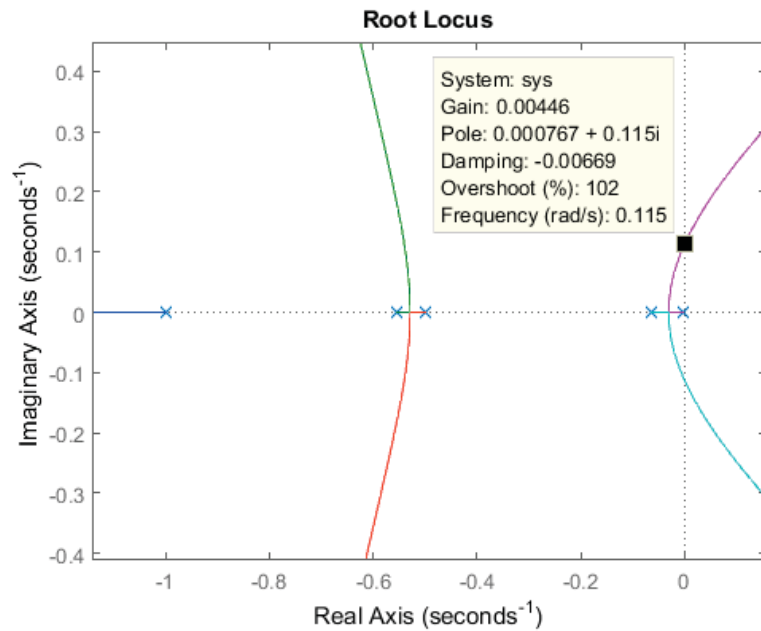
(a)
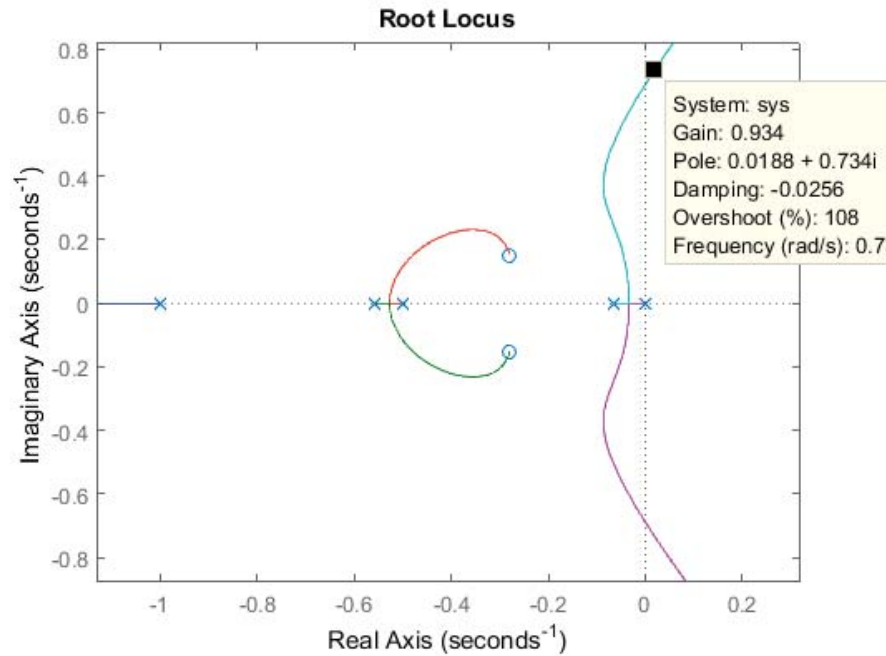
(b)

Figure 6.10 Root locus analysis of (a) conventional control (b) cascade control

Using the transfer functions discussed earlier and the test case, a Simulink model is developed, and for the same controller settings results are compared in Figure 6.11. Both plots show the supply air temperature and room air temperature. In both the cases, same pulse disturbance is given to the system and the room air temperature is maintained close to the setpoint. However, in the case of conventional control the supply air temperature fluctuates over a wide range compared to the result obtained using cascade control with same controller gain settings. Figure 6.11(a) represents the practical problem discussed in Figure 2.7 where the zone setpoint is maintained however the supply air temperature fluctuates over a wide range that leads loss of humidity control in SZ AHU system. This problem may go undetected if the supply air temperature is unnoticed and only room air temperature is considered for maintaining indoor air quality. The cascade control method

measures the supply air temperature to correct the chilled water valve position, and the

supply air temperature does not vary over a wide range as seen in Figure 6.11(b).
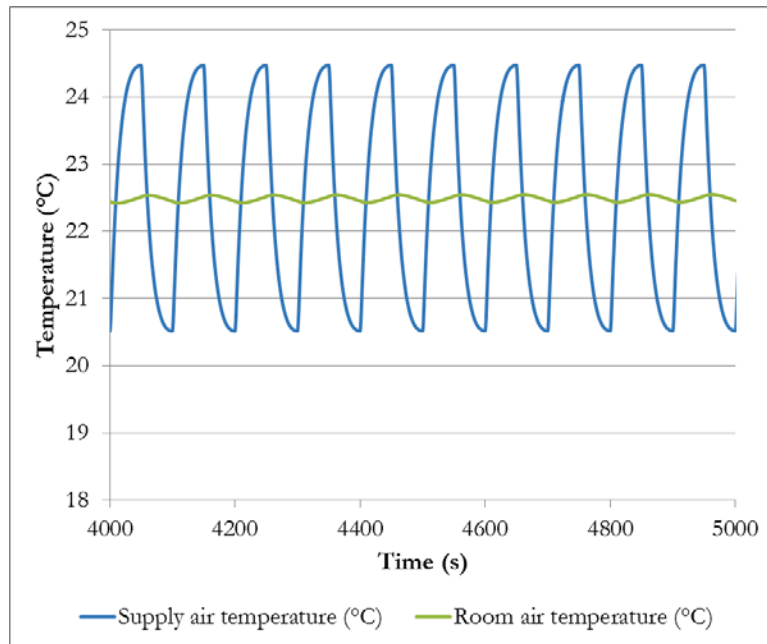
(a)
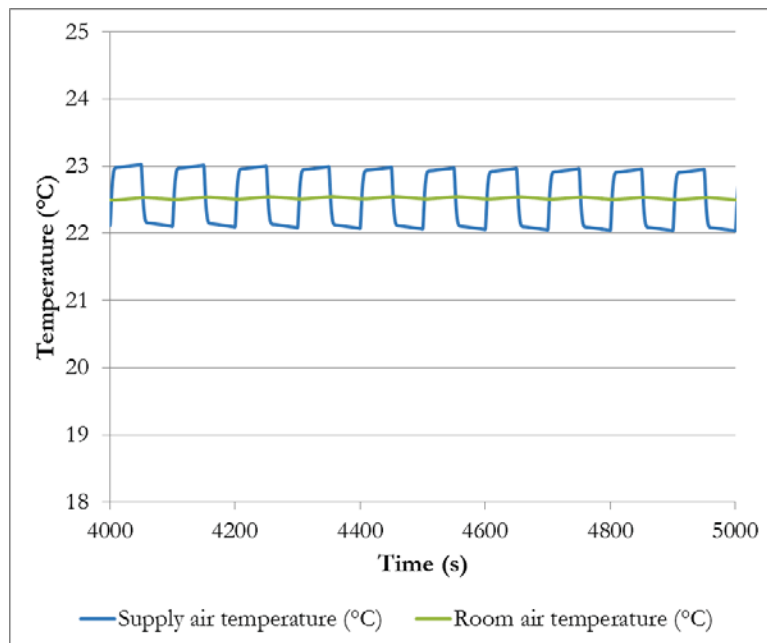
(b)

Figure 6.11 Simulink results of (a) conventional control (b) cascade control

From above discussion, it is clear that the cascade control reduces the system sensitivity to the controller gain, and provides a good range of controller gain to work with. In the case of return fan control, it also gets a feedback from building pressure sensor which makes it responsive to the changes in building static pressure due to unaccounted variables in volume tracking. In cooling coil valve control, cascade control stabilizes the supply air temperature variation that will maintain the humidity level in the building and avoid the simultaneous heating and cooling.

CHAPTER 7. CONCLUSIONS AND FUTURE WORK

From the results in Chapter 4 and 6 conclusions for the two objectives of the thesis are drawn. These conclusions are discussed in subsections of this chapter. In the end, based on the conclusion scope for future work is been identified.

7.1. Conclusions

The Chapter 2 of this thesis describes the two broad objectives and five problem statements for this study. The five problem statements are related to five specific applications in AHUs. Results of these applications are described in detail in chapter 4 and 6. Following conclusions are drawn from the results.

7.1.1 Energy and Control Performance

For the first problem statement, both the fan energy and control performance of five airflow-pressure control methods in an AHU are investigated through simulation using the nonlinear network solution. The SF and RF head and total fan power are applied to evaluate the fan energy performance. The system gain ratios in outdoor air control with the damper command and four interactive disturbance factors, including disturbance factors on the space static pressure and supply airflow by the airflow-pressure control as well as disturbance factors on the outdoor airflow ratio by the SF and RF speeds, are applied to evaluate the system control performance.

The study shows that two (open OAD and decoupled RLD) sequenced control methods have better fan energy performance but the worst control performance, and that traditional controls have the best control performance among the five airflow-pressure control methods, increasing the fan power by 4%, for the studied AHU.

For control purposes, it is recommended that the traditional airflow-pressure control method be selected for AHU pressure-airflow control. In general, control performance degradation needs to be considered in order to determine the optimal airflow-pressure control method.

7.1.2 Controllability of BPP and BPA Methods

The controllability of passive and active type of control, i.e. BPP and BPA at limiting cases of the damper position is studied for this problem statement.

For the study relief airflow and building static pressure of an AHU are simulated at different outdoor airflow rate from lower outdoor airflow ratio to 100% using the nonlinear network solution for both the BPP and BPA controls with the decoupled RLD. The simulation results show that both the controls can well prevent the reverse relief airflow by fully closing the decoupled relief air damper. However, the BPP control may result in negative building static pressure at lower outdoor airflow ratio and excessively positive building static pressure under a low relief air plenum static pressure setpoint at higher outdoor airflow ratio. Even though increasing the relief air plenum static pressure setpoint can fix the positive building static pressure issues at the higher outdoor airflow ratio, it will results in excessive RF energy consumption at the lower outdoor airflow ratio. On the other hand, the BPA control shows robust control over the building static pressure.

7.1.3 OA and Building Static Pressure Control without Sensors

The outdoor airflow ratio and building static pressure are simulated using two alternative control methods on an AHU with the lack of reliable and accurate airflow and pressure sensors for different airflow-pressure control methods. The alternative methods include:

1) the fixed damper position method on the minimum outdoor airflow due to the lack of an outdoor airflow sensor only; 2) the fixed damper position method on the minimum outdoor airflow and the RF speed tracking method on the building static pressure due to the lack of the outdoor, supply and return airflow and building static pressure sensors.

The simulation results reveal a supply airflow independent correlation between the outdoor airflow ratio and damper position with a 2% error. These results were obtained for the supply airflow ratio variation of 40% to 100% with the traditional damper connection and when the return fan perfectly controls the building static pressure. The consistent correlation can be easily calibrated using the CO_2 measurements of the outdoor air, return air and mixed air in AHUs during occupied hours as well as the damper command and will provide a method to calculate the outdoor airflow using the damper command along with the measured supply airflow rate.

The fixed damper position combined with the RF speed linear tracking method maintains a positive building static pressure when traditional airflow-pressure control method is used. The simulation results for the linear tracking are better than the proportional or offset tracking. The building static pressure varies from 0 to 7 Pa (from 0 to 0.03 inch of water) for the traditional connection. The RF linear tracking method may provide a substitute control to maintain the slightly positive building static pressure with the lack of airflow and pressure sensors in AHUs.

7.1.4 Return Fan Speed Control

For this problem statement control performance of cascade control was compared with direct pressure control and volume tracking control after deriving the equations for open and closed loop plant transfer functions in each case, with the help of root locus analysis.

It was observed that the direct pressure control is stable for change in operating condition if the controller is tuned well. However if the controller gain is not tuned well it makes the system unstable not only for change in the operating condition but also at design condition. This makes the direct pressure control highly sensitive to the controller gain and to use this control for building pressurization, fine tuning of the controller is required.

Volume tracking control which is based on differential flow between supply and return airflow is highly stable. The system stability is independent of controller gain. However, volume tracking control does not have a feedback from the building pressure sensor this makes the system unresponsive to any change in building static pressure due to infiltration, exhaust airflow, wind and thermal effects. This system may not respond well to the exhaust fan schedules, opening and closing of doors and pressure changes caused by these factors cannot be corrected by the controller.

The cascade control reduces the system sensitivity to the controller gain, eliminating the need of fine tuning, and provides a good range of controller gain to work with. This type of control also gets a feedback from building pressure sensor which makes it responsive to the changes in building static pressure due to unaccounted variables in volume tracking.

7.1.5 Cooling Coil Valve Control
For SZ AHUs the control performance of cascade control was compared with conventional control method after deriving the equations for open loop plant gain, with the help of root locus analysis. The results indicate that the SZ AHU system is non-linear in nature due to non-linearity of the coil performance. High gain and time delay at low

chilled water flow rate suggest that the system is more likely to be unstable at part load or at minimum airflow conditions.

It was observed that the conventional control is stable at design condition if the controller is tuned well. However if the controller gain is not tuned well, it makes the system unstable not only for change in the operating condition but also at design condition due to limited stability range. This makes the conventional control method highly sensitive to the controller gain and to use this method fine tuning of the controller is required. From the test case it was observed that the cascade control increased the range of the system gain over which the control loop is stable. For the given test case the gain stability range increased by about 200 times and this improvement will change with different system parameters. This increased stability range handles the change in system gain due to non-linearity. This also eliminates the need of seasonal controller gain reset reducing the maintenance work and fine tuning of the controller.

In conventional control method, the lack of control over the supply air temperature, may lead to loss of zone humidity control or sometimes simultaneous heating and cooling. Continuously changing supply air temperature due change in valve position leads to additional pump energy consumption. These problems can be solved with cascade control method which maintains the supply air temperature in close range.

7.2. Future Work
In this section based on the conclusion, future research opportunities are been identified.

- Energy and control performance of five airflow-pressure control methods is studied for the first problem statement and the recommendation is given for the

studied AHU based on the simulation. The method can be applied to any AHU with different system configuration. Moreover, the energy and control performance is analyzed based on the steady state performance. For further detail study, in the future, the system time response can be simulated. The conclusions can be supported with an experimental verification.

- The controllability study of BPP and BPA resulted in conclusion that the BPA control shows a robust control over the building static pressure. Similar to the first conclusion this conclusion is based on the steady state simulation. It will be interesting to compare the dynamic response of the BPP and BPA control method. This conclusion also could be validated experimentally.

- In absence of pressure and airflow sensors, the simulation study concluded that a supply airflow independent correlation between the outdoor airflow ratio and damper position. With the use of virtual flow meter at the supply fan the amount of OA flow can be determined with the OAD position. This conclusion should be verified with an experiment and this could lead to eliminate requirement of flow sensor for OA measurement. Also the experimental verification of building static pressure control with linear return fan speed tracking could eliminate need of pressure and flow sensors used in conventional control methods i.e. direct pressure control and volume tracking control.

- The root locus analysis concluded that cascade control could stabilize the return fan speed control. The stability and responsiveness of the three methods i.e. direct pressure control, volume tracking control and cascade control can be experimentally validated for the same building.

- The dynamic simulation using root locus analysis of SZ AHU concluded that cascade control improves the stability range of the system. The cascade control can be easily implemented and the results can be validated in SZ AHU system.

REFERENCES

ABB. (2008) "Application Notes: VAV with Fan Tracking Positive Pressure." ABB, Helsinki, Finland

Anderson, M., Buehner, M., Young, P., Hittle, D., Anderson, C., Tu, J., & Hodgson, D. (2005) "MIMO Robust Control for Heating, Ventilating and Air Conditioning (HVAC) Systems." IEEE Transactions on Control Systems Technology, 101-116.

Apte, M.G. (2006) "A Review of Demand Control Ventilation (LBNL-60170)." Technical Report under DOE Contract DE-AC03-76SF00098. Lawrence Berkeley National Laboratory, Berkeley, CA

ASHRAE. (2009). "2009 ASHRAE Fundamentals Handbook - Measurement and Instruments." American Society of Heating, Refrigerating and Air-conditioning Engineers, Inc., Atlanta, GA.

ASHRAE. (2010a) "Ventilation for Acceptable Indoor Air Quality, ANSI/ASHRAE Standard 62.1-2010." American Society of Heating, Refrigerating and Air-conditioning Engineers, Inc., Atlanta, GA.

ASHRAE. (2010b) "ASHRAE Standard 90.1-2010. Energy Standard for Buildings except Low-Rise Residential Buildings." American Society of Heating, Refrigerating and Air-conditioning Engineers, Inc., Atlanta, GA.

ASHRAE. (2010c) "Selecting Outdoor, Return, and Relief Dampers for Air-side Economizer Systems." ASHRAE Guideline 16-2010, American Society of Heating, Refrigerating and Air-conditioning Engineers, Inc., Atlanta, GA.

ASHRAE. (2011) "ASHRAE Handbook - HVAC Applications." American Society of Heating, Refrigerating and Air-conditioning Engineers, Inc., Atlanta, GA.

Astrom, K. J. (2002) "Control System Design." chapter 6, page 216. Department of Mechanical and Environmental Engineering, University of California, Santa Barbara.

Brandemuel, M.J., S. Gabel, I. Andersen. (1993) "A Toolkit for Secondary HVAC System Energy Calculation." American Society of Heating, Refrigerating and Air-conditioning Engineers, Inc., Atlanta, GA.

CEC. (2003) "Advanced Variable Air Volume System Design Guide." California Energy Commission.

D&R International. (2012) "2011 Buildings Energy Data Book" Buildings Technologies Program, Energy Efficiency and Renewable Energy, U.S. Department of Energy under Contract to Pacific Northwest National Laboratory. Silver Spring, Maryland.

EnTech. (1998) "Control Valve Dynamic Specification." Version 3.0, Emerson Process Management, Austin, TX

Felker, L.G., and T.L. Felker. (2010) "Dampers and Airflow Control." American Society of Heating, Refrigerating and Air-Conditioning Engineers, Inc., Atlanta, GA, 2010.

Greenheck. (2011) "Centrifugal Roof Downblast Exhaust Fans." Greenheck Fan Corp. Schofield, WI.

Haugen, F. (2004) "Cascade Control" PID Control (pp. 253-261). Fagbokforlaget .

Hitchings, D. (2001) "Laboratory Space Pressurization Control Systems." SAFELAB Corporation.

Honeywell. (1998). "Building Airflow System Control Application." Honeywell Inc. Minneapolis, MN

Janu, G., Wenger, J. D., Nesler, C. G. (1995) "Strategies for Outdoor Airflow Control from a System Perspective." ASHRAE Transactions, 101(2), 631, 1995.

Krarti, M. (2011) "Energy Audit of Building Systems: An Engineering Approach." CRC Press, Taylor & Francis Group, Boca Raton, FL

Kraisuntronlertphop, A., & Gunpanich, S. (2012) "Analysis Parameter PID with the Root Locus Theory by used M-file Mat Lab." International MultiConference of Engineers & Computer Scientists, Vol. 2. Hong Kong: IMECS.

Karunakaran R., et al. (2009) "Efficient Variable Air Volume Air Conditioning System Based on Fuzzy Logic Control for Buildings." Thammasat International Journal of Science and Technology Vol. 14, No. 1, January-March 2009

Levenhagen, J.I. (1998) "HAVC Control System Design Diagrams." First Edition. McGraw-Hill. New York

Liu, G., Zhang, J., & Dasu, A. (2012) "Review of Literature on Terminal Box Control, Occupancy Sensing Technology and Multi-zone Demand Control Ventilation (DCV)." Richland, WA: Pacific Northwest National Laboratory, U.S. Department of Energy.

Lizardos, E. and K. M. Elovitz. (2000) "Damper Sizing Using Damper Authority." ASHRAE Journal, April 2000

Marlin, T. (2000) "Cascade Control." In Process Control (pp. 457-482). McGraw-Hill. Boston, MA

McFarlane, D. (2012) "Top Ten Reasons Building HVAC Systems Do Not Perform as Intended." National Environmental Balancing Bureau, pp. 2-6. , July 2012.

McQuiston, F.C., J.D. Parker, and J.D. Spitler. (2005) "Heating, Ventilating and Air-Conditioning – Analysis and Design." Sixth Edition, John Wiley & Sons, Inc.

Montgomery, R., and R. McDowall. (2008) "Fundamentals of HVAC Control Systems" American Society of Heating, Refrigerating and Air-Conditioning Engineers, Inc. Atlanta, GA.

Nassif, N. and S. Moujaes. (2008) "A New Operating Method for Economizer Dampers of VAV System." Energy and Buildings, 40 (2008), 289–299.

Nassif, N. (2010) "Performance Analysis of Supply and Return Fans for HVAC Systems under Different Operating Strategies of Economizer Dampers." Energy and Buildings, 42 (2010), 1026-1037.

Phalak, K., G. Wang. (2016a) "Minimum Outdoor Air Control and Building Pressurization with Lack of Airflow and Pressure Sensors in Air Handling Units." Journal of Architectural Engineering. DOI: 10.1061/(ASCE)AE.1943-5568.0000190.

Phalak, K., G. Wang. (2016b) "Performance Comparison of Cascade Control with Conventional Controls in Air Handling Units for Building Pressurization." 2016 ASHRAE Winter Conference, Jan 23-27, 2016, Orlando, FL.

Phalak, K., G. Wang, J. Varona. (2016) "Improving Valve Operation Using Cascade Control in Single Zone Air Handling Units." 2016 ASHRAE Annual Conference, June 25-29, St. Louis, MO.

PSU. (2010) "PSU Standard Sequences of Operation Guideline." The Pennsylvania State University Physical Plant Building, University Park, PA.

Siemens Building Technologies Division (2003). "Room Pressurization Control Methods: Volumetric Airflow Tracking vs. Differential Pressure Sensing." Buffalo Grove, IL: Siemens Industry, Inc.

Siemens. (2013) "System with Multiple Storage Elements." In Control Technology (p. 36). Zug, Switzerland: Siemens Switzerland Ltd.

Seem, J.E., J.M. House, G.E. Kelly, C.J. Klaassen. (2000) "A Damper Control System for Preventing Reverse Airflow through the Exhaust Air Damper of Variable-Air-Volume Air-Handling Units." HVAC&R Research, 6(2)(2000),135–148.

Stanke, D., & Bradley, B. (2002) "Managing the Ins and Outs of Commercial Building Pressurization." La Crosse, WI: Trane Engineers Newsletter (Volume 31, No. 2).

Taylor, S. (2014a) "Return Fans in VAV Systems." ASHRAE Journal, October 2014.

Taylor, S. (2014b) "Select & Control Economizer Dampers in VAV Systems." ASHRAE Journal, 50-56.

Trane. (2002) "Commercial Building Pressurization." Engineers Newsletter. Volume 31, No. 2.

Trane. (2014) "Trane Official Product Selection System." TOPSS™ version 6.3, Trane U.S. Inc.

Underwood, C.P. (1999) "HVAC Control Systems: Modeling, Analysis and Design." E&FN SPON, London.

Wang G., Ayala E., Wright J., Ayala L. (2010) "Energy Efficient Method Development for Sport Facility." American Society of Civil Engineers (ASCE).

Wang, G., K. Phalak. (2016) "Reverse Relief Airflow Prevention and Building Pressurization with a Decoupled Relief Air Damper in Air Handling Units." ASHRAE Transactions. Volume 122, part 1.

Wang, G., L. Song, K. Phalak, (2015) "Investigation on the Energy and Control Performance of Different Damper Control Strategies in Air Handling Units." ASHRAE Transactions. Volume 121, part1.

Wang, G., L. Song. (2012) "Air Handling Unit Supply Air Temperature Optimal Control During Economizer Cycles." Energy and Buildings, Elsevier, 310-316.